

Evaluating Sensitivity to the Stick-Breaking Prior in Bayesian Nonparametrics

Ryan Giordano ^{*†} Runjing Liu ^{*‡}

Michael I. Jordan [‡] Tamara Broderick [†]

October 28, 2021

Bayesian models based on the Dirichlet process and other stick-breaking priors have been proposed as core ingredients for clustering, topic modeling, and other unsupervised learning tasks. Prior specification is, however, relatively difficult for such models, given that their flexibility implies that the consequences of prior choices are often relatively opaque. Moreover, these choices can have a substantial effect on posterior inferences. Thus, considerations of robustness need to go hand in hand with nonparametric modeling. In the current paper, we tackle this challenge by exploiting the fact that variational Bayesian methods, in addition to having computational advantages in fitting complex nonparametric models, also yield sensitivities with respect to parametric and nonparametric aspects of Bayesian models. In particular, we demonstrate how to assess the sensitivity of conclusions to the choice of concentration parameter and stick-breaking distribution for inferences under Dirichlet process mixtures and related mixture models. We provide both theoretical and empirical support for our variational approach to Bayesian sensitivity analysis.

1 Introduction

Scientists and engineers working in a wide range of fields are often interested in inferring the number of clusters in a given data set, as well as inferring which data points belong together. Such inferential questions can be posed naturally within a Bayesian nonparametric (BNP) framework, building on tools such as the Dirichlet process [Ferguson, 1973, Sethuraman, 1994]. The Dirichlet process has two useful attributes that have made it be suggested as a natural model of clustering phenomena. First, it is a combinatorial stochastic process, exhibiting discrete structure that allows multiple data points to be associated with the same

^{*}Equal contribution author

[†]Department of EECS, MIT

[‡]Department of Statistics, UC Berkeley

underlying value of a parameter. Second, its nonparametric nature means that the number of unique parameter values generally grows with the size of the data set, accommodating growth in the number of inferred clusters as data accrue. Such growth is appropriate in many real-world settings; for example, we might expect to keep discovering new species as we examine more individual organisms, and we might expect to discover more topics as we read more articles in a scientific literature. Finally, the overall Bayesian framework in which the Dirichlet process is embedded allows clustering to be treated as one aspect of a larger inferential problem. In particular, the Dirichlet process can be flexibly incorporated into more complex models that exhibit other forms of structure, including hierarchical, spatio-temporal, and topological structure.

Although the BNP framework offers flexibility, it is important to recognize that it is not a black-box method. As with any Bayesian methodology, the deployment of a BNP model involves choices of hyperparameters. Often, these choices are made for reasons of mathematical or computational convenience. Indeed, the nonparametric nature of BNP models can make it particularly difficult to express prior belief subjectively. For example, the latent frequencies of clusters provided by the Dirichlet process are obtained by recursively removing beta-distributed fractions of probability mass from the unit interval. The use of the beta distribution is motivated by its mathematical tractability under recursion and by the fact that it yields a form of conditional conjugacy that can be exploited by Gibbs sampling. These are appealing properties, but it is difficult to imagine justifying this specific choice subjectively, particularly given that observable consequences of the choice are indirect. Even having accepted the beta distribution as a choice of convenience, there remains the problem of choosing the parameter α associated with this distribution. The implications of this choice are again difficult to assess subjectively. In practice the choice is often made based on previous applications or by simply employing a heuristic [Teh et al., 2006, Gelman et al., 2013, Chapter 23].

In summary, it is important to recognize that there will exist many possible values of α , and many possible forms of stick-breaking prior, that might correspond to one's prior beliefs, but which the Dirichlet process framework and other complex BNP models bundle in a way that makes it difficult to understand and to specify *a priori*. Choices of convenience are therefore made, and, unfortunately, these choices can change the results of a data analysis. For instance, α has a direct, proportional relationship to the number of clusters obtained asymptotically in draws from the Dirichlet process. Thus the number of clusters inferred at any particular data size may depend strongly on α . If our scientific conclusions varied substantially because of such dependence, we might worry that these conclusions were driven not by the data and meaningful prior beliefs but instead by our arbitrary or default choices. It behooves us, then, to check how sensitive our conclusions are to these choices.

The outputs of Bayesian inference arise not just from a model and collection of data but also via the use of some posterior approximation. Accordingly, when we assess sensitivity, we should assess the sensitivity of this full procedure to our

model choices. In the current paper we focus on Dirichlet process mixture (DPM) models and Variational Bayesian (VB) posterior approximations based on reverse Kulback-Leibler (KL) divergence. VB methods have several favorable properties that motivate their use in the DPM setting. First, they exhibit fast computational scaling due to their use of gradient-based optimization. Second, they avoid the label-switching problem exhibited by MCMC in the mixture-model setting [[Jasra et al., 2005](#)]. Third, their implementation has become increasingly straightforward due to automatic differentiation tools [[Ranganath et al., 2013](#), [Kucukelbir et al., 2016](#)]. Finally, and of particular interest in the current paper, the variational formulation makes it possible to compute closed-form derivative-based expansions of posterior distributions as a function of model hyperparameters [[Giordano et al., 2018](#)]. Thus VB provides a natural pathway to quantifying the robustness of Bayesian inference.

Concretely, with a fully specified model and inference procedure in hand in the setting of DPM models, we can ask how sensitive some quantity of interest is to the choices of α and the stick-breaking distributions. One option is to propose a number of potential α values, compute the variational approximation at each α value, and report our quantity of interest for each α value. We might similarly assess sensitivity to the stick-breaking distribution over a range of distributional choices. There are at least two major issues with this proposal: (1) while VB is a relatively fast form of approximate Bayesian inference in general, it may still be prohibitively expensive to have to re-run it many times, and (2) it is unclear how best to choose a collection of α and (especially) the stick-breaking distribution values—and how many to choose.

In this work, we address these challenges by making full use of the variational nature of VB methodology. We show how to approximate the nonlinear dependence of the VB optimum on prior choices using a first-order Taylor series expansion. We build on the local robustness tools developed by [Giordano et al. \[2018\]](#) for VB and [Gustafson \[1996a\]](#) for the exact posterior and MCMC approximations. To enable their application to DPM models, we solve a number of open problems: (1) we establish that the optimal VB parameters are a continuously differentiable function of α and a particular parametrization of the stick-breaking form; (2) we show that the sensitivity of the VB approximation to functional prior perturbations takes the form of an integral against a computationally tractable *influence function*—and illustrate how the influence function can provide an interpretable summary of the effect of arbitrary changes to the prior density; (3) to justify using linear approximations over a ball describing different stick-breaking densities, we show that our method is a *uniformly* good approximation by establishing Fréchet differentiability; (4) we show how to compute our approximation efficiently in high-dimensional problems; and (5) we establish the accuracy, practicality, and computational efficiency of our approximation for a variety of models that use stick-breaking, and for various quantities of interest in both clustering and topic modeling. Though our present focus is on DPM models, many of our results apply to VB approximations in general.

The remainder of the paper is organized as follows. In Section 2, we review the stick-breaking construction of the Dirichlet process and our chosen variational approximation. In Section 3, we derive the form of local prior robustness measures for VB approximations. We consider functional perturbations to the stick-breaking density in Section 4, and define the influence function from which we can construct influential and worst-case perturbations. We review related work in Section 5. In Section 6, we address scalability and other computational considerations for computing local sensitivity on real applications. In Section 7, we apply our tools to assess the sensitivity of BNP models in several data analysis problems.

2 The Model and Variational Approximation

2.1 A stick-breaking model for clustering

Consider a standard Bayesian nonparametric generative model for clustering, with observed data $x = (x_n)_{n=1}^N$. We assume a countable infinity of latent components, with frequencies $\pi = (\pi_1, \pi_2, \dots)$, such that $\pi_k \in [0, 1]$ for all $k \in \{1, 2, \dots\}$, and $\sum_k \pi_k = 1$. For the n th data point, the vector $z_n = (z_{n1}, z_{n2}, \dots)$ is an indicator vector; $z_{nk} = 1$ represents the assignment of the n th data point to the k th component, with all other vector elements set equal to zero. We generate $z_{nk} = 1$ with probability π_k , i.i.d. across n . To generate the x_n , we assume the k th component is characterized by a component-specific parameter, $\beta_k \in \Omega_\beta \subseteq \mathbb{R}^{D_\beta}$, and that a data point arising from component k is generated as $\mathcal{P}(x_n | \beta_k)$. Then $\mathcal{P}(x_n | z_n, \beta) = \prod_{k=1}^{\infty} \mathcal{P}(x_n | \beta_k)^{z_{nk}}$. The β_k in turn are generated i.i.d. from a prior $\mathcal{P}_{\text{base}}(\beta_k)$. For instance, in a Gaussian mixture model, β_k could be a vector representing the mean and covariance of a Gaussian distribution.

It remains to place a prior on the component frequencies π . We will focus on stick-breaking priors for π , so we first replace π with a stick-breaking representation. Let $\nu = (\nu_1, \nu_2, \dots)$ represent proportions: $\nu_k \in [0, 1]$. Take

$$\pi_k := \nu_k \prod_{k' < k} (1 - \nu_{k'}). \quad (1)$$

We then define a stick-breaking prior by placing a prior on the ν_k . Fix a density, $\mathcal{P}_{\text{stick}}(\cdot)$, with respect to the Lebesgue measure on $[0, 1]$ and let $\nu_k \stackrel{\text{iid}}{\sim} \mathcal{P}_{\text{stick}}(\nu_k)$ for $k \in \{1, 2, \dots\}$. A common choice of $\mathcal{P}_{\text{stick}}$ is Beta(1, α), with *concentration parameter* $\alpha > 0$. With this choice, the π are distributed according to the size-biased weights associated with the atoms of a draw from a Dirichlet process. This particular beta stick-breaking prior is often favored due to its convenient mathematical properties and ease of use in inference.

Posterior quantities of interest. In theory, with our generative model and observed data in hand, we can find the Bayesian posterior $\mathcal{P}(\beta, z, \nu | x)$ and report any posterior summaries of interest. For instance, the posterior $\mathcal{P}(\beta, z, \nu | x)$ induces a posterior distribution on the number of clusters $G_{\text{cl}}(z)$, where *clusters* are

components to which at least one data point has been assigned:

$$G_{\text{cl}}(z) := \sum_{k=1}^{\infty} \mathbb{I} \left(\left(\sum_{n=1}^N z_{nk} \right) > 0 \right),$$

where $\mathbb{I}(\cdot)$ is the indicator function taking value 1 when the argument is true and 0 otherwise.

In practice, though, neither the posterior nor the posterior summary is readily accessed. An approximation must be used instead.

2.2 Variational approximation

To assess the sensitivity of a procedure in practice, we need to consider the approximate Bayesian inference algorithm used as well. Here we focus on a variational Bayes approximation due to [Blei and Jordan \[2006\]](#).

Variational Bayes (VB) posits a class of tractable distributions over the model parameters and chooses the element of this class that minimizes the reverse Kullback-Leibler (KL) divergence to the exact posterior. One approach to apply VB to Dirichlet process stick-breaking models assumes $\nu_{K_{\max}} = 1$ for all distributions in the variational class and some truncation level K_{\max} . Let ζ collect the first $K_{\max} - 1$ elements of ν , the first K_{\max} elements of β , and the first K_{\max} elements of z_n across n . In what follows, then, we effectively consider the reverse KL divergence to the posterior marginal $\mathcal{P}(\zeta|x)$. By setting K_{\max} sufficiently large, one can make this truncation as accurate as desired.

Mean-field VB is a particularly popular VB variant where the tractable approximating distributions \mathcal{Q} factorize over the parameters. In our case, then, we consider approximations of the form

$$\mathcal{Q}(\zeta|\eta) = \left(\prod_{k=1}^{K_{\max}-1} \mathcal{Q}(\nu_k|\eta) \right) \left(\prod_{k=1}^{K_{\max}} \mathcal{Q}(\beta_k|\eta) \right) \left(\prod_{n=1}^N \mathcal{Q}(z_n|\eta) \right), \quad (2)$$

where $\eta \in \Omega_\eta \subseteq \mathbb{R}^{D_\eta}$ represents *variational parameters* that determine the factors of the \mathcal{Q} distribution. When the observation likelihood $\mathcal{P}(x_n|\beta_k)$ is conditionally conjugate with the component-parameter prior $\mathcal{P}_{\text{base}}(\beta_k)$, no further assumptions are needed on the form of $\mathcal{Q}(\beta_k|\eta)$; one can show that it will take the form of the conjugate exponential family after the KL optimization [\[Blei et al., 2017\]](#). Similarly, when $\mathcal{P}_{\text{stick}}$ is a beta distribution, no further assumptions are needed on $\mathcal{Q}(\nu_k|\eta)$; it will take a beta form. However, since we will consider non-beta forms of $\mathcal{P}_{\text{stick}}$, we must specify a more generic approximation—one that will work even when conditional conjugacy does not hold. To that end, we first transform the ν_k to a value that is unbounded and then use a Gaussian approximation. Define the logit-transformed stick-breaking proportions $\tilde{\nu}_k$:

$$\tilde{\nu}_k := \log(\nu_k) - \log(1 - \nu_k) \quad \Leftrightarrow \quad \nu_k = \frac{\exp(\tilde{\nu}_k)}{1 + \exp(\tilde{\nu}_k)}.$$

We take $\mathcal{Q}(\tilde{\nu}_k|\eta)$ to be a normal distribution, which induces a logit-normal distribution on ν_k . We approximate all resulting integrals over $\mathcal{Q}(\tilde{\nu}_k|\eta)$, as in the KL objective for VB or in our later sensitivity calculations, with Gauss–Hermite (GH) quadrature; see Appendix D.4.

GH quadrature yields an approximation, which we call $\text{KL}(\eta)$, to the full KL, $\text{KL}(\mathcal{Q}(\zeta|\eta)||\mathcal{P}(\zeta|x))$. We minimize that approximation to perform approximate posterior inference:

$$\text{KL}(\mathcal{Q}(\zeta|\eta)||\mathcal{P}(\zeta|x)) = \mathbb{E}_{\mathcal{Q}(\zeta|\eta)} [\log \mathcal{Q}(\zeta|\eta) - \log \mathcal{P}(x, \zeta)] + \log \mathcal{P}(x) \quad (3)$$

$$\hat{\eta} := \underset{\eta \in \Omega_\eta}{\operatorname{argmin}} \text{KL}(\eta) \quad \text{where} \quad \text{KL}(\eta) \approx \text{KL}(\mathcal{Q}(\zeta|\eta)||\mathcal{P}(\zeta|x)). \quad (4)$$

Our final approximation to the marginal posterior $\mathcal{P}(\zeta|x)$ is $\mathcal{Q}(\zeta|\hat{\eta})$.

Posterior quantities of interest. To approximate any functional of the exact posterior, we apply the equivalent functional to $\mathcal{Q}(\zeta|\hat{\eta})$. For instance, the approximation to the posterior expected number of clusters among the N observed data points is

$$\mathbb{E}_{\mathcal{Q}(\zeta|\hat{\eta})} [G_{\text{cl}}(z)] = \mathbb{E}_{\mathcal{Q}(z|\hat{\eta})} [G_{\text{cl}}(z)] = \sum_{k=1}^{K_{\text{max}}-1} \left(1 - \prod_{n=1}^N (1 - \mathbb{E}_{\mathcal{Q}(z_n|\hat{\eta}_z)} [z_{nk}]) \right). \quad (5)$$

We will see examples in Section 7 where our quantity of interest is (a) the expected posterior number of clusters in the observed data, (b) the expected posterior number of clusters in a new set of (as yet unobserved) data, (c) some aspect of a co-clustering matrix, or (d) the topic assignments of certain data points. In all of these cases, as in Eq. 5, we can express our (approximate) posterior quantity of interest as some function g of the optimized variational parameters $\hat{\eta}$: $g(\hat{\eta})$.

Once we have an (approximate) posterior quantity of interest, we can ask how this quantity would change—and whether our substantive scientific conclusions would change—if we had made reasonably different prior choices.

3 A Local Approximation for Sensitivity

We would like to understand how our quantity of interest $g(\hat{\eta})$ changes when the concentration parameter or, more generally, the stick-breaking density $\mathcal{P}_{\text{stick}}$ changes. To efficiently compute these changes, we use a first-order Taylor series approximation in the optimal VB parameters. In this section, we first present the Taylor series and then show how to compute its terms.

Sensitivity to the concentration parameter. First, we show how to approximate the sensitivity of $g(\hat{\eta})$ to the choice of concentration parameter α . Let $\hat{\eta}(\alpha)$ represent the value of $\hat{\eta}$ for a particular choice of α . For our approximation, we choose some initial value α_0 of the concentration parameter and solve the

optimization problem to compute $\hat{\eta}(\alpha_0)$. We then approximate $\hat{\eta}(\alpha)$ with the linear approximation $\hat{\eta}^{\text{lin}}(\alpha)$, and in turn approximate $g(\hat{\eta}(\alpha))$ with $g(\hat{\eta}^{\text{lin}}(\alpha))$:

$$\hat{\eta}^{\text{lin}}(\alpha) := \hat{\eta}(\alpha_0) + \frac{d\hat{\eta}(\alpha)}{d\alpha} \bigg|_{\alpha_0} (\alpha - \alpha_0) \quad \text{and} \quad g(\hat{\eta}(\alpha)) \approx g(\hat{\eta}^{\text{lin}}(\alpha)). \quad (6)$$

If $\alpha \mapsto \hat{\eta}(\alpha)$ is continuously differentiable, and g is sufficiently smooth, then we expect $g(\hat{\eta}(\alpha)) \approx g(\hat{\eta}^{\text{lin}}(\alpha))$ when $|\alpha - \alpha_0|$ is small. We will show in Theorem 1 below that the map $\alpha \mapsto \hat{\eta}(\alpha)$ is continuously differentiable for our chosen VB approximation.

Sensitivity to the stick-breaking density. Next, we show how to approximate the sensitivity of $g(\hat{\eta})$ to the choice of concentration stick distribution $\mathcal{P}_{\text{stick}}$. Technically, perturbations of α are perturbations of $\mathcal{P}_{\text{stick}}$. But here we consider more general perturbations of the form of $\mathcal{P}_{\text{stick}}$, potentially outside the beta class. To define our perturbations, let $\tilde{\mathcal{P}}$ represent a potentially unnormalized (but normalizable) density with respect to Lebesgue measure; the same notation without the tilde will give the normalized density. Now start from an initial setting of $\mathcal{P}_{\text{stick}}$ at \mathcal{P}_0 ; we will typically start from Dirichlet-process stick-breaking; i.e., $\mathcal{P}_0 = \text{Beta}(1, \alpha_0)$ for some α_0 . Then take any Lebesgue-measurable function $\phi(\cdot)$ on $[0, 1]$. We consider a range of alternative (potentially unnormalized) stick-breaking forms $\tilde{\mathcal{P}}(\cdot|t)$ defined on $[0, 1]$ by

$$\log \tilde{\mathcal{P}}(\cdot|t) = \log \mathcal{P}_0(\cdot) + t\phi(\cdot). \quad (7)$$

Note that the perturbation applies equally to every stick break ν_k . This style of multiplicative functional perturbation was proposed by [Gustafson \[1996a\]](#); we deviate from [Gustafson \[1996a\]](#) by considering VB (rather than MCMC) approximations and by allowing ϕ to take on negative values.

If we now let $\hat{\eta}(t)$ represent the value of $\hat{\eta}$ for a particular choice of $\tilde{\mathcal{P}}(\cdot|t)$, we can form an approximation analogous to Eq. 6:

$$\hat{\eta}^{\text{lin}}(t) := \hat{\eta}(0) + \frac{d\hat{\eta}(t)}{dt} \bigg|_{t=0} (t - 0) \quad \text{and} \quad g(\hat{\eta}(t)) \approx g(\hat{\eta}^{\text{lin}}(t)). \quad (8)$$

As in the case of expansions with respect to α , Eq. 8 is useful only if the map $t \mapsto \hat{\eta}(t)$ is continuously differentiable for the chosen ϕ . As we will show in Theorem 1 below, a sufficient condition for differentiability is given in terms of the following norm on the perturbation ϕ .

$$\text{Define } \|\phi\|_{\infty} := \underset{\nu_0 \sim \mathcal{P}_0}{\text{esssup}} |\phi(\nu_0)| \quad \text{and} \quad \mathcal{B}_{\phi}(\delta) := \{\phi : \|\phi\|_{\infty} < \delta\}. \quad (9)$$

The set of priors that arise by considering functional perturbations $\phi \in \mathcal{B}_{\phi}(\delta)$ live in a multiplicative band around the original prior, \mathcal{P}_0 , as shown in Figure 1. Theorem 1 below states that $t \mapsto \hat{\eta}(t)$ is continuously differentiable whenever $\|\phi\|_{\infty} < \infty$. So, for sufficiently smooth g , we expect the approximation Eq. 8 to be good for small t , given a particular choice of ϕ with $\|\phi\|_{\infty} < \infty$.

The functional perturbation given in Eq. 7 is useful because, if we consider any other distribution \mathcal{P}_1 for $\mathcal{P}_{\text{stick}}$, we can continuously warp \mathcal{P}_0 to \mathcal{P}_1 by setting $\phi(\cdot) = \log(\mathcal{P}_1(\cdot)/\mathcal{P}_0(\cdot))$ so long as $\mathcal{P}_1 \ll \mathcal{P}_0$; i.e., \mathcal{P}_1 is absolutely continuous with respect to \mathcal{P}_0 . We will see in Section 4 that we can compute an *influence function* to provide an interpretable summary of the effect of arbitrary changes ϕ . Using the influence function and the $\|\cdot\|_\infty$ norm, we are able to find a worst-case choice of ϕ in $\mathcal{B}_\phi(\delta)$.

However, we note that restricting to $\|\phi\|_\infty < \infty$ limits the kinds of alternative priors \mathcal{P}_1 that can be formed using Eq. 7. Although we show in Lemma 1 of Appendix A.3 that functional perturbations with $\|\phi\|_\infty < \infty$ yield valid priors, the converse is not true: there exist valid priors \mathcal{P}_1 such that the corresponding $\|\phi\|_\infty = \infty$. For instance, perturbing the beta stick-breaking form by changing α provides a counterexample since the log of the beta density is unbounded below; see Example 3 of Appendix A.3 for more details. The limited expressiveness of $\mathcal{B}_\phi(\delta)$ may at first seem like a shortcoming of the perturbation given by Eq. 7. However, we show in Section 4 that, among a class of potential functional perturbations such as those proposed by Gustafson [1996a], only the one we defined in Eq. 7 is *Fréchet differentiable*—and thus can be used to safely reason about worst-case ϕ .

Computing the terms in the Taylor series. It remains to show that $\alpha \mapsto \hat{\eta}(\alpha)$ and $t \mapsto \hat{\eta}(t)$ are continuously differentiable, and to provide a computable formula for the derivative. Differentiability naturally requires some regularity conditions on the VB parameterization and on the optimum. We state sufficient conditions in the following Assumption 1, which is satisfied for any local optimum of a smooth, unconstrained parameterization of the variational approximation.

Assumption 1. *Assume that: (1) the map $\eta \mapsto \text{KL}(\eta)$ is twice continuously differentiable at $\hat{\eta}$; (2) the Hessian matrix $\frac{\partial^2 \text{KL}(\eta)}{\partial \eta \partial \eta^T} \Big|_{\hat{\eta}}$ is non-singular; and (3) there exists an open ball $\mathcal{B}_\eta \subseteq \mathbb{R}^{D_\eta}$ such that $\hat{\eta} \in \mathcal{B}_\eta \subseteq \Omega_\eta$.*

Our next result establishes the differentiability of $\hat{\eta}$ and provides a computable formula for the derivative.

Theorem 1. *Let Assumption 1 hold for the VB approximation given in Section 2.2. Either take $\varepsilon = t$ under the perturbation given by $\log \tilde{\mathcal{P}}(\nu_k | t) = \log \mathcal{P}_0(\nu_k) + t\phi(\nu_k)$ with $\|\phi\|_\infty < \infty$, or take $\varepsilon = \alpha - \alpha_0$ in a perturbation to the concentration parameter α of the unnormalized beta distribution $\log \tilde{\mathcal{P}}(\nu_k | \alpha) = \alpha \log(1 - \nu_k)$. Then the map*

$\varepsilon \mapsto \hat{\eta}(\varepsilon)$ is continuously differentiable at $\varepsilon = 0$ with derivative

$$\frac{d\hat{\eta}(\varepsilon)}{d\varepsilon} \Big|_{\varepsilon=0} = -\hat{H}^{-1}\hat{J}, \quad \text{where } \rho_k(\nu_k) := \frac{\partial \log \tilde{\mathcal{P}}(\nu_k|\varepsilon)}{\partial \varepsilon} \Big|_{\varepsilon=0}, \quad (10)$$

$$\hat{H} := \frac{\partial^2 \text{KL}(\eta)}{\partial \eta \partial \eta^T} \Big|_{\eta=\hat{\eta}}, \quad \mathcal{S}(\zeta|\eta) := \frac{\partial \log \mathcal{Q}(\zeta|\eta)}{\partial \eta} \Big|_{\eta}, \quad \text{and} \quad (11)$$

$$\hat{J} := \frac{\partial}{\partial \eta} \mathbb{E}_{\mathcal{Q}(\zeta|\eta)} \left[\sum_{k=1}^{K_{\max}-1} \rho_k(\nu_k) \right] \Big|_{\eta=\hat{\eta}} = \mathbb{E}_{\mathcal{Q}(\zeta|\hat{\eta})} \left[\mathcal{S}(\zeta|\hat{\eta}) \sum_{k=1}^{K_{\max}-1} \rho_k(\nu_k) \right]. \quad (12)$$

Proof. The result follows from Theorem 4 of Appendix A.1, which states general conditions for the differentiability of VB optima. We show in Appendices A.2 and A.3 that the conditions of Theorem 4 are satisfied in the case of our present BNP problem. The equivalence of the expressions for \hat{J} follows by differentiating through the expectation; see Lemma 3 of Appendix B for more details. \square

Eq. 10 requires computation of two terms: \hat{H}^{-1} and \hat{J} . Typically, \hat{J} , which is a derivative of a variational expectation, is straightforward to evaluate: the requisite expectation is evaluated either in closed form or approximated numerically; then, in either case, an application of automatic differentiation provides the gradient [Baydin et al., 2018]. Forming and inverting or factorizing \hat{H} can present a challenge due to its high dimensionality—it has dimensions $D_\eta \times D_\eta$, where D_η is the dimension of η . However, in many cases—including the BNP problem that is our focus—we can take advantage of model sparsity to efficiently compute Eq. 10 (see Section 6), and our experiments confirm that we can compute $\frac{d\hat{\eta}(\varepsilon)}{d\varepsilon} \Big|_{\varepsilon=0}$ much more efficiently than re-optimizing the VB objective directly (Section 7.4). Moreover, the savings increases dramatically when we are interested in a range of ε values because $\frac{d\hat{\eta}(\varepsilon)}{d\varepsilon} \Big|_{\varepsilon=0}$ can be re-used to for any chosen value of ε .

4 The Influence Function and Worst-Case Functional Perturbations

We next show how to find influential and worst-case functional perturbations to the stick-breaking density. We start by showing how to compute an influence function to summarize the effect of different choices of ϕ . Using the influence function, we are able to design stick-breaking densities that produce a large change in a quantity of interest, including computing the worst-case perturbation in $\mathcal{B}_\phi(\delta)$. To justify such uses of the influence function, we prove that, for multiplicative perturbations and the ∞ -norm, the VB objective is Fréchet differentiable—i.e., that it admits a uniformly good linear approximation in a neighborhood of the null perturbation. Finally, we show that our Fréchet differentiability result is unique among a broad class of alternative choices of functional perturbation.

The influence function and worst-case perturbations. We begin by defining the influence function Ψ and discussing its usefulness for understanding the effect of functional perturbations ϕ . Suppose we have a one-dimensional, differentiable quantity of interest, $g(\cdot) : \Omega_\eta \mapsto \mathbb{R}$, and are considering various alternative priors as given by ϕ in Eq. 7. Under the approximation in Eq. 8, the dependence of $g(\hat{\eta}^{\text{lin}}(t))$ on ϕ is not simple if $g(\cdot)$ is non-linear. However, for a particular choice of ϕ , by applying the chain rule with Theorem 1, we can derive a fully linear approximation $g(\hat{\eta}(t)) \approx g(\hat{\eta}) + \frac{dg(\hat{\eta}(t))}{dt} \Big|_{t=0} (t - 0)$. The advantage of linearizing g in this way is that the map $\phi \mapsto \frac{dg(\hat{\eta}(t))}{dt} \Big|_{t=0}$ has a particularly simple form, as given by the following result.

Corollary 1. *Under the conditions of Theorem 1, using Eq. 7 with $\|\phi\|_\infty < \infty$ and $\varepsilon = t$, let $g(\cdot) : \Omega_\eta \mapsto \mathbb{R}$ denote a continuously differentiable, real-valued function of interest. Define the influence function $\Psi : [0, 1] \mapsto \mathbb{R}$:*

$$\Psi(\cdot) := - \sum_{k=1}^{K_{\max}-1} \frac{dg(\eta)}{d\eta^T} \Big|_{\hat{\eta}} \hat{H}^{-1} \mathcal{S}_k(\cdot | \hat{\eta}) \mathcal{Q}_k(\cdot | \hat{\eta}), \quad (13)$$

where $\mathcal{S}_k(\cdot | \hat{\eta})$ and $\mathcal{Q}_k(\cdot | \hat{\eta})$ replace $\mathcal{Q}(\zeta | \eta)$ with just the factor of \mathcal{Q} for ν_k . Then the derivative in Eq. 10 can be written as

$$\frac{dg(\hat{\eta}(t))}{dt} \Big|_0 = \int_0^1 \Psi(\nu_0) \phi(\nu_0) d\nu_0. \quad (14)$$

Proof. The form of the influence function is given applying the chain rule, gathering terms in Eq. 10, and re-writing the variational expectation as an integral over $[0, 1]$. We establish an analogous general result for general VB approximations in Corollary 3 of Appendix A.3, specializing to the BNP case in Example 4 of Appendix A.3. \square

By choosing perturbations ϕ that align with the influence function, we can form priors that we expect to be influential for the function of interest, $g(\cdot)$. For example, in our experiments of Section 7, we show that by choosing ϕ to be a Gaussian bump aligned with particularly high-magnitude positive or negative values of the influence function, one can ensure a large positive or negative gradient, and hence a large predicted change.

Further, with Corollary 1 in hand, we can find a closed-form expression for the worst-case choice of $\phi \in \mathcal{B}_\phi(\delta)$, which is essentially a VB analogue to Gustafson [1996a, Result 11].

Corollary 2. *Under the conditions of Corollary 1,*

$$\sup_{\phi \in \mathcal{B}_\phi(\delta)} \frac{dg(\hat{\eta}(t))}{dt} \Big|_0 = \delta \int |\Psi(\nu_0)| \mu(d\nu_0),$$

and the supremum is achieved at the perturbation $\phi^*(\cdot) = \delta \text{sign}(\Psi(\cdot))$.

Proof. The result follows immediately from applying Hölder’s inequality to Eq. 14. We establish a similar but much more general result for VB approximations with general choices of model and parameters in Corollary 4 of Appendix A.4. The present result is a special case using Example 4 of Appendix A.4. \square

In our experiments of Section 7, we use Corollaries 1 and 2 to choose influential perturbations, and then use the partially linearized Eq. 8 to make predictions about the effect of the perturbations.

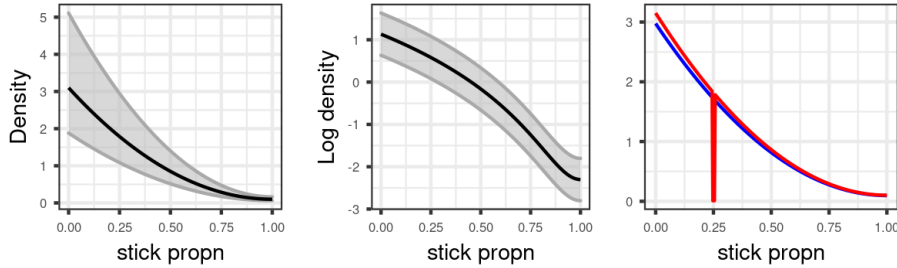


Figure 1: Left two: A multiplicative ball $\mathcal{B}_\phi(\delta)$. Right: Two densities that are distant according to reverse KL divergence and $\|\cdot\|_\infty$ but close according to $\|\cdot\|_p$ for $p \in [1, \infty)$.

Multiplicative perturbations are continuously Fréchet differentiable. The influence function provides a succinct summary of the effect of all perturbations $\phi \in \mathcal{B}_\phi(\delta)$, which we might hope to be accurate for sufficiently small δ . However, the accuracy of our approximation within $\mathcal{B}_\phi(\delta)$ is not guaranteed by Theorem 1 alone. Specifically, Theorem 1 states only that, for a *particular* direction ϕ , $t \mapsto \hat{\eta}(t)$ is continuously differentiable—i.e. that, for a fixed ϕ , one can make t sufficiently small so that the error $|\hat{\eta}(t) - \hat{\eta}^{\text{lin}}(t)|$ goes to zero faster than t . But, if we write $\hat{\eta}(t\phi)$ and $\hat{\eta}^{\text{lin}}(t\phi)$ to make the dependence on ϕ explicit, then Theorem 1 does not imply that for a fixed δ (no matter how small), the worst-case error $\sup_{\phi \in \mathcal{B}_\phi(\delta)} |\hat{\eta}(\phi) - \hat{\eta}^{\text{lin}}(\phi)|$ is bounded, much less that it goes to zero faster than δ .

Thus, to be assured that the influence function is a meaningful summary of the effect of all $\phi \in \mathcal{B}_\phi(\delta)$, we wish to establish that the linear approximation given by Eq. 8 is uniformly accurate over all ϕ of interest within a sufficiently small neighborhood of the zero function. Specifically, observing that ϕ is a point in the Banach space L_∞ [Dudley, 2018, Theorem 5.2.1], we wish to establish that the map $\phi \mapsto \hat{\eta}(\phi)$ from L_∞ to \mathbb{R}^{D_η} is *Fréchet differentiable*, as we now formally define.

Definition 1. (Fréchet differentiability, [Zeidler, 1986, Definition 4.5]) Let B_1 and B_2 denote Banach spaces, and let $\mathcal{B}_1 \subseteq B_1$ define an open neighborhood of $\phi_0 \in B_1$. A function $f : \mathcal{B}_1 \mapsto B_2$ is *Fréchet differentiable* at ϕ_0 if there exists a

bounded linear operator, $f^{\text{lin}} : B_1 \mapsto B_2$, such that, for $\phi \in B_1$,

$$f(\phi) - f(\phi_0) - f_{\phi_0}^{\text{lin}}(\phi - \phi_0) = o(\|\phi - \phi_0\|) \quad \text{as } \|\phi - \phi_0\| \rightarrow 0.$$

The function f is *continuously Fréchet differentiable* if the map $\phi_0 \mapsto f_{\phi_0}^{\text{lin}}(\cdot)$ is continuous as a map from B_1 to the space of all continuous linear operators from B_1 to B_2 equipped with the operator norm. \square

By [Zeidler \[1986, Proposition 4.8\]](#), if a function is Fréchet differentiable, then the linear operator f^{lin} is given precisely by the directional derivative $df(\phi_0 + t(\phi - \phi_0))/dt$. Thus, if $\phi \mapsto \hat{\eta}(\phi)$ is Fréchet differentiable, its derivative is given by [Corollary 1](#). Fréchet differentiability guarantees that, for sufficiently small δ , the error of the linear approximation given by [Corollary 1](#) does not blow up in the ball $\mathcal{B}_\phi(\delta)$.

We emphasize that Fréchet differentiability is neither sufficient nor necessary for a derivative to be useful. For example, it is possible in principle for a function to be Fréchet differentiable but still have a very large finite second derivative, and so fail to extrapolate meaningfully to any alternatives one cares about. Conversely, if a function fails to be Fréchet differentiable, the derivative may still perform well in particular directions, including that chosen by [Corollary 2](#). Nevertheless, Fréchet differentiability is a strong local result, and provides some assurance that one can use results such as [Corollary 2](#) without uncovering pathological behavior.

Finally, then, we prove that our perturbation is continuously Fréchet differentiable.

Theorem 2. *Under the conditions of [Theorem 1](#), the map $\phi \mapsto \hat{\eta}(\phi)$ is well-defined and continuously Fréchet differentiable in a neighborhood of the zero function as a map from L_∞ to \mathbb{R}^{D_η} , with the derivative given in [Corollary 1](#).*

Proof. Our result here is a special case of our general result for VB approximations given in [Theorem 5](#) of [Appendix A.4](#). \square

Many other functional perturbations and norms are not Fréchet differentiable. So far we have focused on the multiplicative functional perturbations in [Eq. 7](#) combined with the infinity norm in [Eq. 9](#). We now ask whether we could perform a similar analysis for other functional perturbations. We show that, of the perturbations proposed by [Gustafson \[1996a\]](#), only multiplicative perturbations yield Fréchet differentiable VB optima.

Specifically, [Gustafson \[1996a\]](#) examines general perturbations, from initial prior \mathcal{P}_0 to alternative \mathcal{P}_1 , that take the following form—with θ a parameter $\theta \in \Omega_\theta \subseteq \mathbb{R}^{D_\theta}$ and $p \in [1, \infty)$:

$$\tilde{\mathcal{P}}(\theta|t_p) := \left((1 - t_p)\mathcal{P}_0(\theta)^{1/p} + t_p \frac{1}{p} \mathcal{P}_1(\theta)^{1/p} \right)^p. \quad (15)$$

Again, let ϕ represent the perturbation, now with:

$$\phi(\theta|\mathcal{P}_1, p) := \mathcal{P}_1(\theta)^{1/p} - \mathcal{P}_0(\theta)^{1/p} \quad \text{and} \quad \|\phi\|_p := \left(\int_0^1 |\phi(\theta)|^p d\theta \right)^{1/p}. \quad (16)$$

The limit $p \rightarrow \infty$ recovers our multiplicative perturbation in Eq. 7 with infinity norm in Eq. 9. The choice $p = 1$ recovers a purely additive perturbation. [Gustafson \[1996a, Result 2\]](#) states that $\|\phi\|_p < \infty$ ensures that the corresponding $\tilde{\mathcal{P}}(\theta|t_p)$ can be normalized, strongly motivating using the $\|\cdot\|_p$ norm with the perturbation given by Eq. 15.

Our next theorem shows that the reverse KL divergence is discontinuous in $\|\cdot\|_p$ for $p < \infty$. Since Fréchet differentiability implies continuity [[Zeidler, 1986, Proposition 4.8 \(d\)](#)], Theorem 3 implies that it is impossible to derive an analogue of Theorem 2 for perturbations of the form in Eq. 15 with the norms in Eq. 16.

Theorem 3. *Let μ denote a measure on the Borel sets of some domain Ω_θ , with μ absolutely continuous with respect to the Lebesgue measure, and let $\mathcal{Q}(\theta)$ and $\mathcal{P}_0(\theta)$ denote densities with respect to μ . Without loss of generality, assume that $\mathcal{Q}(\theta) > 0$ on Ω_θ . Assume that $\text{KL}(\mathcal{Q}(\theta)||\mathcal{P}_0(\theta))$ is well-defined and finite.*

Then, for any $\epsilon > 0$ and any $M > 0$, we can find a density $\mathcal{P}_1(\theta)$ such that $\|\phi(\theta|\mathcal{P}_1, p)\|_p < \epsilon$ but $|\text{KL}(\mathcal{Q}(\theta)||\mathcal{P}_1(\theta)) - \text{KL}(\mathcal{Q}(\theta)||\mathcal{P}_0(\theta))| > M$.

Proof. See Appendix A.5 for a constructive proof, the key to which is the fact that in any $\|\cdot\|_p$ neighborhood of zero there exist prior densities taking values arbitrarily close to zero on sets of nonzero measure, for which the reverse KL divergence blows up. \square

Recall from Section 3 (and particularly Example 3 of Appendix A.3) that there exist priors that cannot be formed from Eq. 7 using ϕ with $\|\phi\|_\infty < \infty$. In light of the proof of Theorem 3, the limited expressiveness of multiplicative perturbations with the $\|\cdot\|_\infty$ norm looks like a feature rather than a bug. Consider the rightmost panel of Figure 1, which illustrates the tradeoffs between the various norms. The two blue and red densities are far from one another according to reverse KL divergence since the red density takes values that are nearly zero where the blue density has nonzero mass. The two densities are also distant in $\|\cdot\|_\infty$ since it takes a large multiplicative change to turn the nonzero blue density into the nearly zero red density. However, the two densities are close in $\|\cdot\|_p$ since the region where the red density is nearly zero has a small measure. In order for VB approximations to be continuous (a necessary condition for Fréchet differentiability), one must consider a topology on priors that is no coarser than the topology induced by reverse KL divergence. But since valid priors can take values close to zero, a sacrifice in expressiveness of the neighborhood of zero must be made in order to induce a topology that is compatible with reverse KL divergence. Multiplicative changes and the $\|\cdot\|_\infty$ norm implement such a tradeoff in a natural, easy-to-understand way.

In this sense, VB approximations based on reverse KL divergence are inherently non-robust to priors that ablate mass nearly to zero. No parameterization of the space of priors will relieve this non-robustness. Only by basing variational approximations on divergences other than reverse KL might this non-robustness be alleviated.

5 Related Work

Evaluating sensitivity to prior choices is typically a necessary step in applied Bayesian data analysis [Gelman et al., 2013, Chapter 6], and a central aim of Bayesian robustness is to provide methods and metrics to measure sensitivity of posterior quantities to variations in the model [Insua and Ruggeri, 2000]. One family of approaches to robustness quantification, “local robustness,” forms differential approximations to model sensitivity, in light of the fact that more desirable “global sensitivity” measures are computationally expensive or infeasible in all but special cases [Sivaganesan, 2000, Gustafson, 2000]. Two recent papers employing non-local approaches to BNP robustness are Nieto-Barajas and Prünster [2009] and Saha and Kurtek [2019], both of which run new MCMC chains at a set of alternative priors. The present work is essentially a VB extension and application of local Bayesian robustness literature which was based on MCMC samples from the full posterior [Gustafson, 1996a,b]. In contrast to MCMC, for which the derivatives of local robustness must be approximated with (potentially noisy) sample covariances, VB optima admit closed-form derivatives. In addition to extending local robustness methods to VB, we contrast with previous applications of local robustness by evaluating the ability of our linear approximation to *extrapolate* to alternative priors, rather than considering the derivative to be measure of robustness *per se* (as in, for example, Basu [2000]).

Since VB is an optimization procedure, the evaluation of the sensitivity of VB estimates inherits a long tradition of robustness methods in frequentist statistics (e.g. [Jaechel, 1972, Cook, 1986, Hampel et al., 2011]). In particular, our theoretical results extend the results of Giordano et al. [2018], providing more easily verifiable sufficient conditions for Giordano et al. [2018, Theorem 2] and proving results for non-parametric perturbations, including continuous Fréchet differentiability (and non-differentiability).

One of our quantities of interest is the posterior expected number of clusters, a quantity which we find non-robust to prior specification in certain cases (see Sections 7.1 and 7.3 and Appendix E.4). The non-robustness of the posterior expected number of clusters can be seen as a companion result to recent literature showing that BNP models provide inconsistent estimates of the number of clusters when the true data generating process is a finite mixture model (Miller and Harrison [2013, 2014]; Cai et al. [2020, 2021] prove similar results for finite mixture models). As Miller and Harrison [2014] observe empirically, inconsistency can be attributed to a small number of low-probability clusters in the BNP posterior. Similarly, we find that the small, rare clusters account for the non-robustness of the posterior expected number of clusters. Whereas inconsistency says that the posterior number of clusters may be unreliable even as the number of data points tend towards infinity, we show here that with a fixed data set, the number of clusters may be unreliable due to the subjective nature of the prior specification.

6 Fast Computation of the Sensitivity

A principal challenge of computing the sensitivity efficiently is the high-dimensional nature of the parameter ζ and hence the variational parameters η . In particular, we have seen that, in our BNP stick-breaking model, ζ and η both grow linearly with the number of data points N . This growth leads to two major computational challenges: (1) we must solve a high-dimensional optimization problem to extremize the VB objective, and (2) we must solve a linear system given by the Hessian \hat{H} . Here we show how we can use special structure in the model to reduce to low-dimensional problems and thereby enjoy efficient computation.

Global and local parameters. In both cases, the key to reducing to a lower-dimensional problem is separating *global* and *local* parameters. Global variables are common to all data points. Local variables are unique to each data point. For instance, in a Gaussian (or other typical) mixture model, the stick-breaking proportions ν and component parameters β are global, whereas the cluster assignment parameters z are local.

Let γ denote the collection of global parameters. When we use a standard mean-field VB parameterization, the VB distributions on γ have their own variational parameters, which we denote η_γ . Similarly, let ℓ denote the local parameters and let η_ℓ be the corresponding local variational parameters.

Reducing to optimization over the global variational parameters. We next show how to reduce the potentially high-dimensional optimization problem over all of η to optimizing over just the global variational parameters η_γ .

In all models we will consider, the conditional posterior $\mathcal{P}(z|\gamma, x)$ has a tractable closed form. Since we choose a conjugate mean-field approximating family for $\mathcal{Q}(z|\eta)$, the optimal local variational parameters $\hat{\eta}_\ell$ can be written as a closed-form function of the global variational parameters η_γ . For some prior parameter ε (as in Theorem 1), let $\hat{\eta}_\ell(\eta_\gamma; \varepsilon)$ denote this mapping, so that

$$\hat{\eta}_\ell(\eta_\gamma; \varepsilon) := \underset{\eta_\ell}{\operatorname{argmin}} \text{KL}((\eta_\gamma, \eta_\ell), \varepsilon). \quad (17)$$

In Example 6 (Appendix D.1), we illustrate this technique for a Gaussian mixture model. Using Eq. 17, we can rewrite our objective as a function of the global parameters. Define

$$\text{KL}_{\text{glob}}(\eta_\gamma, \varepsilon) := \text{KL}((\eta_\gamma, \hat{\eta}_\ell(\eta_\gamma; \varepsilon)), \varepsilon).$$

The $\hat{\eta}_\gamma(\varepsilon)$ that minimizes $\text{KL}_{\text{glob}}(\eta_\gamma, \varepsilon)$ is the same as the corresponding sub-vector of the $\hat{\eta}(\varepsilon)$ that minimizes $\text{KL}(\eta, \varepsilon)$.

Rather than optimizing the $\text{KL}(\eta)$ over all variational parameters, we numerically optimize KL_{glob} , which is a function only of the relatively low-dimensional global parameters. To minimize $\text{KL}_{\text{glob}}(\eta_\gamma)$ in practice, we run the BFGS algorithm with a loose convergence tolerance followed by the trust-region Newton conjugate gradient method to find a high-quality optimum (the `trust-ncg` method of `scipy.optimize.minimize`, Virtanen et al. [2020]; see also Nocedal and Wright

[2006, Chapter 7]). After the optimization terminates at an optimal $\hat{\eta}_\gamma$, the optimal local parameters $\hat{\eta}_\ell$ can be set in closed form to produce the entire vector of optimal variational parameters, $\hat{\eta} = (\hat{\eta}_\gamma, \hat{\eta}_\ell)$.

6.1 Computing and inverting the Hessian

Since the dimension D_η of η scales with N , we can quickly reach cases where inverting or even instantiating a dense matrix of size $D_\eta \times D_\eta$ in memory would be prohibitive. The key to efficient computation is that \hat{H} is not dense; we will again exploit structure inherent in the global/local decomposition.

For generic variables a and b , let H_{ab} denote the sub-matrix $\partial^2 \text{KL}(\eta) / \partial \eta_a \eta_b^T|_{\hat{\eta}}$, the Hessian with respect to the variational parameters governing a and b . We decompose the Hessian matrix \hat{H} into four blocks according to the global/local decomposition:

$$\hat{H} = \frac{\partial^2 \text{KL}(\eta)}{\partial \eta \partial \eta^T} \Big|_{\hat{\eta}} = \begin{pmatrix} H_{\gamma\gamma} & H_{\gamma\ell} \\ H_{\ell\gamma} & H_{\ell\ell} \end{pmatrix}.$$

Similarly, let \hat{J}_γ be the components of \hat{J} corresponding to the variational parameters η_γ . The local components, \hat{J}_ℓ , are zero since no local variables enter the expectation in Eq. 12 when we are perturbing the stick-breaking distribution.

In this notation,

$$\frac{d\hat{\eta}(t)}{dt} \Big|_{t=0} = - \begin{pmatrix} H_{\gamma\gamma} & H_{\gamma\ell} \\ H_{\ell\gamma} & H_{\ell\ell} \end{pmatrix}^{-1} \begin{pmatrix} \hat{J}_\gamma \\ 0 \end{pmatrix}. \quad (18)$$

Applying the Schur complement and focusing on the global parameters (see Appendix D.2 for more details), we find

$$\frac{d\hat{\eta}_\gamma(t)}{dt} \Big|_{t=0} = -\hat{H}_\gamma^{-1} \hat{J}_\gamma \quad \text{where} \quad \hat{H}_\gamma := (H_{\gamma\gamma} - H_{\gamma\ell} H_{\ell\ell}^{-1} H_{\ell\gamma}), \quad (19)$$

In our model, $H_{\ell\ell}$ is block diagonal, and the size of $H_{\gamma\gamma}$ is relatively small. Thus each term of Eq. 19 can be tractably computed, even on very large datasets. While the Schur complement calculation is illustrative, Eq. 19 is equivalent to applying automatic differentiation to the global-only objective $\text{KL}_{\text{glob}}(\eta_\gamma, t)$; see Appendix D.2 for details.

In our BNP applications, it is not cost-effective to form and invert or factorize \hat{H} in memory. Instead, we numerically solve linear systems of the form $\hat{H}^{-1}v$ using the conjugate gradient (CG) algorithm [Nocedal and Wright, 2006, Chapter 5], which requires only Hessian-vector products that are readily available through automatic differentiation.

A linear approximation only in the global variational parameters. With the tools above, we can separate out the linear approximation in the global

parameters and then directly compute the local parameters. In particular, we compute

$$\hat{\eta}_\gamma^{\text{lin}}(t) := \hat{\eta}_\gamma + \frac{d\hat{\eta}_\gamma(t)}{dt} \Big|_{t=0} t, \quad (20)$$

and then use $\hat{\eta}_\ell(\eta_\gamma)$ e.g. in computing our quantity of interest. By doing so, our approximation is able to retain non-linearities in the map $\eta_\gamma \mapsto \hat{\eta}_\ell(\eta_\gamma)$. We give an example for the expected number of clusters in Appendix D.3. In all our experiments, we use Eq. 20 in this way.

7 Experimental Results

We next evaluate our sensitivity approximations on three real data sets, each with a different model using stick-breaking. We find that our approximations largely agree with ground truth obtained by re-running the VB optimization, but with the evaluation of our derivative an order of magnitude faster than re-optimizing for a given perturbation.

7.1 Gaussian mixture modeling on iris data

We perform a clustering analysis of Fisher’s iris data set [Anderson, 1936]. Here each data point (with $N = 150$ total points) represents $d = 4$ measurements of a particular flower, from one of three iris species. We use a standard Gaussian mixture model with a conjugate Gaussian-Wishart prior for the component parameters (detailed in Appendix E.2) and a mean-field VB approximation with truncation parameter $K_{\max} = 15$. We consider two quantities of interest: (1) g_{cl} , the posterior expected number of clusters among the N observed data points, and (2) $g_{\text{pred,cl}}$, the posterior predictive expected number of clusters in N new (i.e. as-yet-unseen) data points. We set the base stick-breaking prior $\mathcal{P}_0(\nu_k)$ to be the standard Beta($\nu_k|1, \alpha$) distribution with $\alpha = \alpha_0 = 2$. Under the base stick-breaking prior with α_0 , the posterior expected number of clusters matches the three iris species; see also Figure 13 in Appendix E.2 for an illustration.

Sensitivity to the concentration parameter. We approximate the changes in the quantities of interest as α varies over $\alpha \in [0.1, 4.0]$, which corresponds to an *a priori* expected number of clusters among N data points in $[1.5, 15]$ (Appendix E.1). Over this range, the shape of a Beta($1, \alpha$) density varies considerably, as shown in Figure 12 in Appendix E.1.

Figure 2 compares our linear approximation to ground truth on the two quantities of interest as α varies. Over this range of α , the posterior expected number of clusters in the observed data is quite robust; it remains nearly constant at three. The posterior predictive expected number of clusters in N new data points is less robust; it ranges roughly from 3.0 to 5.6 expected species. Our approximation captures this qualitative behavior. As expected, the approximation is least accurate furthest from the α_0 , where the Taylor series is centered.

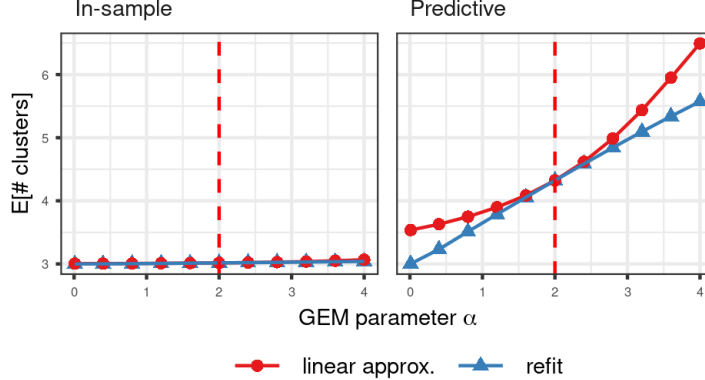


Figure 2: The expected number of clusters in the original data set (g_{cl} , left) and in a new data set of size N ($g_{\text{pred,cl}}$, right) as α varies in the GMM fit of the iris data. We formed the linear approximation at $\alpha_0 = 2$.

Sensitivity to functional perturbations. Insensitivity of the expected number of clusters g_{cl} to α does not rule out sensitivity to other prior perturbations. We now check how our approximation fares for the multiplicative perturbations in Eq. 7. We consider perturbations ϕ that are Gaussian bumps in logit stick space, with each perturbation centered at a different location on the real line. Each row of Figure 3 corresponds to a different ϕ . Each ϕ is shown in gray in the leftmost plot of its row. The middle column of Figure 3 shows the stick-breaking prior $\mathcal{P}(\nu_k|\phi)$ induced by the corresponding ϕ . The rightmost column of Figure 3 shows the changes produced by the ϕ perturbation for that row. We see that our approximation captures the qualitative behavior of the exact changes.

We also see in this example that we can use the influence function to predict the effect of functional changes to the stick-breaking prior. In the leftmost column, we plot in purple the influence function in the logit space.¹ According to Corollary 1, the sign and magnitude of the effect of a perturbation should be determined by its integral against the influence function. Thus, when ϕ lines up with a negative part of Ψ , as in the first row, we expect the change to be negative. Similarly, we expect the perturbation of the bottom row to produce a positive change, and the middle row, in which ϕ overlaps with both negative and positive parts of the influence function, to produce a relatively small change. We see this intuition borne out in the rightmost column.

Worst-case functional perturbation. Finally, Figure 4 shows the worst-case multiplicative perturbation with $\|\phi\|_\infty = 1$, as given by Corollary 2, along with its effect on the prior and g_{cl} . As expected, this worst-case perturbation has a much

¹Corollary 1 expresses the influence function in the stick domain $[0, 1]$, but, for visualization, it is preferable to express the influence function in the logit stick domain \mathbb{R} . The more general Corollary 3 in Appendix A.3 accommodates such transformations.

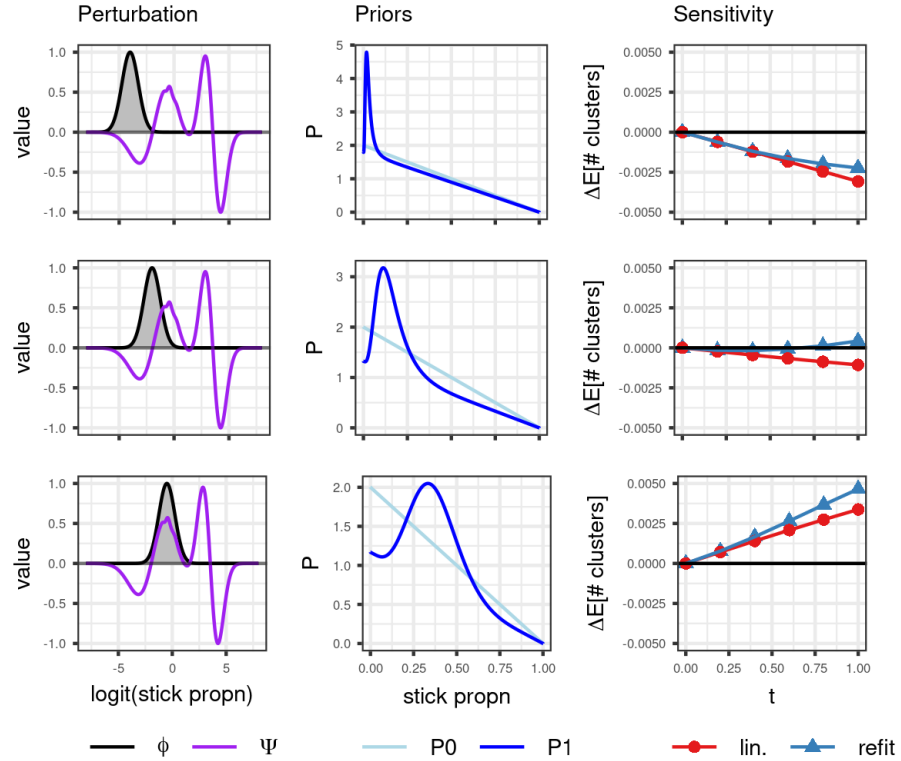


Figure 3: Sensitivity of the expected number of in-sample clusters in the iris data set to three multiplicative perturbations each with $\|\phi\|_\infty = 1$. (Left) The multiplicative perturbation ϕ is in grey. The influence function Ψ , scaled so $\|\Psi\|_\infty = 1$, is in purple. (Middle) The initial $\mathcal{P}_0(\nu_k)$ (light blue) and alternative $\mathcal{P}_1(\nu_k)$ (dark blue) priors. (Right) The effect of the perturbation on the change in expected number of clusters for $t \in [0, 1]$.

larger effect on g_{cl} compared to the other unit-norm perturbations in Figure 3. However, even with the worst-case perturbation—which results in an unreasonably shaped prior density—the change in g_{cl} is still small. We conclude that g_{cl} appears to be a robust quantity for this model and dataset.

7.2 Regression mixture modeling

We next check our approximation on a more complex clustering task: clustering time series, with a co-clustering matrix (and summaries thereof) as the quantity of interest.

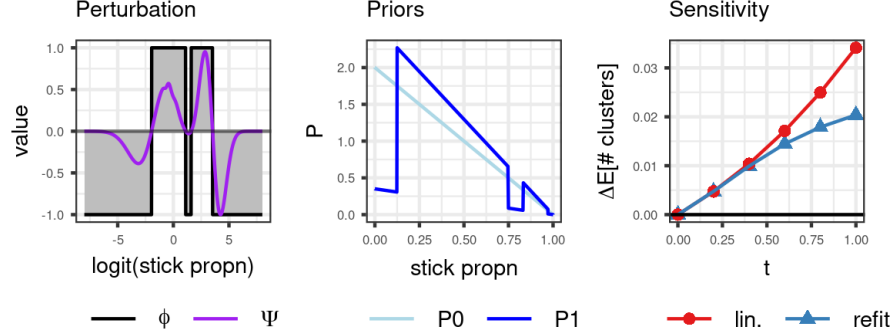


Figure 4: Sensitivity of the expected number of in-sample clusters in the iris data set to the worst-case multiplicative perturbation with $\|\phi\|_\infty = 1$.

Data and model. We use a publicly available data set of mice gene expression [Shoemaker et al., 2015]. Mice were infected with influenza virus, and expression levels of a set of genes were assessed at 14 time points after infection. Three measurements were taken at each time point (called biological replicates), for a total of $M = 42$ measurements per gene.

The goal of the analysis is to cluster the time-course gene expression data under the assumption that genes with similar time-course behavior may have similar function. Clustering gene expressions is often used for exploratory analysis and is a first step before further downstream investigation. It is important, therefore, to ascertain the stability of the discovered clusters.

The left plot of Figure 14 in Appendix E.3 shows the measurements of a single gene over time. We model each gene as belonging to a latent component, where each component defines a smooth expression curve over time. Then, observations are drawn by adding i.i.d. noise to the smoothed curve along with a gene-specific offset. Following Luan and Li [2003], we construct the smoothers using cubic B-splines.

Let $x_n \in \mathbb{R}^M$ be measurements of gene n at M time points. Let A be the $M \times d$ B-spline regressor matrix, so that the ij -th entry of A is the j -th B-spline basis vector evaluated at the i -th time point. The right plot of Figure 14 in Appendix E.3 shows the B-spline basis. The distribution of the data arising from component k is

$$\mathcal{P}(x_n | \beta_k, b_n) = \mathcal{N}(x_n | A\mu_k + b_n, \tau_k^{-1} I_{M \times M}), \quad (21)$$

where b_n is a gene-specific additive offset and I is the identity matrix. We include the additive offset because we are interested in clustering gene expressions based on their patterns over time, not their absolute level. In this model, the component-specific parameters are $\beta_k = (\mu_k, \tau_k)$, the regression coefficients and the inverse noise variance. The component frequencies are determined by stick-breaking

according to ν , and cluster assignments z are drawn as in Section 2.1.

Our variational approximation factorizes similarly to Eq. 2 except with an additional factor for the additive shift. In our variational approximation, we also make a simplification by letting $\mathcal{Q}(\beta_k|\eta) = \delta(\beta_k|\eta)$, where $\delta(\cdot|\eta)$ denotes a point mass at a parameterized location. See Appendix E.3 for further details concerning the model and variational approximation.

Quantity of interest: the co-clustering matrix and summaries. In this application, we are particularly interested in which genes cluster together, so we focus on the posterior co-clustering matrix. Let $g_{cc}(\eta) \in \mathbb{R}^{N \times N}$ denote the matrix whose (i, j) -th entry is the posterior probability that gene i belongs to the same cluster as gene j , given by

$$[g_{cc}(\eta)]_{ij} = \mathbb{E}_{\mathcal{Q}(z|\eta)} [\mathbb{I}(z_i = z_j)] = \begin{cases} \sum_{k=1}^{K_{\max}} \left(\mathbb{E}_{\mathcal{Q}(z_i|\eta)} [z_{ik}] \mathbb{E}_{\mathcal{Q}(z_j|\eta)} [z_{jk}] \right) & \text{for } i \neq j \\ 1 & \text{for } i = j. \end{cases}$$

Figure 5 shows the inferred co-clustering matrix at α_0 .

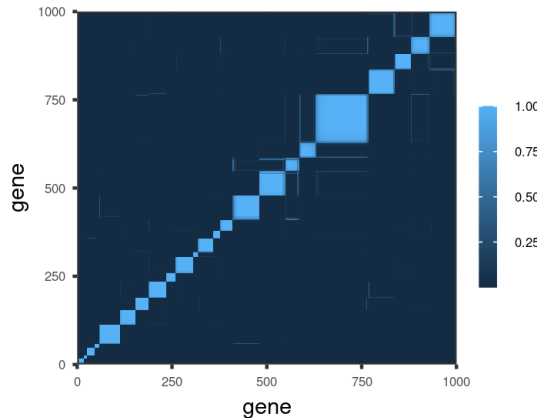


Figure 5: The inferred co-clustering matrix of gene expressions at $\alpha_0 = 6$.

Below, we will use the influence function (Corollary 2) to try and find a perturbation that produces large changes in the co-clustering matrix. To compute the worst-case perturbation, we must choose a univariate summary of the N^2 -dimensional co-clustering matrix whose derivative we wish to extremize. We use the sum of the eigenvalues of the symmetrically normalized graph Laplacian, as given by

$$g_{ev}(\eta) = \text{Tr} \left(I - D(\eta)^{-1/2} g_{cc}(\eta) D(\eta)^{-1/2} \right),$$

where $D(\eta)^{-1/2}$ is the diagonal matrix with entries $d_i = \sum_{j=1}^N [g_{cc}(\eta)]_{ij}$. The quantity g_{ev} is differentiable, and has close connection with the number of distinct

components in a graph [von Luxburg, 2007]. We expect that prior perturbations that produce large changes in g_{ev} will also produce large changes in the full co-clustering matrix.

Sensitivity to the concentration parameter. We first evaluate the sensitivity of the co-clustering matrix g_{cc} to the choice of α in the stick-breaking prior.

We start at $\alpha = \alpha_0 = 6$. We use the linear approximation to extrapolate the co-clustering matrix under prior parameters $\alpha = 0.1$ and $\alpha = 12$. The *a priori* expected number of clusters in the original data at these values is 2 and 50, respectively. Despite this wide prior range, the change in the posterior co-clustering matrix for each α is minuscule (Figure 6). The largest absolute changes in the co-clustering matrix is of order 10^{-2} . Refitting the approximate posterior at $\alpha = 0.1$ and $\alpha = 12$ confirms the insensitivity predicted by the linearized variational global parameters. Beyond capturing insensitivity, the linearized parameters were also able to capture the sign and size of the changes in the individual entries of the co-clustering matrix, even though these changes are small.

Sensitivity to functional perturbations. We now investigate sensitivity of the co-clustering matrix to deviations from the beta prior. In Figure 7, we use the influence function for g_{ev} to construct a nonparametric prior perturbation that we expect to have a large, positive effect. The resulting prior does indeed produce changes an order of magnitude larger than those produced by the perturbations to α shown in Figure 6, and our approximation is again able to capture the qualitative changes. The influence function is also able to explain why α perturbations were unable to produce large changes in this case: Figure 8 shows that changing α (as in Example 3) induces large changes in the prior only where the influence function is small.

However, even with the (unreasonable-looking) selected functional perturbation, the size of the differences in the co-clustering matrix remains modest. It is unlikely that any scientific conclusions derived from the co-clustering matrix would have changed after the functional perturbation. The co-clustering matrix appears robust to perturbations in the stick-breaking distribution.

7.3 Genetic admixture modeling with fastSTRUCTURE

Our final analysis illustrates the use of our approximation for stick-breaking priors beyond clustering; namely, in topic modeling.

Data and model. We use a publicly available dataset that contains genotypes from $N = 155$ individuals of an endangered bird species, the Taita thrush [Galbusera et al., 2000]. Individuals were collected from four regions in southeast Kenya (Chawia, Mbololo, Ngangao, Yale), and each individual was genotyped at $L = 7$ micro-satellite loci. The four regions were once part of a cohesive cloud forest that has been fragmented by human development. For this endangered bird species, understanding the degree to which populations have grown genetically distinct is important for conservation efforts: well-separated populations with little genetic diversity are particularly at risk of extinction. The goal of the analysis is

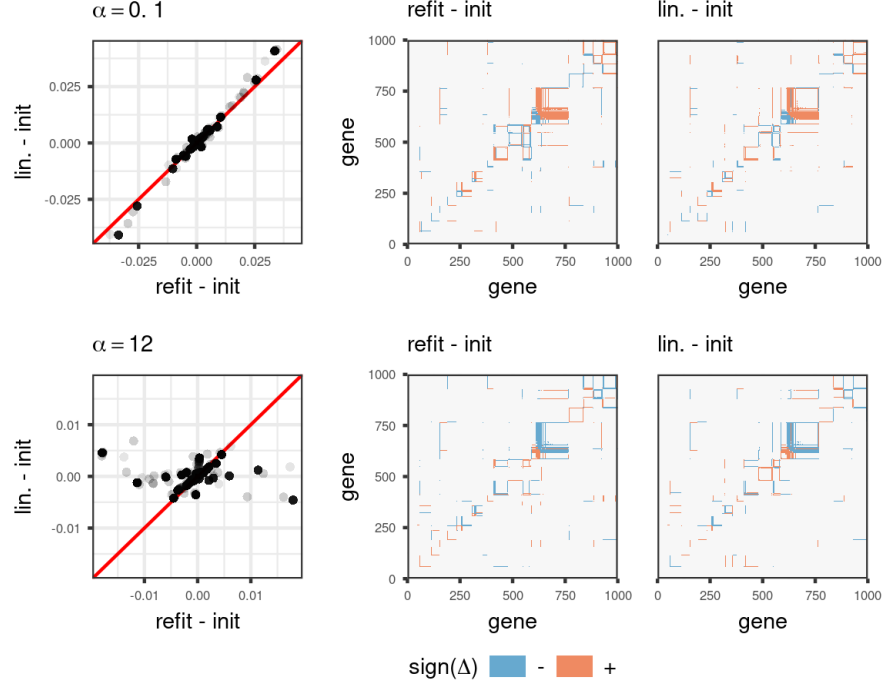


Figure 6: Differences in the co-clustering matrix at $\alpha = 0.1$ (top row) and $\alpha = 12$ (bottom row), relative to the co-clustering matrix at $\alpha_0 = 6$. (Left) A scatter plot of differences under the linear approximation against differences after refitting. Each point represents an entry of the co-clustering matrix. Note the scales of the axes: the largest change in an entry of the co-clustering matrix is ≈ 0.03 . (Middle) Sign changes in the co-clustering matrix observed after refitting, ignoring the magnitude of the change. (Right) Sign changes under the linearly approximated variational parameters. For visualization, changes with absolute value $< 10^{-5}$ are not colored.

to infer the population of origin for specific loci and estimate the degree to which populations are admixed in each individual.

Let $x_{nli} \in \{1, \dots, J_l\}$ be the observed genotype for individual n at locus l and chromosome i . J_l is the number of possible genotypes at locus l . For example, if the measurements are all single nucleotides (A, T, C or G) then $J_l = 4$ for all l .

A latent population is characterized by the collection $\beta_k = (\beta_{k1}, \dots, \beta_{kL})$, where $\beta_{kl} \in \Delta^{J_l-1}$ are the latent frequencies for the J_l possible genotypes at locus l . Let z_{nli} be the assignment of observation x_{nli} to a latent population. Notice that for a given individual n , different loci (or even different chromosomes at a given locus) may have different population assignments. The distribution of

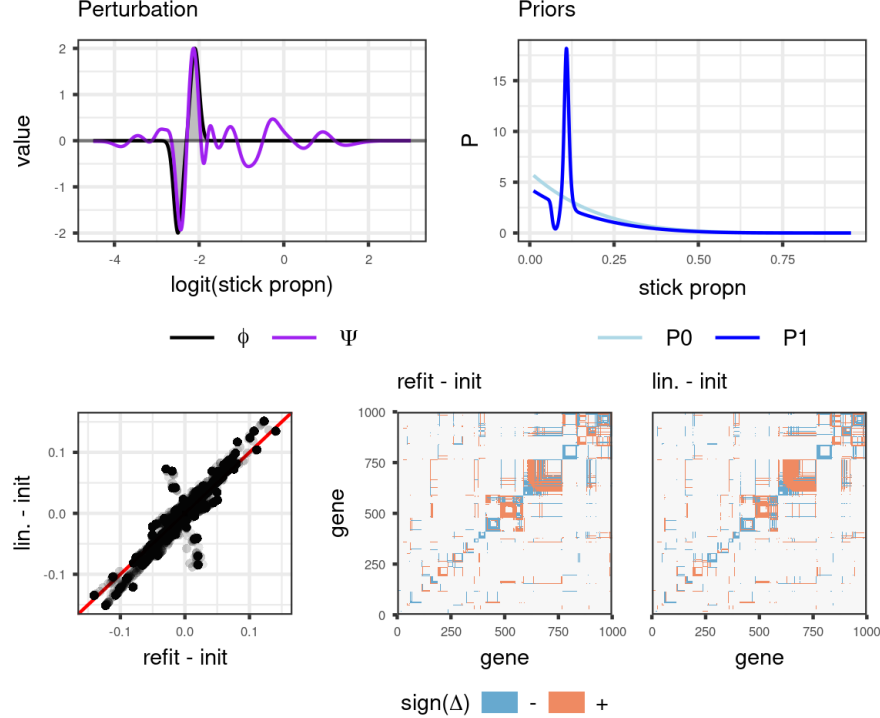


Figure 7: Effect on the co-clustering matrix of a multiplicative functional perturbation. (Top left) The perturbation ϕ is in grey, and the influence function is in purple. (Top right) The effect of this perturbation on the prior density. (Bottom) The effect of this perturbation on the co-clustering matrix. Note the scale of the scatter plot axes compared with the scatter plots in Figure 6.

$x_{nli} \in \{1, \dots, J_l\}$ arising from population k is $\mathcal{P}(x_{nli}|\beta_k) = \text{Categorical}(x_{nli}|\beta_{kl})$.

Unlike the previous models, we now have a stick-breaking process for each individual. Draw sticks

$$\nu_{nk} \stackrel{\text{indep}}{\sim} \mathcal{P}_{\text{stick}}(\nu_{nk}), \quad n = 1, \dots, N; k = 1, 2, \dots$$

The prior assignment probability vector $\pi_n = (\pi_{n1}, \pi_{n2}, \dots)$, now unique to each individual, is formed by the same stick-breaking construction as before,

$$\pi_{nk} = \nu_{nk} \prod_{k' < k} (1 - \nu_{nk'}).$$

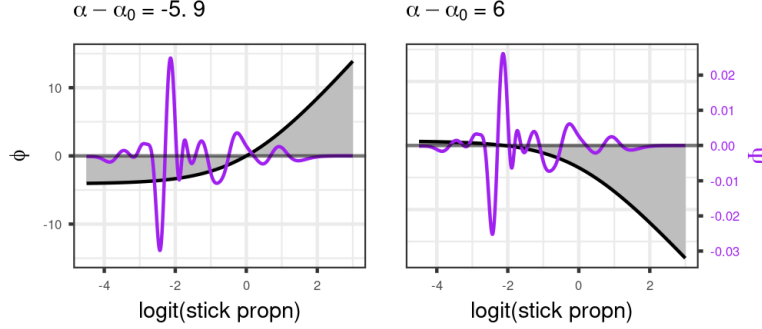


Figure 8: The multiplicative perturbations $\phi_\alpha(\cdot)$ that corresponds to decreasing (left) or increasing (right) the α parameter.

The population assignment z_{nli} is drawn from a multinomial distribution

$$p(z_{nli}|\pi_n) = \prod_{k=1}^{\infty} \pi_{nk}^{z_{nlik}}.$$

In this genetics application, we call π_n the *admixture* of individual n .

Initially we take $\mathcal{P}_{\text{stick}}$ to be Beta(1, α) with parameter $\alpha = \alpha_0 = 3$. The choice of $\alpha_0 = 3$ corresponds to roughly four distinct populations *a priori*, in agreement with the observation that the individuals come from four geographic regions. Below, we will evaluate sensitivity to this prior choice.

This model is identical to fastSTRUCTURE, a model proposed in [Pritchard et al. \[2000\]](#) and [Raj et al. \[2014\]](#), except that we replace the Dirichlet prior in fastSTRUCTURE with an infinite stick-breaking process. The result is a model similar to a hierarchical Dirichlet process for topic modeling [\[Teh et al., 2006\]](#), but without the top-level Dirichlet process. In addition, genotypes at genetic markers take the place of words in a document; in lieu of inferring “topics,” we infer latent populations.

We use a mean-field variational approximation, and all distributions are conditionally conjugate except for the stick-breaking proportions, which remain logit-normal. See [Appendix E.4](#) for further details.

Quantity of interest. The posterior quantities of interest in this application are the admixtures π_n . [Figure 16](#) plots the inferred admixtures $\mathbb{E}_{\mathcal{Q}(\pi_n|\hat{\eta})}[\pi_n]$ for all individuals n .

In the approximate posterior with α_0 , there appear to be three dominant latent populations, which we arbitrarily label as populations 1, 2, and 3 (top panel of [Figure 9](#)). The inferred admixture proportions generally correspond with geographic regions: Mbololo individuals are primarily population 1, Ngangao

individuals are primarily population 2, and Chawia individuals are a mixture of populations 1, 2, and 3 (Figure 16 in Appendix E.4).

Notably, outlying admixtures among individuals from the same geographic region provide clues into the historical migration patterns of this species. For example, while most Mbololo individuals are dominantly population 1, several Mbololo individuals have abnormally large admixture proportions of population 2. Conversely, while most Ngangao individuals are dominantly population 2, several Ngangao individuals have abnormally large admixture proportions of population 1. These patterns suggest that some migration has occurred between the Mbololo and Ngangao regions.

We evaluate the sensitivity of this conclusion to possible prior perturbations. Define the posterior quantity

$$g_{\text{admix}}(\eta; \mathcal{N}, k) = \mathbb{E}_{Q(\pi|\eta)} \left[\frac{1}{|\mathcal{N}|} \sum_{n \in \mathcal{N}} \pi_{nk} \right],$$

the average admixture proportion of population k in a set of individuals \mathcal{N} .

Below, we consider g_{admix} with three different sets of individuals: $\mathcal{N} = \{26, \dots, 31\}$, corresponding to the outlying Mbololo individuals, labeled “A” in Figure 9; $\mathcal{N} = \{125, \dots, 128\}$, corresponding to the four outlying Ngangao individuals, labeled “B”; and $\mathcal{N} = \{139, \dots, 155\}$ corresponding to all Chawia individuals, labeled “C”. For individuals A, we let $k = 2$ in g_{admix} and examine the robustness of the presence of population 2; for individuals B, we use $k = 1$; and for individuals C, we use $k = 3$. The first two posterior quantities relate to the inferred migration between the Mbololo and Ngangao regions. In the last example, we study the robustness of having a third latent population present, a population that primarily appears in Chawia individuals.

Functional sensitivity. We construct worst-case negative perturbations for each of the three variants of g_{admix} , in order to see whether the biologically interesting patterns can be made to disappear with different prior choices. Figure 9 shows the result of the worst-case perturbations on the prior density and g_{admix} . After the worst-case perturbation, the admixture proportion of population 2 in individuals A was nearly halved. On the other hand, the admixture of population 1 in individuals B is more robust. We conclude that the inferred migration from Ngangao to Mbololo is relatively robust to the stick-breaking prior, while conclusions about migration from Mbololo to Ngangao may be dependent on prior choices.

In this data set and model, the conclusions from the linear approximation did not always agree with the conclusions from refitting the variational approximation. For example, the admixture proportion of population 3 in individuals C were predicted to more sensitive by our linear approximation than were actually observed after refitting (Figure 9, bottom row).

Moreover, even though the linear approximation agreed with the refits for individuals A in overall admixture proportion (Figure 9, second row), the approximation does not perform uniformly well over all individuals. Figure 10 plots the inferred admixtures computed using the linearized variational parameters and

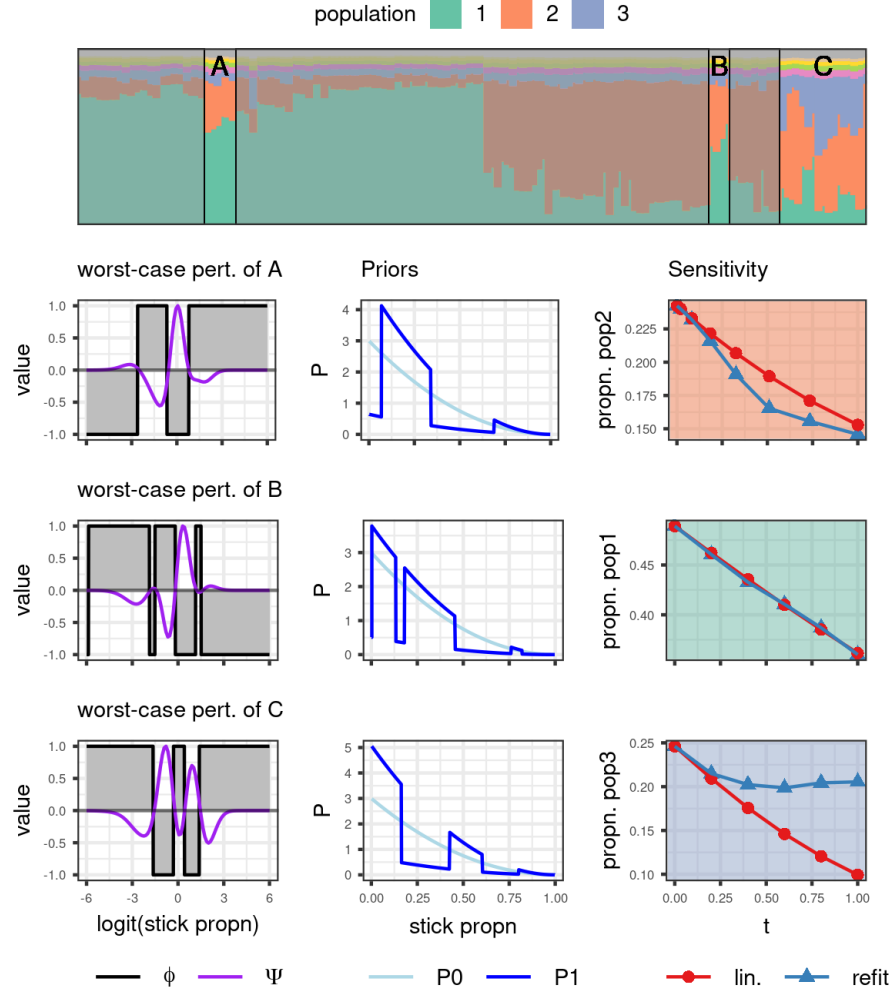


Figure 9: Sensitivity of inferred admixtures for several outlying individuals. For individuals A, we examine the sensitivity of the admixture proportion of population 2. For individuals B, we examine the population 1 admixture. For the individuals C, we examine the population 3 admixture. (Left column) The worst-case negative perturbation with $\|\phi\|_\infty = 1$ in grey, plotted against the influence function in purple (scaled such that $\|\psi\|_\infty = 1$). (Middle column) The effect of the perturbation on the prior density. (Right column) Effects on the inferred admixture.

the refitted variational parameters. The admixture proportion of population 2 in individual $n = 25$ dramatically increased after refitting with the perturbed prior;

the linearized parameters failed to reproduce this change.

Even though linear approximation works less well in this example, the influence function is still able to guide our choice of functional perturbations at which to refit. While the worst-case perturbations we used may be an adversarial choice, the influence function suggests that we can construct a smoother perturbation with a similar effect as the worst-case, as we did in Section 7.2. Importantly, as we will note in the next subsection, the influence function is cheap to compute relative to refitting. For a further discussion of the limitations of the linear approximation, see Appendix F.

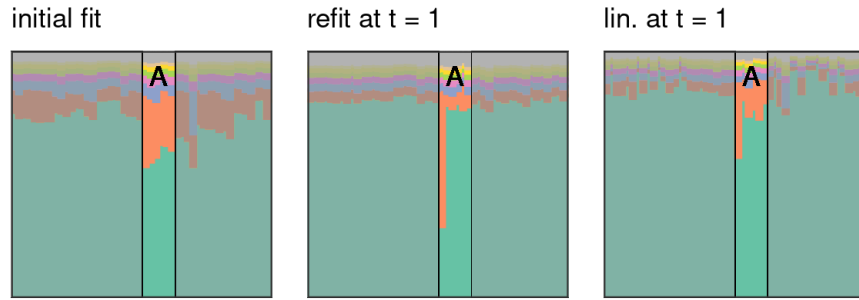


Figure 10: Inferred admixtures after the worst-case perturbation to individuals “A” (see Figure 9 for perturbation).

7.4 Computation time

The relative computational costs of the approximation and re-fitting for our three experiments are shown in Table 1. The data sets we considered in our experiments had varying degrees of complexity, and the computational cost of fitting the variational approximation thus also varies accordingly. However, the cost of forming the linear approximation—the step that requires computing and inverting the Hessian matrix—was consistently roughly an order of magnitude faster than refitting.

Recall from Section 6 that the solution of a linear system involving \hat{H}^{-1} is the computationally intensive part of the linear approximation, and that the linear system needs to be solved only once for a given perturbation, as described in Section 6. Consistent with this observation, in all the examples, after the linear approximation is formed, extrapolating to any new prior parameter $\alpha \neq \alpha_0$ or $t \neq 0$ takes only fractions of a second. For example, in the thrush data and fastSTRUCTURE model, the initial fit took seven seconds, with subsequent refits (which we warm-started with the initial fit) taking between five and ten seconds. Solving a linear system to form the linear approximation for a particular

Table 1: Compute time in seconds of various quantities on each data set. Reported times for $\hat{\eta}(\alpha)$ and $\hat{\eta}^{\text{lin}}(\alpha)$ are median times over the set of considered α 's. The reported influence function time is the time required to evaluate the influence function on a grid of 1000 points.

	iris	mice	thrush
Initial fit	1	30	7
Hessian solve for α sensitivity	0.02	3	0.3
Linear approx. $\hat{\eta}^{\text{lin}}(\alpha)$	0.0008	0.001	0.0008
Refits $\hat{\eta}(\alpha)$	0.5	30	5
The influence function (at 1000 grid points)	0.09	3	0.6
Hessian solve for ϕ	0.02	3	0.4
Linear approx. $\hat{\eta}^{\text{lin}}(\phi)$	0.001	0.001	0.0008
Refit $\hat{\eta}^{\text{lin}}(\phi)$	0.6	20	10

perturbation ϕ took less than a second, and evaluating $\hat{\eta}(\phi)$ was essentially free.

Acknowledgments. We are indebted to helpful discussions with Nelle Varoquaux, Matthew Stephens, Michael C. Hughes, Eric Sudderth, and Jake Soloff. Runjing Liu is supported by the National Science Foundation graduate research fellowship program. Ryan Giordano and Tamara Broderick were supported in part by an NSF CAREER Award and an ONR Early Career Grant.

References

E. Anderson. The species problem in iris. *Annals of the Missouri Botanical Garden*, 23(3):457–509, 1936. [17](#)

V. Averbukh and O. Smolyanov. The theory of differentiation in linear topological spaces. *Russian Mathematical Surveys*, 22(6):201–258, 1967. [46](#)

Sanjib Basu. *Bayesian Robustness and Bayesian Nonparametrics*, pages 223–240. Springer New York, New York, NY, 2000. [14](#)

A. Baydin, B. Pearlmutter, A. Radul, and J. Siskind. Automatic differentiation in machine learning: A survey. *Journal of Machine Learning Research*, 18, 2018. [9](#)

P. Billingsley. *Probability and Measure*. John Wiley and Sons, second edition, 1986. [35](#), [43](#)

C. M. Bishop. *Pattern Recognition and Machine Learning*. Springer, 2006. [53](#)

D. Blackwell and J. B. MacQueen. Ferguson distributions via Polya urn schemes. [57](#)

D. M. Blei and M. I. Jordan. Variational inference for Dirichlet process mixtures. *Bayesian Analysis*, 1(1):121 – 143, 2006. 5

D. M. Blei, A. Kucukelbir, and J. D. McAuliffe. Variational inference: A review for statisticians. *Journal of the American Statistical Association*, 112(518):859–877, 2017. 5, 53

D. Cai, T. Campbell, and T. Broderick. Power posteriors do not reliably learn the number of components in a finite mixture. In *ICBINB@NeurIPS workshop*, 2020. 14

D. Cai, T. Campbell, and T. Broderick. Finite mixture models do not reliably learn the number of components. In *Proceedings of the 38th International Conference on Machine Learning (to appear)*, 2021. 14

D. Cook. Assessment of local influence. *Journal of the Royal Statistical Society: Series B (Methodological)*, 48(2):133–155, 1986. 14

R. Dudley. *Real Analysis and Probability*. CRC Press, 2018. 11, 41

T. S. Ferguson. A Bayesian analysis of some nonparametric problems. *The Annals of Statistics*, pages 209–230, 1973. 1

P. Galbusera, L. Lens, T. Schenck, E. Waiyaki, and E. Matthysen. Genetic variability and gene flow in the globally, critically-endangered taita thrush. *Conservation Genetics*, 1:45–55, 2000. 22

Andrew Gelman, John B. Carlin, Hal S. Stern, David B. Dunson, Aki Vehtari, and Donald B. Rubin. *Bayesian Data Analysis, Third Edition*. Chapman & Hall/CRC Texts in Statistical Science. Taylor & Francis, 2013. 2, 14

R. Giordano, T. Broderick, and M. I. Jordan. Covariances, robustness and variational Bayes. *Journal of Machine Learning Research*, 19(51), 2018. 3, 14

P. Gustafson. Local sensitivity of posterior expectations. *Annals of Statistics*, 24(1):174–195, 1996a. 3, 7, 8, 10, 12, 13, 14, 39, 41, 42

P. Gustafson. Local sensitivity of inferences to prior marginals. *Journal of the American Statistical Association*, 91(434):774–781, 1996b. 14

P. Gustafson. *Local Robustness in Bayesian Analysis*, pages 71–88. Springer New York, New York, NY, 2000. 14

F. Hampel, E. Ronchetti, P. Rousseeuw, and W. Stahel. *Robust Statistics: The Approach Based on Influence Functions*, volume 196. John Wiley & Sons, 2011. 14

D. R. Insua and F Ruggeri. *Robust Bayesian Analysis*. Springer, 2000. 14

L. Jaeckel. The infinitesimal jackknife, memorandum. Technical report, MM 72-1215-11, Bell Lab. Murray Hill, NJ, 1972. [14](#)

A. Jasra, C. C. Holmes, and D. A. Stephens. Markov chain Monte Carlo methods and the label switching problem in Bayesian mixture modeling. *Statistical Science*, 20(1):50 – 67, 2005. [3](#)

S. Krantz and H. Parks. *The Implicit Function Theorem: History, Theory, and Applications*. Springer Science & Business Media, 2012. [34](#), [45](#)

A. Kucukelbir, D. Tran, R. Ranganath, A. Gelman, and D. Blei. Automatic differentiation variational inference. *arXiv preprint arXiv:1603.00788*, 2016. [3](#), [37](#)

Y. Luan and H. Li. Clustering of time-course gene expression data using a mixed-effects model with B-splines. *Bioinformatics*, 19(4):474–482, 2003. [20](#), [58](#)

J. W. Miller and M. T. Harrison. A simple example of dirichlet process mixture inconsistency for the number of components. In C. J. C. Burges, L. Bottou, M. Welling, Z. Ghahramani, and K. Q. Weinberger, editors, *Advances in Neural Information Processing Systems*, volume 26. Curran Associates, Inc., 2013. [14](#)

J. W. Miller and M T. Harrison. Inconsistency of Pitman-Yor process mixtures for the number of components. *Journal of Machine Learning Research*, 15(96): 3333–3370, 2014. URL <http://jmlr.org/papers/v15/miller14a.html>. [14](#)

O. Nielsen. *An Introduction to Integration and Measure Theory*, volume 17. Wiley-Interscience, 1997. [43](#), [49](#)

Luis E. Nieto-Barajas and Igor Prünster. A sensitivity analysis for Bayesian nonparametric density estimators. *Statistica Sinica*, 19(2):685–705, 2009. [14](#)

J. Nocedal and S. Wright. *Numerical Optimization*. Springer Science & Business Media, 2006. [15](#), [16](#)

J. K. Pritchard, M. Stephens, and P. Donnelly. Inference of population structure using multilocus genotype data. *Genetics*, 155(2):945–959, 2000. [25](#)

A. Raj, M. Stephens, and J. K. Pritchard. fastSTRUCTURE: Variational inference of population structure in large SNP data sets. *Genetics*, 197(2):573–589, 2014. [25](#)

Rajesh Ranganath, Sean Gerrish, and David M. Blei. Black box variational inference, 2013. <https://arxiv.org/abs/1401.0118>. [3](#)

J. Reeds. *On the definition of von Mises functionals*. PhD thesis, Statistics, Harvard University, 1976. [46](#)

A. Saha and S. Kurtek. Geometric sensitivity measures for Bayesian nonparametric density estimation models. *Sankhyā Series A.*, 81:104–143, 2019. [14](#)

J. Sethuraman. A constructive definition of Dirichlet priors. *Statistica sinica*, pages 639–650, 1994. [1](#)

J. E. Shoemaker, S. Fukuyama, A. J. Eisfeld, et al. An ultrasensitive mechanism regulates influenza virus-induced inflammation. *PLoS Pathogens*, 11(6):1–25, 2015. [20](#), [57](#)

S. Sivaganesan. Global and local robustness approaches: Uses and limitations. In *Robust Bayesian Analysis*, pages 89–108. Springer, 2000. [14](#)

J. D. Storey, W. Xiao, J. T. Leek, R. G. Tompkins, and R. W. Davis. Significance analysis of time course microarray experiments. *Proceedings of the National Academy of Sciences of the United States of America*, 102(36):12837–42, 2005. [57](#)

Y. W. Teh. Dirichlet processes. In *Encyclopedia of Machine Learning*. Springer, 2010. [57](#)

Y. W. Teh, M. I. Jordan, M. J. Beal, and D. M. Blei. Hierarchical Dirichlet processes. *Journal of the American Statistical Association*, 101(476):1566–1581, 2006. [2](#), [25](#)

P. Virtanen, R. Gommers, T. Oliphant, M. Haberland, T. Reddy, D. Cournapeau, E. Burovski, P. Peterson, W. Weckesser, J. Bright, S. van der Walt, M. Brett, J. Wilson, J. Millman, N. Mayorov, A. Nelson, E. Jones, R. Kern, E. Larson, C. Carey, İ. Polat, Y. Feng, E. Moore, J. VanderPlas, D. Laxalde, J. Perktold, R. Cimrman, I. Henriksen, E. Quintero, C. Harris, A. Archibald, A. Ribeiro, F. Pedregosa, P. van Mulbregt, and SciPy 1.0 Contributors. SciPy 1.0: Fundamental algorithms for scientific computing in Python. *Nature Methods*, 17: 261–272, 2020. doi: 10.1038/s41592-019-0686-2. [15](#)

U. von Luxburg. A tutorial on spectral clustering. *Statistics and Computing*, 17: 395–416, 2007. [22](#)

E. Zeidler. *Nonlinear Functional Analysis and Its Applications I: Fixed point theorems*. Springer Verlag New York, Inc., 1986. [11](#), [12](#), [13](#), [46](#), [48](#), [49](#)

Appendices

A General differentiability results

Our goal is to approximate the dependence of the optimal VB parameters on the prior using a Taylor series, which requires that the optimal VB parameters must be continuously differentiable as a function of the prior specification. In this section we state general conditions under which VB optima based on reverse KL

divergence are differentiable functions of both parametric and nonparametric prior perturbations. We will state our conditions and results in terms of a generic VB approximation and prior perturbation, which we articulate in Definition 2.

Definition 2. For some parameter $\theta \in \Omega_\theta \subseteq \mathbb{R}^{D_\theta}$, let $\mathcal{P}(\theta|t)$ denote a class of probability densities relative to a sigma-finite measure μ , defined for t in an open set $\mathcal{B}_t \subseteq \mathbb{R}$ containing 0. Let $\mathcal{Q}(\theta|\eta)$ be a family of approximating densities, also defined relative to μ .

Let the variational objective factorize as

$$\text{KL}(\eta, t) := \text{KL}(\eta) - \mathbb{E}_{\mathcal{Q}(\theta|\eta)} [(\log \mathcal{P}(\theta|t) - \log \mathcal{P}(\theta|t=0))] \quad (22)$$

$$\hat{\eta}(t) := \operatorname{argmin}_{\eta \in \Omega_\eta} \text{KL}(\eta, t). \quad (23)$$

Let $\hat{\eta}$ with no argument refer to $\hat{\eta}(0)$, the minimizer of $\text{KL}(\eta)$. \square

In general, we expect θ of Definition 2 to be some subset of the model parameters whose prior is being perturbed. The decomposition in Eq. 22 is always possible for VB approximations based on reverse KL divergence, in the sense that one could always take θ to be all model parameters and $\text{KL}(\eta) = 0$. We decompose the objective in this way in order to state strict regularity assumptions only on the part of the reverse KL divergence that is being perturbed. Indeed, we will require little from the $\text{KL}(\eta)$ part of the decomposition other than that it can be differentiated and optimized.

By identifying t with some hyperparameter (e.g. the concentration parameter, as in Example 1 below), we can use Definition 2 to study parametric perturbations. Furthermore, by parameterizing a path through the space of general densities, Definition 2 will allow us to study nonparametric perturbations (e.g. Example 2 below and the detailed analysis of Appendices A.3 to A.5). We can thus study VB prior robustness in general by studying problems of the form in Definition 2.

Example 1. For the BNP model with the $\mathcal{P}_{\text{stick}}$ prior on the stick breaks, take $\theta = (\nu_1, \dots, \nu_{K_{\max}-1})$, and take μ to be the Lebesgue measure on $[0, 1]^{K_{\max}-1}$. Let α_0 be some initial value of the concentration parameter, and let t be $\alpha - \alpha_0$, so that deviations of t away from 0 represent deviations of α away from α_0 .

Expanding the reverse KL divergence in Eq. 3, we see that the prior $\mathcal{P}(\nu_k|\alpha)$ enters the VB objective in a term of the form $\sum_{k=1}^{\infty} \mathbb{E}_{\mathcal{Q}(\nu_k|\eta)} [\log \mathcal{P}(\nu_k|\alpha)]$. Adding and subtracting the this term evaluated at α_0 gives

$$\text{KL}(\eta, \alpha) = \text{KL}(\eta, \alpha_0) - \sum_{k=1}^{K_{\max}-1} \left(\mathbb{E}_{\mathcal{Q}(\nu_k|\eta)} [\log \mathcal{P}(\nu_k|\alpha)] - \mathbb{E}_{\mathcal{Q}(\nu_k|\eta)} [\log \mathcal{P}(\nu_k|\alpha_0)] \right).$$

Plugging in the definition of $\mathcal{P}(\nu_k|\alpha)$, recognizing that the normalizing constant does not depend on ν_k and so can be neglected in the optimization, letting

$\text{KL}(\eta) := \text{KL}(\eta, \alpha_0)$, and substituting $t = \alpha - \alpha_0$ gives

$$\text{KL}(\eta, t) = \text{KL}(\eta, \alpha_0) - t \sum_{k=1}^{K_{\max}-1} \mathbb{E}_{\mathcal{Q}(\nu_k|\eta)} [\log(1 - \nu_k)].$$

△

Example 2. As in Example 1, take $\theta = (\nu_1, \dots, \nu_{K_{\max}-1})$ and μ to be the Lebesgue measure on $[0, 1]^{K_{\max}-1}$. Let $\mathcal{P}_0(\nu_k) := \text{Beta}(\nu_k|1, \alpha_0)$, and let $\mathcal{P}_1(\nu_k)$ be a density, not in the beta family, that shifts mass towards zero:

$$\mathcal{P}_1(\nu_k) := \frac{\exp(-\nu_k) \mathcal{P}_0(\nu_k)}{\int \exp(-\nu'_k) \mathcal{P}_0(\nu'_k) d\nu'_k}.$$

For $t \in [0, 1]$ define the multiplicatively perturbed prior

$$\mathcal{P}(\nu_k|t) := \frac{\mathcal{P}_1(\nu_k)^t \mathcal{P}_0(\nu_k)^{1-t}}{\int \mathcal{P}_1(\nu'_k)^t \mathcal{P}_0(\nu'_k)^{1-t} d\nu'_k}.$$

When $t = 0$, $\mathcal{P}(\nu_k|t) = \mathcal{P}_0(\nu_k)$, when $t = 1$, $\mathcal{P}(\nu_k|t) = \mathcal{P}_1(\nu_k)$. For $t \in (0, 1)$ $\mathcal{P}(\nu_k|t)$ varies smoothly between \mathcal{P}_0 and \mathcal{P}_1 .

As in Example 1, up to constants not depending on ν_k we can write

$$\begin{aligned} \log \mathcal{P}(\nu_k|t) - \log \mathcal{P}(\nu_k|t=0) &= -t \log \mathcal{P}_0(\nu_k) + t \log \mathcal{P}_1(\nu_k) + C \\ &= -t\nu_k + C \Rightarrow \\ \text{KL}(\eta, t) &= \text{KL}(\eta) - t \mathbb{E}_{\mathcal{Q}(\nu_k|\eta)} [\nu_k] + C. \end{aligned}$$

Different choices for $\mathcal{P}_1(\nu_k)$ would give different additive perturbations to the reverse KL divergence. △

A.1 Parametric prior perturbations

We now state conditions under which $t \mapsto \hat{\eta}(t)$, as defined by Definition 2, is continuously differentiable. Our key theoretical tool will be the implicit function theorem [see, e.g., Krantz and Parks, 2012], applied to the first-order conditions for the VB optimization problem.

Our results can be expressed in terms of unnormalized densities, which can simplify some computation. To that end, let $\tilde{\mathcal{Q}}$ and $\tilde{\mathcal{P}}$ refer to potentially unnormalized (but normalizable) versions of the respectively corresponding \mathcal{Q} and \mathcal{P} given in Definition 2, so that

$$\mathcal{Q}(\theta|\eta) := \frac{\tilde{\mathcal{Q}}(\theta|\eta)}{\int \tilde{\mathcal{Q}}(\theta'|\eta) \mu(d\theta')} \quad \text{and} \quad \mathcal{P}(\theta|t) := \frac{\tilde{\mathcal{P}}(\theta|t)}{\int \tilde{\mathcal{P}}(\theta'|t) \mu(d\theta')}.$$

In Assumption 1, stated in Section 3 above, we require some mild regularity conditions for the “initial problem,” $\text{KL}(\eta)$. As we discuss in Appendix A.2,

Assumption 1 states conditions that are typically satisfied when $\text{KL}(\eta)$ can be optimized numerically using unconstrained optimization.

Next, we will require some differentiability conditions for the perturbation and the variational approximation.

Assumption 2. *Assume that the map $\eta \mapsto \log \tilde{Q}(\theta|\eta)$ is twice continuously differentiable, and that the map $t \mapsto \log \tilde{P}(\theta|t)$ is continuously differentiable.*

Further, assume that we can exchange the order of integration and differentiation in the expressions $\int \tilde{Q}(\theta|\eta) \log \tilde{P}(\theta|t) \mu(d\theta)$ and $\int \tilde{Q}(\theta|\eta) \mu(d\theta)$ at $\eta = \hat{\eta}$ and $t = 0$ for the derivatives $\partial/\partial\eta$, $\partial^2/\partial\eta^2$, and $\partial^2/\partial\eta\partial t$.

In certain cases, one can verify Assumption 2 directly, such as when $\mathbb{E}_{\tilde{Q}(\theta|\eta)} [\log \tilde{P}(\theta|t)]$ has a closed form. For more general situations, the following assumptions allow us to satisfy Assumption 2 using the dominated convergence theorem [Billingsley, 1986, Theorem 16.8].

Assumption 3. *Let $f(\theta, \eta, t)$ be a function taking values in \mathbb{R} . Assume that the partial derivatives $\partial/\partial\eta$, $\partial^2/\partial\eta^2$, and $\partial^2/\partial\eta\partial t$ of f exist, are continuous functions of η and t , and are μ -measurable functions of θ on some open set $\mathcal{B}_\eta \times \mathcal{B}_t$.*

Let $M(\theta) > 0$ be a measurable function with $\int M(\theta) \mu(d\theta) < \infty$. Assume that, for all $\eta, t \in \mathcal{B}_\eta \times \mathcal{B}_t$, $M(\theta)$ is μ -almost everywhere greater than each of the following functions: $|f(\theta, \eta, t)|$, $\|\partial f(\theta, \eta, t)/\partial\eta\|_2$, $\|\partial^2 f(\theta, \eta, t)/\partial\eta\partial\eta^T\|_2$, and $\|\partial^2 f(\theta, \eta, t)/\partial\eta\partial t\|_2$.

Assumption 4. *(Sufficient conditions for Assumption 2.) Let Assumption 3 hold with the function $f(\theta, \eta, t) = \tilde{Q}(\theta|\eta) \log \tilde{P}(\theta|t)$ as well as with $f(\theta, \eta, t) = \tilde{Q}(\theta|\eta)$.*

By the dominated convergence theorem, Assumption 4 implies Assumption 2 (see Lemma 2 in Appendix B for a proof). The advantage of Assumption 4 over Assumption 2 is that the conditions of Assumption 4 can typically be verified even when the expectation $\mathbb{E}_{\tilde{Q}(\theta|\eta)} [\log \tilde{P}(\theta|t)]$ does not have a closed form. In Appendix A.2, we will discuss how different choices of variational approximations for the stick lengths lend themselves to either Assumption 2 or Assumption 4. Furthermore, Assumption 3 will be essential to analyzing nonparametric perturbations in Appendix A.3.

We are now in a position to define the quantities that occur in the derivative and state our main result.

Definition 3. Under the conditions of Definition 2, when Assumptions 1 and 2 hold, define

$$\begin{aligned} \hat{H} &:= \left. \frac{\partial^2 \text{KL}(\eta)}{\partial\eta\partial\eta^T} \right|_{\hat{\eta}} \quad \text{and} \\ \mathcal{S}(\theta|\eta) &:= \nabla_\eta \log \tilde{Q}(\theta|\eta) - \mathbb{E}_{\tilde{Q}(\theta|\eta)} [\nabla_\eta \log \tilde{Q}(\theta|\eta)]. \end{aligned}$$

Further, define

$$\hat{J} := \left. \frac{\partial \mathbb{E}_{\mathcal{Q}(\theta|\eta)} \left[\frac{\partial \log \tilde{\mathcal{P}}(\theta|t)}{\partial t} \right]_{t=0}}{\partial \eta} \right|_{\eta=\hat{\eta}} = \mathbb{E}_{\mathcal{Q}(\theta|\hat{\eta})} \left[\mathcal{S}(\theta|\hat{\eta}) \frac{\partial \log \tilde{\mathcal{P}}(\theta|t)}{\partial t} \right]_{t=0},$$

where the final equality follows from differentiating under the integral using Assumption 2 (see Lemma 3 in Appendix B for more details). \square

Theorem 4. *Under the conditions of Definitions 2 and 3, let Assumptions 1 and 2 hold. Then the map $t \mapsto \hat{\eta}(t)$ is continuously differentiable at $t = 0$ with derivative*

$$\left. \frac{d\hat{\eta}(t)}{dt} \right|_0 = -\hat{H}^{-1} \hat{J}. \quad (24)$$

(For a proof, see Appendix B Proof B.)

A.2 Differentiability of BNP models with respect to α

In this section, we return to the BNP problem and prove carefully that the map $\alpha \mapsto \hat{\eta}(\alpha)$ satisfies Assumptions 1 and 2, and so the conditions of Theorem 4. As in Example 1, we will take μ to be the Lebesgue measure on $[0, 1]^{K_{\max}-1}$.

Recall from Section 2.2 that we take $\mathcal{Q}(\nu_k|\eta)$ to be a normal density on the logit-transformed sticks, $\tilde{\nu}_k$. For the duration of this section, write $\mathcal{Q}(\tilde{\nu}_k|\eta) = \mathcal{N}(\tilde{\nu}_k|\mu_k, \sigma_k^2)$, so that the subvector of η parameterizing $\mathcal{Q}(\tilde{\nu}_k|\eta)$ is $\eta_{\nu_k} = (\mu_k, \sigma_k)$. By the formula for transformation of probability densities,

$$\mathcal{Q}(\nu_k|\eta_{\nu_k}) = \mathcal{N} \left(\log \left(\frac{\nu_k}{1-\nu_k} \right) \middle| \mu_k, \sigma_k^2 \right) \frac{1}{\nu_k(1-\nu_k)},$$

where we have used the fact that $\left. \frac{d\tilde{\nu}_k}{d\nu_k} \right|_{\nu_k} = \frac{1}{\nu_k(1-\nu_k)}$. Similarly, for any function $f(\nu_k)$ of the stick lengths, we can transform the expectations as $\mathbb{E}_{\mathcal{Q}(\nu_k|\eta_{\nu_k})} [f(\nu_k)] = \mathbb{E}_{\mathcal{Q}(\tilde{\nu}_k|\eta_{\nu_k})} \left[f \left(\frac{\exp(\tilde{\nu}_k)}{1+\exp(\tilde{\nu}_k)} \right) \right]$, using the fact that $\nu_k = \frac{\exp(\tilde{\nu}_k)}{1+\exp(\tilde{\nu}_k)}$.

Differentiability of $\text{KL}(\eta)$ (Assumption 1 (Item (1))) is immediately satisfied for the η that parameterize $\mathcal{Q}(\beta|\eta)$ and $\mathcal{Q}(z|\eta)$ by our use of conjugate approximating families and standard parameterizations. The stick length density, $\mathcal{Q}(\nu_k|\eta_{\nu_k})$ is not a standard exponential family², so we must show that the entropy

²In this section, we continue to take μ to be the Lebesgue measure on $[0, 1]$ as in Example 1. We could have equivalently taken μ to be the Lebesgue measure on \mathbb{R} and analyzed $\mathcal{P}(\tilde{\nu}_k|\alpha)$ instead of $\mathcal{P}(\nu_k|\alpha)$. Had we done so, the log Jacobian term $\log(\nu_k(1-\nu_k))$ now appearing in the entropy would have instead appeared in the $\log \tilde{\mathcal{P}}(\tilde{\nu}_k|\alpha)$ term, and so been part of Assumption 2 rather than Assumption 1 (Item (1)). Nevertheless, the needed assumptions would be substantively the same. For essentially this reason, the choice of dominating measure in Definition 2 does not matter.

$\mathbb{E}_{\mathcal{Q}(\nu_k|\eta_{\nu_k})}[\log \mathcal{Q}(\nu_k|\eta_{\nu_k})]$ is twice continuously differentiable. The entropy is given up to a constant by

$$\begin{aligned} & \mathbb{E}_{\mathcal{Q}(\nu_k|\eta_{\nu_k})}[\log \mathcal{Q}(\nu_k|\eta_{\nu_k})] \\ &= \mathbb{E}_{\mathcal{Q}(\nu_k|\eta_{\nu_k})} \left[\log \mathcal{N} \left(\log \left(\frac{\nu_k}{1-\nu_k} \right) \middle| \mu_k, \sigma_k^2 \right) \right] + \mathbb{E}_{\mathcal{Q}(\nu_k|\eta_{\nu_k})}[\log(\nu_k(1-\nu_k))] \\ &= \mathbb{E}_{\mathcal{Q}(\tilde{\nu}_k|\eta_{\nu_k})} \left[\log \mathcal{N} \left(\tilde{\nu}_k \middle| \mu_k, \sigma_k^2 \right) \right] + \mathbb{E}_{\mathcal{Q}(\tilde{\nu}_k|\eta_{\nu_k})}[\tilde{\nu}_k] \\ &= \frac{1}{2} \log \sigma_k^2 + \mu_k + C, \end{aligned}$$

which is twice continuously differentiable by inspection. Indeed, Assumption 1 (Item (1)) is typically satisfied in VB problems; when it is not, many black-box optimization methods also do not apply.

Non-singularity of the Hessian matrix \hat{H} (Assumption 1 (Item (2))) is satisfied whenever $\hat{\eta}$ is at a local optimum of $\text{KL}(\eta)$. In practice, we compute $\hat{\eta}$ and (approximately) check Assumption 1 (Item (2)) numerically as part of computing the sensitivity $\hat{H}^{-1}\hat{J}$. As with Assumption 1 (Item (1)), if Assumption 1 (Item (2)) is violated, then the user will probably have difficulty optimizing $\text{KL}(\eta)$.

Assumption 1 (Item (3)) essentially requires that $\text{KL}(\eta)$ be well-defined in an \mathbb{R}^{D_η} neighborhood of $\hat{\eta}$, and can require some care in choosing the parameterization η . As an example of a parameterization that would violate Assumption 1 (Item (3)), consider parametrizing $\mathcal{Q}(z_n|\eta)$ by the K_{\max} expectations $m_k := \mathbb{E}_{\mathcal{Q}(z_n|\eta)}[z_{nk}]$.

The set $(m_1, \dots, m_{K_{\max}})$ completely specify $\mathcal{Q}(z_n|\eta)$, but violate Assumption 1 (Item (3)), since any valid parameterization satisfies $\sum_{k=1}^{K_{\max}} m_k = 1$, and so no open ball in \mathbb{R}^{D_η} can be contained in Ω_η . However, Assumption 1 (Item (3)) is satisfied we use an *unconstrained parameterization* for $\mathcal{Q}(\zeta|\eta)$. Unconstrained parameterizations of variational distributions allow the use of unconstrained optimization for variational inference and are a good practice when available [Kucukelbir et al., 2016]. For details on our parameterizations, see the corresponding appendices.

Verifying Assumption 2 is the principal technical challenge of satisfying the conditions of Theorem 4. Recall from Example 1 that $\log \tilde{\mathcal{P}}(\nu_k|t) = t \log(1 - \nu_k)$, so we need to establish Assumption 2 for

$$-\mathbb{E}_{\mathcal{Q}(\nu_k|\eta_{\nu_k})}[t \log(1 - \nu_k)] = \mathbb{E}_{\mathcal{Q}(\tilde{\nu}_k|\eta_{\nu_k})}[t \log(1 + \exp(\tilde{\nu}_k))].$$

Since the preceding equality holds for all t and η_{ν_k} , it suffices to establish that we can exchange the order of integration and differentiation for the right hand side. Since the normal density has a term of the form $\exp(-C\tilde{\nu}_k^2)$, and since $\log(1 + \exp(\tilde{\nu}_k)) \exp(-|\tilde{\nu}_k|) < \infty$ for all $\tilde{\nu}_k \in \mathbb{R}$ as long as the variational variance is finite, one can show that the conditions of Assumption 4 are satisfied within $\mathcal{B}_\eta \times \mathcal{B}_t$. (See Lemma 7 in Appendix B for a proof.) Note that derivatives with

respect to any components of η other than η_{ν_k} are zero and so Assumption 2 is trivially satisfied.

Assumption 4 implies Assumption 2. Since both Assumptions 1 and 2 are satisfied, Theorem 4 applies, and the map $\alpha \mapsto \hat{\eta}(\alpha)$ is continuously differentiable.

We end this section by observing that the only real technical challenge was showing that the assumptions were satisfied for the logit-normal densities $\mathcal{Q}(\nu_k | \eta_{\nu_k})$. Had we instead used the conjugate beta density parameterized by its natural parameters, then both Assumption 1 and Assumption 2 would follow immediately by standard properties of the Beta distribution. In particular, the expectation $\mathbb{E}_{\mathcal{Q}(\nu_k | \eta_{\nu_k})} [t \log(1 - \nu_k)]$ needed for Assumption 1 is simply t times the Beta distribution's moment parameter, which is known to be an infinitely-differentiable function of the natural parameters.

A.3 Nonparametric prior perturbations

We now show how, by parameterizing a path between two arbitrary densities, we can apply Theorem 4 to nonparametric perturbations of the prior density. Again let us return to the abstract setting of Definition 2. Let us fix an initial prior density, $\mathcal{P}_0(\theta)$, at which we have computed a VB approximation, and suppose we wish to ask what the variational optimum would have been had we used some alternative prior density, $\mathcal{P}_1(\theta)$. Let us write $\hat{\eta}(\mathcal{P}_0)$ and $\hat{\eta}(\mathcal{P}_1)$ for these two approximations, respectively, so we are interested in quantifying the change $g(\hat{\eta}(\mathcal{P}_1)) - g(\hat{\eta}(\mathcal{P}_0))$. If this change is large, we say that our quantity of interest is not robust to replacing \mathcal{P}_0 with \mathcal{P}_1 .

To approximately assess robustness using the local sensitivity approach, we must somehow define a continuous path from $\mathcal{P}_0(\theta)$ to $\mathcal{P}_1(\theta)$ parameterized, say, by $t \in [0, 1]$. One way to do so is to define a multiplicative path

$$\log \tilde{\mathcal{P}}(\theta|t) = (1 - t) \log \mathcal{P}_0(\theta) + t \log \mathcal{P}_1(\theta). \quad (25)$$

Under Eq. 25, when $t = 0$, $\mathcal{P}(\theta|t) = \mathcal{P}_0(\theta)$, when $t = 1$, $\mathcal{P}(\theta|t, \mathcal{P}_0, \mathcal{P}_1) = \mathcal{P}_1(\theta)$, and $t \in (0, 1)$ smoothly parameterizes a path between the two. If we can verify that Theorem 4 applies to the perturbation given in Eq. 25, then, just as in the parametric case, we can form the Taylor series approximation,

$$\hat{\eta}(\mathcal{P}_1) \approx \hat{\eta}(\mathcal{P}_0) + \left. \frac{d\hat{\eta}(t)}{dt} \right|_{t=0} (1 - 0).$$

Our first task is then to state conditions under which Theorem 4 applies to Eq. 25. In Eq. 25 we have assumed that \mathcal{P}_1 is a density, but it will be more convenient to observe that, when $\mathcal{P}_1 \ll \mathcal{P}_0$, we can re-write

$$\log \tilde{\mathcal{P}}(\theta|t) = \log \mathcal{P}_0(\theta) + t \log \frac{\tilde{\mathcal{P}}_1(\theta)}{\tilde{\mathcal{P}}_0(\theta)} + C. \quad (C \text{ does not depend on } \theta)$$

Defining the generic function $\phi(\theta) := \log \frac{\tilde{\mathcal{P}}_1(\theta)}{\mathcal{P}_0(\theta)}$ motivates consideration of perturbations of the form $\log \tilde{\mathcal{P}}(\theta|t) = \mathcal{P}_0(\theta) + t\phi(\theta)$, where $\phi(\theta)$ is some generic measurable function. We can then ask what ϕ give rise to valid densities as well as differentiable maps $t \mapsto \hat{\eta}(t)$.

Definition 4. Let μ denote a measure on the Borel sets of Ω_θ and fix $\mathcal{P}_0(\theta)$, a density with respect to μ . Assume that $\mu(\{\theta : \mathcal{P}_0(\theta) = 0\}) = 0$, so that (in a slight abuse of notation) $\mu \ll \mathcal{P}_0$. For any measurable $\phi : \Omega_\theta \mapsto \mathbb{R}$ for which the expressions are well-defined, let

$$\tilde{\mathcal{P}}(\theta|\phi) := \mathcal{P}_0(\theta) \exp(\phi(\theta)).$$

As usual, when $0 < \int \tilde{\mathcal{P}}(\theta|\phi) \mu(d\theta) < \infty$, we let $\mathcal{P}(\theta|\phi)$ be the normalized version of $\tilde{\mathcal{P}}(\theta|\phi)$. Further, define the norm $\|\phi\|_\infty := \text{esssup}_{\theta \sim \mu} |\phi(\theta)|$, and let $\mathcal{B}_\phi(\delta) := \{\phi : \|\phi\|_\infty < \delta\}$. \square

The class of perturbations defined in Definition 4 are one of the family of “nonlinear” functional perturbations given by [Gustafson \[1996a\]](#), though we deviate from [Gustafson \[1996a\]](#) by allowing ϕ to take on negative values. The following result, which motivates the use of the $\|\cdot\|_\infty$ norm to measure the “size” of a perturbation ϕ , is only a minor modification of the corresponding result from [Gustafson \[1996a\]](#) to allow negative perturbations.

Lemma 1. ([Gustafson \[1996a\]](#)) Fix the quantities given in Definition 4. For a fixed probability measure $\mathcal{P}_1 \ll \mu$ with density $\mathcal{P}_1(\theta)$ with respect to μ , let $\phi(\theta|\mathcal{P}_1) := \log \mathcal{P}_1(\theta)/\mathcal{P}_0(\theta)$. Then $\mathcal{P}_1 \mapsto \|\phi(\cdot|\mathcal{P}_1)\|_\infty$ is a norm, does not depend on μ , and is invariant to invertible transformations of θ .

Furthermore, for any ϕ with $\|\phi\|_\infty < \infty$, the quantity $\tilde{\mathcal{P}}(\theta|\phi)$ gives rise to a valid prior, in the sense that $\tilde{\mathcal{P}}(\theta|\phi) \geq 0$ μ -almost everywhere, and $0 < \int \tilde{\mathcal{P}}(\theta|\phi) \mu(d\theta) < \infty$. (See [Proof B](#) on page [45](#).)

The set of priors $\{\mathcal{P}(\theta|\phi) : \phi \in \mathcal{B}_\phi(\delta)\}$ live in a multiplicative band around the original prior, \mathcal{P}_0 , as shown in Figure 1. Although Lemma 1 proves that every ϕ with $\|\phi\|_\infty$ is a valid prior, the converse is not true, and the Beta prior perturbation of Example 1 is a counterexample.

Example 3. Take μ to be the Lebesgue measure on $[0, 1]$, let $\mathcal{P}_0(\theta) = \text{Beta}(\theta|1, \alpha_0)$ and $\mathcal{P}_1(\theta) = \text{Beta}(\theta|1, \alpha_1)$ for $\alpha_0 \neq \alpha_1$. Taking $\phi(\theta) = (\alpha_1 - \alpha_0) \log(1 - \theta)$ parameterizes a path from \mathcal{P}_0 to \mathcal{P}_1 as in Eq. 25, and

$$\|\phi\|_\infty = |\alpha_1 - \alpha_0| \sup_{\theta \in [0, 1]} |\log(1 - \theta)| = \infty.$$

Therefore, in general, there exist valid priors that cannot be expressed by Definition 4 with ϕ with $\|\phi\|_\infty < \infty$. \triangle

We now show that, when $\|\phi\|_\infty < \infty$, we can apply Theorem 4. We still require the following assumption on the VB density, which is strictly weaker than Assumption 4.

Assumption 5. Assume that Assumption 3 applies with the function $f(\theta, \eta, t) = \mathcal{Q}(\theta|\eta)$ (no t dependence).

Corollary 3. Fix the quantities given in Definition 4, and let Assumptions 1 and 5 hold. Let $g(\eta) : \Omega_\eta \mapsto \mathbb{R}$ denote a continuously differentiable real-valued function of interest. Define the “influence function” $\Psi : \Omega_\theta \mapsto \mathbb{R}$:

$$\Psi(\theta) := - \frac{dg(\eta)}{d\eta^T} \Big|_{\hat{\eta}} \hat{H}^{-1} \mathcal{S}(\theta|\hat{\eta}) \mathcal{Q}(\theta|\hat{\eta}). \quad (26)$$

Then, if $\|\phi\|_\infty < \infty$, the map $t \mapsto g(\hat{\eta}(t\phi))$ is continuously differentiable at $t = 0$ with derivative

$$\frac{dg(\hat{\eta}(t\phi))}{dt} \Big|_0 = \int \Psi(\theta) \phi(\theta) \mu(d\theta). \quad (27)$$

Proof. It suffices to show that Assumption 5 implies Assumption 2 for the perturbation given in Definition 4 when $\|\phi\|_\infty < \infty$. Observe that $\log \hat{\mathcal{P}}(\theta|t) = t\phi(\theta)$, so, for any $f(\theta, \eta, t)$ that satisfies the conditions of Assumption 3, $\phi(\theta)f(\theta, \eta, t) \leq \|\phi\|_\infty M(\theta)$. Therefore Assumption 3 is satisfied by $\phi(\theta)f(\theta, \eta, t)$ as well. It follows that Assumption 5 \Rightarrow Assumption 4 \Rightarrow Assumption 2. The form of the influence function is then given by gathering terms in Eq. 24. \square

The influence function can be a useful summary of the effect of making generic changes to the prior density, as we will show in the experiments of Section 7. For visualization, it can be useful to reduce the dimension of the domain of the influence function, as we discuss in the following example.

Example 4. In the BNP example, we are perturbing each of the sticks, so we take $\theta \in [0, 1]^{K_{\max}-1}$. Formally, $\phi : [0, 1]^{K_{\max}-1} \mapsto \mathbb{R}$ can express different perturbations for the density of each of the $K_{\max}-1$ sticks. However, when we describe “changing the stick breaking density,” we mean changing each stick’s prior density in the same way.

To represent perturbing all the sticks simultaneously, take some univariate perturbation $\phi_u : [0, 1] \mapsto \mathbb{R}$, and set $\phi(\nu_1, \dots, \nu_{K_{\max}-1}) = \sum_{k=1}^{K_{\max}-1} \phi_u(\nu_k)$. By linearity of the derivative Corollary 3,

$$\frac{dg(\hat{\eta}(t\phi))}{dt} \Big|_0 = \int \Psi(\theta) \left(\sum_{k=1}^{K_{\max}-1} \phi_u(\nu_k) \right) d\nu_1 \dots d\nu_{K_{\max}-1}.$$

By definition, $\mathbb{E}_{\mathcal{Q}(\theta|\hat{\eta})} [\mathcal{S}(\theta|\hat{\eta})] = 0$, so $\int \Psi(\theta) \mu(d\theta) = 0$. By the mean-field assumption, $\Psi(\nu_1, \dots, \nu_{K_{\max}-1}) = \prod_{k=1}^{K_{\max}-1} \Psi_k(\nu_k)$, where $\Psi_k(\nu_k)$ is derived from Eq. 26 but using $\theta = \nu_k$. Letting $\nu_0 \in [0, 1]$ denote the variable of integration and plugging in the preceding observations gives

$$\int \Psi(\theta) \phi(\theta) \mu(d\theta) = \int_0^1 \left(\sum_{k=1}^{K_{\max}-1} \Psi_k(\nu_0) \right) \phi_u(\nu_0) d\nu_0.$$

Thus we can say that the influence function for perturbing all the stick breaking densities simultaneously is given by the sum of the individual sticks' influence functions, which maps $[0, 1] \mapsto \mathbb{R}$. \triangle

A.4 Worst-case prior perturbations and Fréchet differentiability

As we saw in Corollary 3, the derivative of perturbations given by Definition 4 takes the form of an integral of the influence function against the perturbation. It is natural to use the influence function to *explore* the space of priors, e.g., to find alternative priors with large influence but small $\|\phi\|_\infty$. Consider as an example the following corollary, which is the VB analogue of [Gustafson \[1996a, Result 11\]](#).

Corollary 4. *The “worst-case” derivative in $\mathcal{B}_\phi(\delta)$ is given by*

$$\sup_{\phi \in \mathcal{B}_\phi(\delta)} \frac{dg(\hat{\eta}(t\phi))}{dt} \Big|_0 = \delta \int |\Psi(\theta)| \mu(d\theta),$$

which is achieved at the perturbation $\phi^(\theta) = \delta \text{sign}(\Psi(\theta))$.*

Proof. The result follows immediately from applying Hölder’s inequality [[Dudley, 2018](#), Theorem 5.1.2 and subsequent discussion] to Eq. 27. \square

As discussed in Section 4 above, we also wish to show that the map $\phi \mapsto g(\hat{\eta}(\phi))$ is continuously Fréchet differentiable as a map from L_∞ to \mathbb{R}^{D_η} .

Theorem 5. *Let Assumptions 1 and 5 hold. Then the map $\phi \mapsto \hat{\eta}(\phi)$ is well-defined and continuously Fréchet differentiable in a neighborhood of 0 as a map from L_∞ to \mathbb{R}^{D_η} , with the derivative given in Corollary 3.*

(For a proof, see [Appendix B Proof B](#).)

A.5 Other nonparametric prior perturbations

One might ask whether one could consider paths through the space of priors other than multiplicative, such as additive perturbations. In this section, we briefly consider a broader class of nonlinear perturbations investigated by [Gustafson \[1996a\]](#), of which additive and multiplicative perturbations are special cases, and show that, within this class, only multiplicative perturbations lead to Fréchet differentiable VB optima.

As in [Appendix A.3](#), suppose we have an initial prior \mathcal{P}_0 and an alternative \mathcal{P}_1 , and that we wish to parameterize a continuous path between them. Deviating from multiplicative perturbations, for some $p \in [1, \infty)$, let

$$\tilde{\mathcal{P}}(\theta|t_p) := \left((1 - t_p)\mathcal{P}_0(\theta)^{1/p} + t_p \frac{1}{p} \mathcal{P}_1(\theta)^{1/p} \right)^p. \quad (28)$$

As with Eq. 25, $\mathcal{P}(\theta|t_p = 0) = \mathcal{P}_0(\theta)$, $\mathcal{P}(\theta|t_p = 1) = \mathcal{P}_1(\theta)$, and $\mathcal{P}(\theta|t_p)$ moves continuously between the two in $t_p \in (0, 1)$. When $p = 1$, $\tilde{\mathcal{P}}(\theta|t_p)$ defines an “additive perturbation,” and the limit as $p \rightarrow \infty$ gives the multiplicative perturbation of Eq. 25.

Gustafson [1996a, Result 2] states a result analogous to Lemma 1 for Eq. 28, where the $\|\cdot\|_\infty$ norm is replaced by

$$\phi(\theta|\mathcal{P}_1, p) := \mathcal{P}_1(\theta)^{1/p} - \mathcal{P}_0(\theta)^{1/p} \quad \text{and} \quad \|\phi\|_p := \left(\int |\phi(\theta)|^p \right)^{1/p}. \quad (29)$$

We refer the reader to Gustafson [1996a] for details.³ For our present discussion, what matters is that the use of the perturbation in Eq. 28 strongly motivates the use of the norm $\|\phi(\theta|\mathcal{P}_1, p)\|_p$ when forming, for example, worst-case perturbations as in Corollary 4.

Though the $\|\phi(\theta|\mathcal{P}_1, p)\|_p$ norm does not appear to cause major difficulties for the full Bayesian posterior,⁴ the $\|\phi(\theta|\mathcal{P}_1, p)\|_p$ norm is not compatible with KL divergence, in the sense that reverse KL divergence is *discontinuous* in this norm. Prior changes that are arbitrarily small according to $\|\phi(\theta|\mathcal{P}_1, p)\|_p$ can induce arbitrarily large changes in the reverse KL divergence, and so (in general) arbitrarily large changes in its optimum. The precise result is stated in Theorem 3 of Section 4 above; we now provide the proof.

Proof of Theorem 3. For the duration of the proof, we will use the shorthand that a density applied to a set represents the integral of the density over the set. For example, for a set S , $\mathcal{P}(S) = \int_S \mathcal{P}(\theta) \mu(d\theta)$.

The proof will be constructive, based on an alternative $\mathcal{P}_1(\theta)$ formed by driving $\mathcal{P}_0(\theta)$ to zero in a small interval. By making the interval narrow, we can make $\|\phi(\theta|\mathcal{P}_1, p)\|_p$ small, but by making the $\mathcal{P}_1(\theta)$ sufficiently close to zero, we can make the reverse KL divergence difference large irrespective of how narrow the interval is.

³Gustafson [1996a] in fact considers only pointwise positive perturbations $\phi(\theta|\mathcal{P}_1, p) > 0$, μ -almost everywhere. It is not hard to extend Lemma 1 [Gustafson, 1996a, Result 2] to permit negative perturbations, except for the fact that $\|\cdot\|_p$ -neighborhoods of the zero function will always contain pointwise negative “priors.” We allow for negative $\phi(\theta|\mathcal{P}_1, p)$ because otherwise $\|\cdot\|_p$ leads to counter intuitive notions of the “size” of prior perturbations, as we discuss in Appendix C, and because standard results in functional analysis used in the proof of Theorem 5 require open neighborhoods.

However, we must acknowledge that the main result of this section, Theorem 3 below, relies on the possibility that $\phi(\theta|\mathcal{P}_1, p)$ can be negative. In light of this, one might reasonably wonder whether we should in fact restrict to positive perturbations in an attempt to avoid the consequences of Theorem 3. In the view of the authors, restricting to pointwise positive perturbations is a somewhat artificial solution to a fundamental disconnect between the $\|\cdot\|_p$ norm and reverse KL divergence which we discuss at the end of the present section. We believe that the disconnect is resolved more transparently and naturally through the use of the $\|\cdot\|_\infty$ norm and multiplicative perturbations which are allowed to be negative.

⁴Other than the fact that there exist pointwise negative priors induced by $\phi(\theta|\mathcal{P}_1, p)$ in every neighborhood of the zero function.

First, observe that

$$\text{KL}(q(\theta)||\mathcal{P}_1(\theta)) - \text{KL}(q(\theta)||\mathcal{P}_0(\theta)) = \mathbb{E}_{\mathcal{Q}(\theta)} \left[\log \frac{\mathcal{P}_1(\theta)}{\mathcal{P}_0(\theta)} \right].$$

For any set S with $\mathcal{P}_0(S) = \epsilon$, define

$$\mathcal{P}_1(\theta|S, \delta) := \frac{\delta^{\mathbb{I}(\theta \in S)}}{1 + \epsilon(1 - \delta)} \mathcal{P}_0(\theta).$$

Then $\mathcal{P}_1(\theta|S, \delta)$ is a valid density, and

$$\text{KL}(q(\theta)||\mathcal{P}_1(\theta)) - \text{KL}(q(\theta)||\mathcal{P}_0(\theta)) = \mathcal{Q}(S) \log \delta - \log(1 + \epsilon(1 - \delta)).$$

By Eq. 29,

$$\begin{aligned} \phi(\theta|\mathcal{P}_1, p) &= \mathcal{P}_0(\theta)^{1/p} \left(\frac{(\delta^{1/p})^{\mathbb{I}(\theta \in S)}}{(1 + \epsilon(1 - \delta))^{1/p}} - 1 \right) \quad \text{and} \\ \|\phi(\theta|\mathcal{P}_1, p)\|_p^p &= \epsilon \left(\frac{(\delta^{1/p})}{(1 + \epsilon(1 - \delta))^{1/p}} - 1 \right) + (1 - \epsilon) \left(\frac{1}{(1 + \epsilon(1 - \delta))^{1/p}} - 1 \right). \end{aligned}$$

Since μ is absolutely continuous with respect to the Lebesgue measure, there exists a sequence $\epsilon_n \rightarrow 0$ with $\epsilon_n > 0$ and a sequence of corresponding sets S_n such that $\mathcal{P}_0(S_n) = \epsilon_n$. (See Lemma 6 for a proof of this fact, which is a straightforward consequence of Nielsen [1997, Proposition 15.5] and the continuity of the Lebesgue measure.) Since $\mathcal{Q}(\theta) > 0$ on Ω_θ , $\mathcal{Q}(S_n) > 0$ for all n . Since $\text{KL}(\mathcal{Q}(\theta)||\mathcal{P}_0(\theta))$ is finite, we must have $\lim_{n \rightarrow \infty} \mathcal{Q}(S_n) = 0$.

Take $\delta_n = \exp(-1/(\mathcal{Q}(S_n)^2))$, and take $\mathcal{P}_1(\theta) = \mathcal{P}_1(\theta|S_n, \delta_n)$. Then $\epsilon_n(1 - \delta_n) \rightarrow 0$, and $\mathcal{Q}(S_n) \log \delta_n = -1/\mathcal{Q}(S_n)$, so

$$\begin{aligned} |\text{KL}(q(\theta)||\mathcal{P}_1(\theta|S_n, \delta_n)) - \text{KL}(q(\theta)||\mathcal{P}_0(\theta))| &\rightarrow \infty, \quad \text{but} \\ \|\phi(\theta|\mathcal{P}_1(\cdot|S_n, \delta_n), p)\|_p^p &\rightarrow 0. \end{aligned}$$

Thus, for sufficiently large n , the conclusion follows. \square

B Detailed Proofs

In this section, we provide detailed proofs for results stated above.

A standard consequence of the dominated convergence theorem is the ability to exchange integration and differentiation. Since we will use this result frequently, we state it here in our own notation as Theorem 6.

Theorem 6. [Billingsley, 1986, Theorem 16.8] *Let μ be sigma-finite measure on Ω_θ , and let $S_t \subseteq \mathbb{R}$. Let $f : \Omega_\theta \times S_t \mapsto \mathbb{R}$.*

If there exists a function $M(\theta)$ with $\int M(\theta)\mu(d\theta) < \infty$ such that $|f(\theta, t)| \leq M(\theta)$, μ -almost surely, for all $t \in S_t$, then the map $t \mapsto \int f(\theta, t)\mu(d\theta)$ is continuous.

Further, suppose that the derivative $\left. \frac{\partial f(\theta, t)}{\partial t} \right|_t$ exist μ -almost surely for $t \in S_t$. If there exists an $M'(\theta)$ such that $\int M'(\theta)\mu(d\theta) < \infty$ and $\left| \left. \frac{\partial f(\theta, t)}{\partial t} \right|_t \right| \leq M'(\theta)$, μ -almost surely and for all $t \in S_t$, then

$$\left. \frac{\partial \int f(\theta, t)\mu(d\theta)}{\partial t} \right|_t = \int \left. \frac{\partial f(\theta, t)}{\partial t} \right|_t \mu(d\theta).$$

Lemma 2. Under Assumption 3, at any $\eta, t \in \mathcal{B}_\eta \times \mathcal{B}_t$, we can exchange the order of integration and differentiation in $\int f(\theta, \eta, t)\mu(d\theta)$ for the derivatives $\partial/\partial\eta$, $\partial^2/\partial\eta^2$, and $\partial^2/\partial\eta\partial t$.

Proof. Let η_d denote the d -th entry of the vector η . Then

$$\begin{aligned} |\partial f(\theta, \eta, t)/\partial\eta_d| &\leq \|\partial f(\theta, \eta, t)/\partial\eta\|_2, \\ |\partial^2 f(\theta, \eta, t)/\partial\eta_d\partial t| &\leq \|\partial f(\theta, \eta, t)/\partial\eta\partial t\|_2, \text{ and} \\ |\partial^2 f(\theta, \eta, t)/\partial\eta_{d_1}\partial\eta_{d_2}| &\leq \|\partial f(\theta, \eta, t)/\partial\eta\partial\eta^T\|_2. \end{aligned}$$

The conclusion follows by repeatedly applying Theorem 6 to the components of the derivatives. \square

Lemma 3. Under Assumption 2, the map $\eta, t \mapsto \mathbb{E}_{\mathcal{Q}(\theta|\eta)} [\log \tilde{\mathcal{P}}(\theta|t)]$ has continuous partial derivatives $\partial/\partial\eta$, $\partial^2/\partial\eta^2$, and $\partial^2/\partial\eta\partial t$ at all $\eta, t \in \mathcal{B}_\eta \times \mathcal{B}_t$. Furthermore,

$$\left. \frac{\partial \mathbb{E}_{\mathcal{Q}(\theta|\eta)} [\log \tilde{\mathcal{P}}(\theta|t)]}{\partial\eta} \right|_\eta = \mathbb{E}_{\mathcal{Q}(\theta|\eta)} [\mathcal{S}(\theta|\eta) \log \tilde{\mathcal{P}}(\theta|t)] \quad (30)$$

$$\left. \frac{\partial^2 \mathbb{E}_{\mathcal{Q}(\theta|\eta)} [\log \tilde{\mathcal{P}}(\theta|t)]}{\partial\eta\partial t} \right|_{\eta, t} = \mathbb{E}_{\mathcal{Q}(\theta|\eta)} \left[\mathcal{S}(\theta|\eta) \left. \frac{\partial \log \tilde{\mathcal{P}}(\theta|t)}{\partial t} \right|_t \right]. \quad (31)$$

Proof. We can write

$$R(a, b) := \frac{a}{b} \Rightarrow \mathbb{E}_{\mathcal{Q}(\theta|\eta)} [\psi(\theta, t)] = R \left(\int \tilde{\mathcal{Q}}(\theta|\eta) \psi(\theta, t) \mu(d\theta), \int \tilde{\mathcal{Q}}(\theta|\eta) \mu(d\theta) \right).$$

If necessary, we can shrink \mathcal{B}_η so that the denominator $\int \tilde{\mathcal{Q}}(\theta|\eta) \mu(d\theta)$ is bounded below by a positive constant for all $\eta \in \mathcal{B}_\eta$. With the denominator strongly positive, $R(a, b)$ is a continuously differentiable function to all orders for all $t, \eta \in \mathcal{B}_t \times \mathcal{B}_\eta$. The desired results follow from Assumption 2 by the chain rule. \square

Proof of Theorem 4. By Assumption 1 (Item (1)) and Lemma 3, $\eta \mapsto \text{KL}(\eta, t)$ is continuously differentiable for all $\eta, t \in \mathcal{B}_\eta \times \mathcal{B}_t$. So, for all $t \in \mathcal{B}_t$, the optimal $\hat{\eta}(t)$ satisfies the first order condition:

$$\frac{\partial \text{KL}(\eta, t)}{\partial \eta} \bigg|_{\hat{\eta}(t), t} = \frac{\partial \text{KL}(\eta)}{\partial \eta} \bigg|_{\hat{\eta}(t)} + \frac{\partial \mathbb{E}_{\mathcal{Q}(\theta|\eta)} [\log \tilde{\mathcal{P}}(\theta|t)]}{\partial \eta} \bigg|_{\hat{\eta}(t)} = 0 \quad (32)$$

We wish to apply the implicit function theorem [Krantz and Parks, 2012, Theorem 3.3.1] to the estimating equation defined by Eq. 32. Again, by Assumption 1 (Item (1)) and Lemma 3, the estimating equation given is continuously differentiable in both η and t . The Jacobian of the estimating equation is nonsingular by Assumption 1 (Item (2)), and valid in an open ball by Assumption 1 (Item (3)). Finally, the form of the derivative is given by Krantz and Parks [2012, Theorem 3.3.1], together with Eq. 31 of Lemma 3.

For convenience, Table B shows the correspondence between our notation and that of Krantz and Parks [2012, Theorem 3.3.1].

Krantz & Parks notation	Our notation
$\Phi(x)$	$\text{KL}(\eta, t)$
Q	1
M	D_η
U	$\mathcal{B}_\eta \times \mathcal{B}_t$
W	\mathcal{B}_t
x_1, \dots, x_Q	t
x_{Q+1}, \dots, x_N	η
$f_1(x_a), \dots, f_M(x_a)$	$\hat{\eta}(t)$

□

Proof of Lemma 1. Let μ and μ' denote two mutually absolutely continuous candidate dominating measures for \mathcal{P}_0 , with respective densities (Radon-Nikodym derivatives) $\mathcal{P}_0(\theta)$ and $\mathcal{P}'_0(\theta)$. Let the respective densities of the measure \mathcal{P} be denoted $\mathcal{P}_1(\theta)$ and $\mathcal{P}'_1(\theta)$ as well. Let $R(\theta) = \frac{d\mu}{d\mu'} \bigg|_\theta$ denote the Radon-Nikodym derivative of μ with respect to μ' , and note that $\mathcal{P}'_0(\theta) = R(\theta)\mathcal{P}_0(\theta)$ and $\mathcal{P}'_1(\theta) = R(\theta)\mathcal{P}_1(\theta)$.

We have that the perturbations for μ and μ' are given respectively by

$$\begin{aligned} \phi(\theta|\beta, \mathcal{P}_1) &= \log \mathcal{P}_1(\theta) - \log \mathcal{P}_0(\theta) + \log \beta \\ \phi'(\theta|\beta, \mathcal{P}'_1) &= \log \mathcal{P}'_1(\theta) - \log \mathcal{P}'_0(\theta) + \log \beta \\ &= \log \mathcal{P}_1(\theta) - \log R(\theta) - \log \mathcal{P}_0(\theta) + \log R(\theta) + \log \beta \\ &= \phi(\theta|\beta, \mathcal{P}_1). \end{aligned}$$

It follows that $\|\phi(\cdot|\beta, \mathcal{P}_1)\|_\infty = \|\phi'(\cdot|\beta, \mathcal{P}'_1)\|_\infty$.

Next, let $\tau := \tau(\theta)$ be an invertible transformation with Jacobian $J(\theta) := \det\left(\frac{d\tau}{d\theta}\right|_\theta\right)$. For the dominating measure μ , let $\mathcal{P}_0(\theta)$ and $\mathcal{P}_1(\theta)$ denote the densities of θ and $\mathcal{P}_0'(\tau)$ and $\mathcal{P}_1'(\tau)$ denote the densities of τ . The desired result follows by the exact same formal argument as for the change of measure, except with $J(\theta)\mu(d\theta)$ and $\mu(d\tau)$ taking the place of $R(\theta)\mu(d\theta)$ and $\mu'(d\theta)$, respectively.

We now prove that ϕ gives rise to valid priors when $\|\phi\|_\infty < \infty$. Since the exponential function is positive, for any $\phi(\theta)$,

$$\tilde{\mathcal{P}}(\theta|\phi) = \mathcal{P}_0(\theta) \exp(\phi(\theta)) > 0,$$

μ -almost everywhere. Furthermore, since $\int \mathcal{P}_0(\theta) \lambda(d\theta) = 1$,

$$\exp(-\|\phi\|_\infty) \leq \int \mathcal{P}_0(\theta) \exp(\phi(\theta)) \mu(d\theta) \leq \exp(\|\phi\|_\infty).$$

so that $0 < \int \tilde{\mathcal{P}}(\theta|\phi) \mu(d\theta) < \infty$ whenever $\|\phi\|_\infty < \infty$. \square

Lemma 4. *Under Definition 4, Assumption 5 implies Assumption 2 when $\|\phi\|_\infty < \infty$.*

Proof. Since $\tilde{\mathcal{Q}}(\theta|\eta)\phi(\theta) \leq \tilde{\mathcal{Q}}(\theta|\eta)\delta$, and $\tilde{\mathcal{Q}}(\theta|\eta)$ satisfies Assumption 3 with some $M(\theta)$ by Assumption 5, we can satisfy Assumption 3 for $\tilde{\mathcal{Q}}(\theta|\eta)\phi(\theta)$ with $\max\{1, \delta\}M(\theta)$. Finally, Lemma 2 implies that Assumption 2 is satisfied. \square

Lemma 5. *Under Assumption 5, the map $\eta, \phi \mapsto \partial_{\mathcal{Q}(\theta|\eta)} \mathbb{E}[\phi(\theta)] / \partial\eta$ is continuously Fréchet differentiable as a map from $\mathbb{R}^{D_\eta} \times L_\infty \mapsto \mathbb{R}^{D_\eta}$.*

Proof. The map $\eta, \phi \mapsto \partial_{\mathcal{Q}(\theta|\eta)} \mathbb{E}[\phi(\theta)] / \partial\eta$ is a map from the Banach space $\mathbb{R}^{D_\eta} \times L_\infty$ into the Banach space \mathbb{R} . Let us take the L2 norm $\|\cdot\|_2$ on \mathbb{R}^{D_η} and \mathbb{R} . Let \mathcal{B} denote the ball $\mathcal{B}_\eta \times \{\phi : \|\phi\|_\infty < \delta\}$ for some $\delta > 0$. Let \mathcal{L} denote a linear operator from \mathcal{B} to \mathbb{R}^{D_η} , and define the dual norm

$$\|\mathcal{L}\|^* := \sup_{\Delta\eta: \|\Delta\eta\|_2 \leq 1} \sup_{\Delta\phi: \|\Delta\phi\|_\infty \leq 1} \|\mathcal{L}(\Delta\eta, \Delta\phi)\|_2.$$

Formally, $\Delta\eta$ and $\Delta\phi$ are members of \mathbb{R}^{D_η} and L_∞ respectively, but in the preceding display they can be thought of as directions on which the linear operator \mathcal{L} operates.

Observe that the directional derivatives are linear operators, and so $\|\cdot\|^*$ defines a norm on the space of linear operators. We will prove Fréchet differentiability using the fact that a functional is Fréchet differentiable if its directional derivatives are continuous in $\|\cdot\|^*$ as a function of the location at which they are evaluated (Zeidler [1986, Proposition 4.8(c)], Averbukh and Smolyanov [1967, Corollary 1.4] and [Reeds, 1976, Appendix A]). Further, it suffices by Zeidler [1986, Proposition 4.14(c)] to show that the partial derivatives with respect to η and ϕ are continuously Fréchet to show that the joint map is continuously Fréchet differentiable.

First, consider the partial derivative with respect to η . Observe that, by Lemma 4, Lemma 3 applies with $\log \tilde{P}(\theta|t) = \phi(\theta)$ (no t dependence). Consequently the map $\eta \mapsto \mathbb{E}_{\mathcal{Q}(\theta|\eta)} [\phi(\theta)]$ is twice continuously differentiable. The linear operator corresponding to the directional derivative in the $\Delta\eta$ direction is given by

$$\mathcal{L}_\eta(\Delta\eta, \Delta\phi) = \left. \frac{\partial^2 \mathbb{E}_{\mathcal{Q}(\theta|\eta)} [\phi(\theta)]}{\partial\eta \partial\eta^T} \right|_{\eta} \Delta\eta,$$

with no dependence on $\Delta\phi$. Define for the moment the the $D_\eta \times D_\eta$ matrix $\mathcal{H}(\eta, \phi) := \partial^2 \mathbb{E}_{\mathcal{Q}(\theta|\eta)} [\phi(\theta)] / \partial\eta \partial\eta^T$. Then the dual norm of the derivative is simply the operator norm of \mathcal{H} , i.e., $\|\mathcal{L}_\eta\|^* = \|\mathcal{H}(\eta, \phi)\|_{op}$. Thus we must show that $\|\mathcal{H}(\eta, \phi)\|_{op}$ is continuous in η, ϕ . For any η', ϕ' and η'', ϕ'' in $\mathcal{B}_\eta \times \mathcal{B}_\phi(\delta)$,

$$\begin{aligned} & \|\mathcal{H}(\eta', \phi') - \mathcal{H}(\eta'', \phi'')\|_{op} \\ & \leq \|\mathcal{H}(\eta', \phi') - \mathcal{H}(\eta', \phi'')\|_{op} + \|\mathcal{H}(\eta', \phi'') - \mathcal{H}(\eta'', \phi'')\|_{op}. \end{aligned}$$

For the first term in the preceding display, for all η' ,

$$\begin{aligned} & \|\mathcal{H}(\eta', \phi') - \mathcal{H}(\eta', \phi'')\|_{op} \leq \left. \frac{\partial^2 \mathbb{E}_{\mathcal{Q}(\theta|\eta)} [1]}{\partial\eta \partial\eta^T} \right|_{\eta'} \|\phi' - \phi''\|_\infty \Rightarrow \\ & \lim_{\phi' \rightarrow \phi''} \|\mathcal{H}(\eta', \phi') - \mathcal{H}(\eta', \phi'')\|_{op} = 0. \end{aligned}$$

For the second term, by Lemma 3, for all ϕ'' ,

$$\lim_{\eta' \rightarrow \eta''} \|\mathcal{H}(\eta', \phi'') - \mathcal{H}(\eta'', \phi'')\|_{op} = 0.$$

It follows that $\|\mathcal{H}(\eta, \phi)\|_{op}$ is continuous in η, ϕ , and so the partial derivative with respect to η is a continuous Fréchet derivative.

Next, we consider the partial derivative with respect to ϕ . By Eq. 30, we can write

$$\left. \frac{\partial \mathbb{E}_{\mathcal{Q}(\theta|\eta)} [\phi(\theta)]}{\partial\phi} \right|_{\eta} = \mathbb{E}_{\mathcal{Q}(\theta|\eta)} [\mathcal{S}(\theta|\eta)\phi(\theta)].$$

Since this expression is linear in ϕ , the linear operator for the partial derivative with respect to ϕ is given by

$$\mathcal{L}_\phi(\Delta\eta, \Delta\phi) = \mathbb{E}_{\mathcal{Q}(\theta|\eta)} [\mathcal{S}(\theta|\eta)\Delta\phi(\theta)],$$

with no dependence on $\Delta\eta$.

In order to be a valid partial derivative, we must verify that \mathcal{L}_ϕ is a bounded linear operator. Boundedness follows from Hölder's inequality and Assumption 5 since

$$\begin{aligned} \sup_{\Delta\phi: \|\Delta\phi\|_\infty \leq 1} \|\mathcal{L}_\phi(\Delta\eta, \Delta\phi)\|_2 &\leq \mathbb{E}_{\mathcal{Q}(\theta|\eta)} [\|\mathcal{S}(\theta|\eta)\|_1] \|\Delta\phi\|_\infty \\ &\leq \sqrt{D_\eta} \mathbb{E}_{\mathcal{Q}(\theta|\eta)} [\|\mathcal{S}(\theta|\eta)\|_2] \\ &\leq \sqrt{D_\eta} \int M(\theta) \mu(d\theta) < \infty. \end{aligned}$$

Similarly, the dual norm of the ϕ partial derivative is given by

$$\|\mathcal{L}_\phi\|^* = \mathbb{E}_{\mathcal{Q}(\theta|\eta)} [\|\mathcal{S}(\theta|\eta)\|_1].$$

We thus need to show that $\eta \mapsto \mathbb{E}_{\mathcal{Q}(\theta|\eta)} [\|\mathcal{S}(\theta|\eta)\|_1]$ is a continuous function of η (there is no ϕ dependence). To show this, observe that

$$\mathbb{E}_{\mathcal{Q}(\theta|\eta)} [\|\mathcal{S}(\theta|\eta)\|_1] = \frac{\int \tilde{\mathcal{Q}}(\theta|\eta) \|\mathcal{S}(\theta|\eta)\|_1 \mu(d\theta)}{\int \tilde{\mathcal{Q}}(\theta|\eta) \mu(d\theta)}. \quad (33)$$

By Assumption 5, we have that there exists a finitely integrable envelope function $M(\theta)$ such that, for all $\eta \in \mathcal{B}_\eta$,

$$\begin{aligned} \tilde{\mathcal{Q}}(\theta|\eta) &\leq M(\theta) \quad \text{and} \\ \tilde{\mathcal{Q}}(\theta|\eta) \|\mathcal{S}(\theta|\eta)\|_1 &\leq \sqrt{D_\eta} \tilde{\mathcal{Q}}(\theta|\eta) \|\mathcal{S}(\theta|\eta)\|_2 \leq M(\theta). \end{aligned}$$

Therefore, by the dominated convergence theorem, we can exchange limits and integrals in the numerator and denominator of Eq. 33. It follows that, for any η' and η'' in \mathcal{B}_η ,

$$\begin{aligned} \lim_{\eta' \rightarrow \eta''} \left| \int \tilde{\mathcal{Q}}(\theta|\eta') \mu(d\theta) - \int \tilde{\mathcal{Q}}(\theta|\eta'') \mu(d\theta) \right| &\leq \lim_{\eta' \rightarrow \eta''} \int \left| \tilde{\mathcal{Q}}(\theta|\eta') - \tilde{\mathcal{Q}}(\theta|\eta'') \right| \mu(d\theta) \\ &= \int \lim_{\eta' \rightarrow \eta''} \left| \tilde{\mathcal{Q}}(\theta|\eta') - \tilde{\mathcal{Q}}(\theta|\eta'') \right| = 0. \end{aligned}$$

Thus the numerator of Eq. 33 is continuous in η . The denominator of Eq. 33 is also continuous by an analogous argument. Since the denominator of Eq. 33 is bounded away from zero, $\mathbb{E}_{\mathcal{Q}(\theta|\eta)} [\|\mathcal{S}(\theta|\eta)\|_1]$ is a continuous composition of continuous functions, and itself continuous. It follows that the ϕ partial derivative is continuously Fréchet differentiable.

Since its partial derivatives are continuous, it follows by Zeidler [1986, Proposition 4.14(c)] that the joint map $\eta, \phi \mapsto \partial \mathbb{E}_{\mathcal{Q}(\theta|\eta)} [\phi(\theta)] / \partial \eta$ is continuously Fréchet differentiable.

□

Proof of Theorem 5. Recall that, by Lemma 4, Lemma 3 applies with $\log \tilde{\mathcal{P}}(\theta|t) = \phi(\theta)$ (no t dependence). Therefore, as in the proof of Theorem 4, for any $\phi \in \mathcal{B}_\phi(\delta)$, $\hat{\eta}(\phi)$ satisfies the first-order condition

$$\frac{\partial \text{KL}(\eta)}{\partial \eta} \bigg|_{\hat{\eta}(\phi)} + \frac{\partial \mathbb{E}_{\mathcal{Q}(\theta|\eta)}[\phi(\theta)]}{\partial \eta} \bigg|_{\hat{\eta}(\phi)} = 0. \quad (34)$$

As in the proof of Theorem 4, we wish to employ an implicit function theorem, but this time for general Banach spaces. We will use [Zeidler \[1986, Theorem 4.B\]](#).

First, [Zeidler \[1986, Chapter 4 Condition 21b\]](#) holds since \hat{H} is invertible by Assumption 1 (Item (2)). So we satisfy conditions (i), (ii), and (iii) of [Zeidler \[1986, Theorem 4.B\(c\)\]](#), giving that the function $\hat{\eta}(\phi)$ exists.

Moreover, by Assumption 1 (Item (1)) and Lemma 5, the estimating equation Eq. 34 is continuously Fréchet differentiable (C^1 in the notation of Zeidler) in a neighborhood of $\hat{\eta}, 0$. It follows from [Zeidler \[1986, Theorem 4.B\(d\)\]](#), $\hat{\eta}(\phi)$ is also continuously Fréchet differentiable. \square

Lemma 6. *If μ is absolutely continuous with respect to the Lebesgue measure, and \mathcal{P}_0 is a probability measure with a density relative to μ , then there exists a sequence $\epsilon_n \rightarrow 0$ with $\epsilon_n > 0$ and a sequence of corresponding sets S_n such that $\mathcal{P}_0(S_n) = \epsilon_n$.*

Proof. Let $\epsilon'_n = n^{-1}$. Since $\mathcal{P}_0 \ll \mu \ll \lambda$ (where λ is the Lebesgue measure), by applying [Nielsen \[1997, Proposition 15.5\]](#), for each n there exists a δ'_n such that, for any measurable set A with $\mu(A) < \delta'_n$, $\mathcal{P}_0(A) < \epsilon'_n$. Again applying [Nielsen \[1997, Proposition 15.5\]](#), there similarly exists a δ_n such that for any measurable set A with $\lambda(A) < \delta_n$, $\mu(A) < \delta'_n \Rightarrow \mathcal{P}_0(A) < \epsilon'_n$.

For each n , partition Ω_θ into a countable number of sets A_m such that $\sum_m \lambda(A_m) = 1$ and $\lambda(A_m) < \delta_n$. (This is possible by dividing Ω_θ into sufficiently small rectangles, for example.) Then $\mathcal{P}_0(A_m) < \epsilon'_n$ for all m . Since \mathcal{P}_0 is a probability measure, $\sum_m \mathcal{P}_0(A_m) = 1$, so there must exist at least $1/\epsilon'_n$ indices m' such that $\mathcal{P}_0(A_{m'}) > 0$. Take any such m' and let $\epsilon_n = \mathcal{P}_0(A_{m'})$ and $S_n = A_{m'}$. \square

Lemma 7. *Let μ denote the Lebesgue measure on \mathbb{R} . Let σ denote the standard deviation of a normal distribution, let η denote a continuously differentiable function of the normal distribution's natural parameters, let $\mathcal{N}(\theta|\eta)$ denote a normal density with respect to μ , and let \mathcal{B}_η denote an open ball in \mathbb{R}^2 such that $0 < \sigma < \infty$ for all $\eta \in \mathcal{B}_\eta$. Let \mathcal{B}_t denote an open ball in \mathbb{R} , and let $\psi(\theta, t)$ be a function such that $\theta \mapsto \psi(\theta, t)$ is μ -measurable for all $t \in \mathcal{B}_t$.*

If there exists a constant $C > 0$ such that

$$\sup_{t \in \mathcal{B}_t} |\psi(\theta, t)| \leq C \exp(|\theta|) \quad \text{and} \quad \sup_{t \in \mathcal{B}_t} \left| \frac{\partial \psi(\theta, t)}{\partial t} \right| \leq C \exp(|\theta|),$$

then one can exchange the order of expectation and differentiation in the expression $\mathbb{E}_{\mathcal{N}(\theta|\eta)} [\psi(\theta, t)]$ for the derivatives $\partial/\partial\eta$, $\partial^2/\partial\eta\partial\eta$, and $\partial^2/\partial\eta\partial t$, evaluated at any $t \in \mathcal{B}_t$ and $\eta \in \mathcal{B}_\eta$.

Proof. For the moment, let η denote the exponential family natural parameters of the normal distribution. By properties of the exponential family,

$$\begin{aligned} \frac{\partial \log \tilde{\mathcal{Q}}(\theta|\eta)}{\partial \eta} \bigg|_{\eta} &= (\theta, \theta^2)^T \quad \text{and} \quad \frac{\partial^2 \log \tilde{\mathcal{Q}}(\theta|\eta)}{\partial \eta \partial \eta^T} \bigg|_{\eta} = 0_{2 \times 2} \Rightarrow \\ \left\| \frac{\partial \log \tilde{\mathcal{Q}}(\theta|\eta)}{\partial \eta} \bigg|_{\eta} \right\|_2^2 &= \theta^2 + \theta^4 \quad \text{and} \quad \left\| \frac{\partial^2 \log \tilde{\mathcal{Q}}(\theta|\eta)}{\partial \eta \partial \eta^T} \bigg|_{\eta} \right\|_2 = 0. \end{aligned}$$

Let $\bar{\mathcal{B}}_\eta$ denote the closure of \mathcal{B}_η , and let

$$\eta^* := \operatorname{argmax}_{\eta \in \bar{\mathcal{B}}_\eta} \mathbb{E}_{\mathcal{Q}(\theta|\eta)} [\exp(|\theta|)].$$

By standard properties of the normal and the boundedness of $\sigma(\eta)$, the right hand side of the preceding display is finite. Then

$$\begin{aligned} \int \mathcal{Q}(\theta|\eta) \psi(\theta, t) \mu(d\theta) &\leq \left(\sup_{\theta} \sup_{t \in \mathcal{B}_t} |\psi(\theta, t)| \exp(-|\theta|) \right) \int \mathcal{Q}(\theta|\eta) \exp(\theta) \mu(d\theta) \\ &\leq C \mathbb{E}_{\mathcal{Q}(\theta|\eta^*)} [\exp(|\theta|)]. \quad (C \text{ does not depend on } \eta, t) \end{aligned}$$

Therefore, for Assumption 3, we can take $M(\theta) \propto \mathcal{Q}(\theta|\eta^*) \exp(|\theta|)$. The other terms follow similarly, since each multiplier of $\mathcal{Q}(\theta|\eta)$ is dominated by $\exp(-|\theta|)$. The final $M(\theta)$ simply takes the largest of the five constants.

Finally, if $\tilde{\eta}$ is a twice-continuously differentiable function of the natural parameters η (e.g the mean and variance), then the derivatives with respect to $\tilde{\eta}$ are equal to the derivatives with respect to η times bounded (on \mathcal{B}_η) functions of η that do not depend on θ . Thus a constant multiple of $M(\theta)$ will bound the new derivatives. \square

C Positive Perturbations Are Counterintuitive

The following example illustrates how, by requiring perturbations to be positive, one can induce counterintuitive notions of the “size” of a perturbation that ablates prior mass.

Example 5. Take μ to be the Lebesgue measure on $[0, 1]$. Let $\mathcal{P}_0(\theta) = \mathbb{I}(0 \leq \theta \leq 1)$. For some $\delta > 0$ and $0 < \epsilon \ll 1$, let

$$\mathcal{P}_1(\theta) := \left(\frac{1 - \delta\epsilon}{1 - \epsilon} \right) \mathbb{I}(\epsilon \leq \theta \leq 1) + \delta \mathbb{I}(0 \leq \theta \leq \epsilon).$$

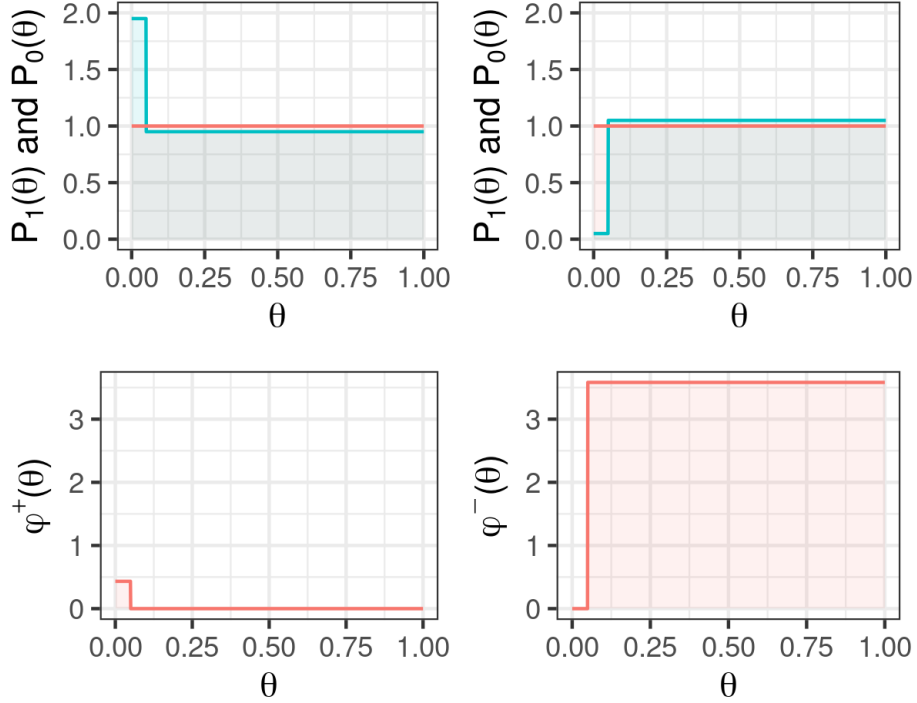


Figure 11: A plot of the perturbations from Example 5 with $p = 2$ and $\epsilon = 0.05$. Positive ϕ can only add mass, so to remove a small amount of mass requires adding mass everywhere else and re-normalizing, resulting in a large perturbation according to $\|\cdot\|_p$.

We can use Eq. 28 to give $\tilde{\mathcal{P}}(\theta|t_p = 1) = \mathcal{P}_1(\theta)$ by using, for any $\alpha > 0$,

$$\phi(\theta) = \left(\alpha \left(\frac{1 - \delta\epsilon}{1 - \epsilon} \right)^{1/p} - 1 \right) \mathbb{I}(\epsilon \leq \theta \leq 1) + \left(\alpha\delta^{1/p} - 1 \right) \mathbb{I}(0 \leq \theta \leq \epsilon).$$

It follows that

$$\|\phi\|_p = \left(\alpha \left(\frac{1 - \delta\epsilon}{1 - \epsilon} \right)^{1/p} - 1 \right) (1 - \epsilon) + \left(\alpha\delta^{1/p} - 1 \right) \epsilon.$$

For ϕ to be positive, we require

$$\alpha^p \geq \frac{1 - \epsilon}{1 - \delta\epsilon} \quad \text{and} \quad \alpha^p \geq \frac{1}{\delta}.$$

First, let us consider adding a small amount of prior mass, taking $\delta = 2 - \epsilon$; let the corresponding perturbation be ϕ^+ . For $\delta > 1$, then we achieve $\phi \geq 0$ by taking

$\alpha^p = \frac{1-\epsilon}{1-\delta\epsilon}$. Using the fact that $\epsilon \ll 1$ and keeping only leading-order terms,

$$\begin{aligned}\frac{1-\epsilon}{1-\delta\epsilon} &\approx (1-\epsilon)(1+\delta\epsilon) \\ &\approx 1 + (\delta-1)\epsilon \\ &\approx 1 + \epsilon,\end{aligned}$$

so

$$\begin{aligned}\|\phi^+\|_p &= \left(\alpha\delta^{1/p} - 1\right)\epsilon \\ &\approx \left((1+\epsilon)(2-\epsilon)^{1/p} - 1\right)\epsilon \\ &\approx \left(2^{1/p} - 1\right)\epsilon.\end{aligned}$$

Next, consider removing the same amount of mass with the symmetric change $\delta = \epsilon$, letting ϕ^- be the corresponding perturbation. Then we can ensure that $\phi(\theta) \geq 0$ with $\alpha^p \geq \epsilon^{-1}$, and $\epsilon \ll 1$ gives

$$\frac{1-\delta\epsilon}{1-\epsilon} \approx 1-\epsilon,$$

and

$$\begin{aligned}\|\phi^-\|_p &= \left(\alpha\left(\frac{1-\delta\epsilon}{1-\epsilon}\right)^{1/p} - 1\right)(1-\epsilon) \\ &\approx \left(\left(\frac{1-\epsilon}{\epsilon}\right)^{1/p} - 1\right)(1-\epsilon) \\ &\approx \left(\frac{1}{\epsilon}\right)^{1/p}.\end{aligned}$$

Since ϵ is small, $\|\phi^-\|_p \approx \left(\frac{1}{\epsilon}\right)^{1/p} \gg \|\phi^+\|_p \approx (2^{1/p} - 1)\epsilon$, despite the two perturbations respectively removing and adding the same amount of arbitrarily small probability mass.

△

D Computational details

D.1 The optimal local parameters

In all models we consider, the optimal local variational parameters $\hat{\eta}_\ell$ can be written as a closed-form function of the global variational parameters η_γ . Let $\hat{\eta}_\ell(\eta_\gamma; t)$ denote this mapping; that is,

$$\hat{\eta}_\ell(\eta_\gamma; t) := \operatorname{argmin}_{\eta_\ell} \text{KL}((\eta_\gamma, \eta_\ell), t).$$

The next example details this mapping for the Gaussian mixture model.

Example 6 (Optimalility of η_ℓ in a GMM). Recall that under our truncated variational approximation, the cluster assignment z_n is a discrete random variable over K_{\max} categories.

Let η_{z_n} be the categorical parameters in its exponential family natural parameterization. That is, we let $\eta_{z_n} = (\rho_{n1}, \rho_{n2}, \dots, \rho_{n(K_{\max}-1)})$ be an unconstrained vector in $\mathbb{R}^{K_{\max}-1}$; in this parameterization, the assignment probabilities are

$$p_{nk} := \mathbb{E}_{\mathcal{Q}(z_n|\eta_z)} [z_{nk}] = \frac{\exp(\rho_{nk})}{1 + \sum_{k'=1}^{K_{\max}-1} \exp(\rho_{nk})}$$

We use the exponential family parameterization because we require the optimal variational parameters $\hat{\eta}$ to be interior to Ω_η in Theorem 4. In the mean parameterization, $\sum_{k=1}^{K_{\max}} p_{nk} = 1$, so the optimal mean parameters $\hat{\mu}_n$ cannot be interior to $\Delta^{K_{\max}-1}$. On the other hand, η_{z_n} as defined is unconstrained in $\mathbb{R}^{K_{\max}-1}$.

Fixing $\mathcal{Q}(\beta|\eta_\beta)$ and $\mathcal{Q}(\nu|\eta_\nu)$, the optimal $\hat{\eta}_{z_n}$ must satisfy

$$\begin{aligned} \mathcal{Q}(z_n|\hat{\eta}_{z_n}) &\propto \exp(\tilde{\rho}_{nk}) \\ \text{where } \tilde{\rho}_{nk} &:= \mathbb{E}_{\mathcal{Q}(\beta, \nu|\eta)} [\log \mathcal{P}(x_n|\beta_k) + \log \pi_k]. \end{aligned}$$

See [Bishop \[2006\]](#) and [Blei et al. \[2017\]](#) for details. To satisfy this optimality condition, we set the optimal $\hat{\eta}_{z_n}$ to be

$$\hat{\eta}_{z_n} = \left(\log \frac{\tilde{\rho}_{n1}}{\tilde{\rho}_{nK_{\max}}}, \log \frac{\tilde{\rho}_{n2}}{\tilde{\rho}_{nK_{\max}}}, \dots, \log \frac{\tilde{\rho}_{n(K_{\max}-1)}}{\tilde{\rho}_{nK_{\max}}} \right).$$

Thus, as long as the expectations $\tilde{\rho}_{nk}$ can be provided as a closed-form function of (η_β, η_ν) , the optimal $\hat{\eta}_{z_n}$ can be also be set in closed-form as a function of (η_β, η_ν) . \triangle

D.2 More details on computing and inverting the Hessian

We fill in more details for the efficient computation of the Hessian outlined in Section 6.

We start from our formula in Eq. 18,

$$\frac{d\hat{\eta}(t)}{dt} \Big|_{t=0} = - \begin{pmatrix} H_{\gamma\gamma} & H_{\gamma\ell} \\ H_{\ell\gamma} & H_{\ell\ell} \end{pmatrix}^{-1} \begin{pmatrix} \hat{J}_\gamma \\ 0 \end{pmatrix},$$

and an application of the Schur complement gives

$$\frac{d\hat{\eta}(t)}{dt} \Big|_{t=0} = - \begin{pmatrix} I_{\gamma\gamma} \\ H_{\ell\ell}^{-1} H_{\ell\gamma} \end{pmatrix} (H_{\gamma\gamma} - H_{\gamma\ell} H_{\ell\ell}^{-1} H_{\ell\gamma})^{-1} \hat{J}_\gamma,$$

where $I_{\gamma\gamma}$ is the identity matrix with the same dimension as η_γ . Specifically, observe that the sensitivity of the global parameters is given by

$$\frac{d\hat{\eta}_\gamma(t)}{dt} \Big|_{t=0} = -\hat{H}_\gamma^{-1} \hat{J}_\gamma \quad \text{where } \hat{H}_\gamma := (H_{\gamma\gamma} - H_{\gamma\ell} H_{\ell\ell}^{-1} H_{\ell\gamma}),$$

In our model, $H_{\ell\ell}$ is sparse, and the size of $H_{\gamma\gamma}$ does not grow with N . Thus, each term of \hat{H}_{γ} can be tractably computed, stored in memory, and inverted, even on very large datasets.

One can derive the exact same identity using the optimality of $\hat{\eta}_{\ell}(\eta_{\gamma})$. By applying the chain rule, one can verify that

$$\hat{H}_{\gamma} = \frac{\partial^2}{\partial \eta_{\gamma} \partial \eta_{\gamma}^T} \text{KL}_{\text{glob}}(\hat{\eta}_{\gamma}, 0). \quad (35)$$

In practice, we evaluate \hat{H}_{γ} using automatic differentiation and Eq. 35 rather than the Schur complement.

D.3 Expressing g using global parameters only

Given a posterior quantity g , we again take advantage of the fact that the optimal local parameters can be found in closed form given global parameters. In general, g will be a function of the entire vector of variational parameters. However, in the same way that KL_{glob} implicitly sets the local parameters at their optimum and is a function of only global parameters and the prior parameter t , we can construct an analogous mapping for g ,

$$(t, \eta_{\gamma}) \mapsto g\left(\left(\eta_{\gamma}, \hat{\eta}_z(\eta_{\gamma}, t)\right)\right). \quad (36)$$

We illustrate this mapping when our quantity of interest is the in-sample expected posterior number of clusters.

Example 7. Let $g_{\text{cl}}(\eta)$ denote our variational approximation to $\mathbb{E}_{\mathcal{P}(z|x)}[G_{\text{cl}}(z)]$. Using the fact that $\mathcal{P}(z_n|\beta, \nu, x) = \mathcal{Q}(z_n|\hat{\eta}_{z_n})$ is available in closed form, we can then take

$$\begin{aligned} g_{\text{cl}}(\hat{\eta}) &:= \mathbb{E}_{\mathcal{Q}(\beta, \nu|\hat{\eta})} \left[\mathbb{E}_{\mathcal{P}(z|\beta, \nu, x)}[G_{\text{cl}}(z)] \right] \\ &\approx \mathbb{E}_{\mathcal{P}(\beta, \nu|x)} \left[\mathbb{E}_{\mathcal{P}(z|\beta, \nu, x)}[G_{\text{cl}}(z)] \right] = \mathbb{E}_{\mathcal{P}(z|x)}[G_{\text{cl}}(z)] \Rightarrow \\ g_{\text{cl}}(\eta) &= \sum_{k=1}^{K_{\text{max}}-1} \left(1 - \prod_{n=1}^N \left(1 - \mathbb{E}_{\mathcal{Q}(\beta, \nu|\eta_{\beta}, \eta_{\nu})} \left[\mathbb{E}_{\mathcal{P}(z_n|\beta, \nu, x)}[z_{nk}] \right] \right) \right). \end{aligned}$$

In this way, $g_{\text{cl}}(\eta)$ depends only on η_{β} and η_{ν} , which are much lower-dimensional than η_z , and retains nonlinearities in the map

$$\eta_{\beta}, \eta_{\nu} \mapsto \mathbb{E}_{\mathcal{Q}(\beta, \nu|\eta_{\beta}, \eta_{\nu})} \left[\mathbb{E}_{\mathcal{P}(z_n|\beta, \nu, x)}[z_{nk}] \right].$$

△

The mapping Eq. 36 can be constructed for any posterior quantity g . Therefore, linearizing the global parameters using Eqs. 19 and 20 is sufficient: we do not need to invert the full Hessian and linearize the entire set of variational parameters, global and local.

D.4 Evaluating stick expectations

We describe how to compute expectations with respect to the stick-breaking proportion ν_k . Let $f : \mathbb{R} \mapsto \mathbb{R}$ be a smooth function, and we are interested in expectations of the form

$$\mathbb{E}_{\mathcal{Q}(\nu_k|\eta)} [f(\nu_k)].$$

For example, f might be $f(\nu_k) = \log \mathcal{P}(\nu_k)$, whose expectation appears in the KL divergence.

Recall that we chose the distribution on the logit-transformed stick-breaking proportions $\tilde{\nu}_k$ to be normally distributed. Let η_k^μ and η_k^σ be the location and scale, respectively, of the Gaussian distribution on $\tilde{\nu}_k$. Also let s be the sigmoid function, so that $\nu_k = s(\tilde{\nu}_k)$.

To compute expectations of a smooth function $f(\nu_k)$, the law of the unconscious statistician states that

$$\mathbb{E}_{\mathcal{Q}(\nu_k|\eta)} [f(\nu_k)] = \mathbb{E}_{\mathcal{Q}(\tilde{\nu}_k|\eta)} [f \circ s(\tilde{\nu}_k)].$$

By choosing $\mathcal{Q}(\tilde{\nu}_k|\eta)$ to be Gaussian, the right-hand side is a Gaussian integral, which we approximate using GH quadrature with N_{GH} knots, located at ξ_g , weighted by ω_g :

$$\mathbb{E}_{\mathcal{Q}(\tilde{\nu}_k|\eta)} [f \circ s(\tilde{\nu}_k)] \approx \sum_{g=1}^{N_{\text{GH}}} \omega_g f \circ s(\eta_g^\sigma \xi_g + \eta_g^\mu) \quad (37)$$

Using GH quadrature to approximate the expectation is similar to the “reparameterization trick,” only using GH points rather than standard normal draws.

D.5 Unconstrained variational parameterizations

Recall from Theorem 4 that we require the optimal variational parameters $\hat{\eta}$ to be in the interior of its domain. One way to achieve this is to use only *unconstrained* parameterizations for the component distributions of \mathcal{Q} . One such parameterization was presented in Example 6, where we let η_{z_n} , which parameterize the cluster assignments, be allowed to take any value in $\mathbb{R}^{K_{\text{max}}-1}$; the assignment probabilities $m_n \in \mathbb{R}^{K_{\text{max}}}$, which are constrained to sum to one, are then formed with an appropriate transform of the unconstrained parameters η_{z_n} .

Other variables require careful parameterization as well. For instance, instead of parameterizing the normal distribution on logit-sticks $\tilde{\nu}_k$ using a mean and

variance, we let $\eta_{\nu_k} \in \mathbb{R}^2$ be the mean and *log* variance. The variance is constrained to be positive; the log-variance is unconstrained on the real line. In general, a real-valued parameter μ_i which must be constrained $a < \mu_i < b$ can be transformed to its unconstrained parameterization by letting

$$\eta_i = \log(\mu_i - a) - \log(b - \mu_i).$$

In the variational approximation to the GMM model, we let the component variables β_k be Normal-Wishart. In this case, the scale matrix of the Normal-Wishart, $W_k \in \mathbb{R}^{d \times d}$, is constrained to be positive definite. Because W is symmetric, we only need $d(d + 1)/2$ parameters to represent it. To form an unconstrained parameterization, we factorize W using the Cholesky decomposition,

$$W = L^T L,$$

where L is a lower-triangular matrix, with positive diagonal entries. The unconstrained parameterization of W is then taken to be the strictly lower-diagonal entries of L , along with the log of the diagonal entries of L .

E Additional Experimental Details

First, we review the Beta prior on the stick-breaking proportions, which are common to each model we considered. Then, we give some additional modeling details for each experiment.

E.1 The Beta prior

In the iris experiment, we considered $\alpha \in [0.1, 4.0]$. Over this range, the shape of the Beta(1, α) stick-breaking density varies considerably, as shown in Figure 12.

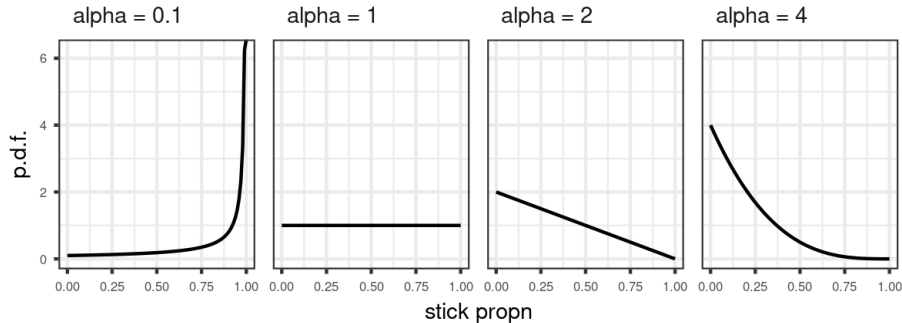


Figure 12: Probability density functions of Beta(1, α) distributions, under various α considered for the iris data set.

To help us understand the effect of the concentration parameter α we often use the following fact. Under the $\text{GEM}(\alpha)$ prior, the *a priori* expected number of distinct clusters in a dataset of size N is given by

$$\mathbb{E}_{\mathcal{P}(z|\pi)\mathcal{P}(\pi|\alpha)} [G_{\text{cl}}(z)] = \sum_{n=1}^N \frac{\alpha}{\alpha + n - 1}. \quad (38)$$

See [Blackwell and MacQueen](#) and [Teh \[2010, Equation 11\]](#).

E.2 Gaussian mixture modeling on iris data

The observations are vectors $x_n \in \mathbb{R}^d$, and we model each component with a multivariate Gaussian. In this model, $\beta_k = (\mu_k, \Lambda_k)$, where $\mu_k \in \mathbb{R}^d$, Λ_k is a $d \times d$ positive definite information matrix, and

$$\begin{aligned} \mathcal{P}(x_n|\beta_k) &= \mathcal{N}(x_n|\mu_k, \Lambda_k^{-1}) \\ \log \mathcal{P}(x_n|\beta_k) &= -\frac{1}{2}(x_n - \mu_k)^T \Lambda_k (x_n - \mu_k) + \frac{1}{2} \log |\Lambda_k| + C. \\ &\quad (C \text{ does not depend on } \beta_k) \end{aligned}$$

We let $\mathcal{P}_{\text{base}}(\beta_k)$ be the conjugate prior, which in this case is normal-Wishart:

$$\begin{aligned} \mathcal{P}_{\text{base}}(\beta_k) &= \mathcal{N}\mathcal{W}(\beta_k|\tau_0, n_0, p_0, V_0) \\ \log \mathcal{P}_{\text{base}}(\beta_k) &= -\frac{\tau_0}{2}(\mu_k - \mu_0)^T \Lambda_k (\mu_k - \mu_0) \\ &\quad + \frac{n_0 - p_0 - 1}{2} \log |\Lambda_k| - \frac{1}{2} \text{Tr}(V_0 \Lambda_k) + C, \end{aligned}$$

where (τ_0, n_0, p_0, V_0) are fixed prior parameters.

In this model, the conditionally conjugate variational distribution on β_k is normal-Wishart, which we denote as $\mathcal{Q}(\beta_k|\eta) = \mathcal{N}\mathcal{W}(\beta_k|\eta_{\beta_k})$, with η_{β_k} the normal-Wishart parameters. The conditionally conjugate variational distribution on z are multinomial.

Figure 13 shows the inferred clustering for $\alpha_0 = 2$, which recovers that there are three iris species.

E.3 Regression mixture modeling

The data. The data come from a publicly available data set of mice gene expression [[Shoemaker et al., 2015](#)]. Our analysis focuses on mice treated with the “A/California/04/2009” strain. We normalize the data as described in [Shoemaker et al. \[2015\]](#) and then apply the differential analysis tool EDGE [[Storey et al., 2005](#)] to rank the genes from most to least significantly differentially expressed. We run our analysis on the top $N = 1000$ genes.

The left plot of Figure 14 shows the measurements of a single gene over time. We model each gene as belonging to a latent component, where each component

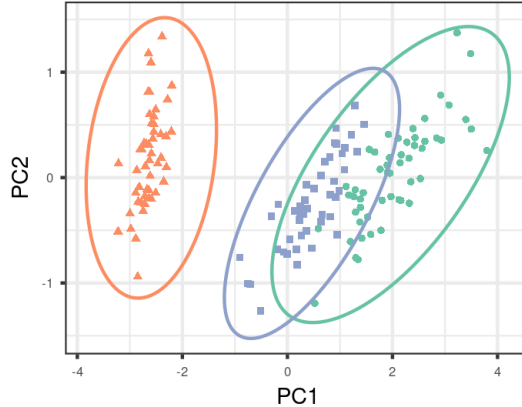


Figure 13: The iris data in principal component space and GMM fit at $\alpha = 2$. Colors denote inferred memberships and ellipses represent estimated covariances.

defines a smooth expression curve over time. Then, observations are drawn by adding i.i.d. noise to the smoothed curve along with a gene-specific offset.

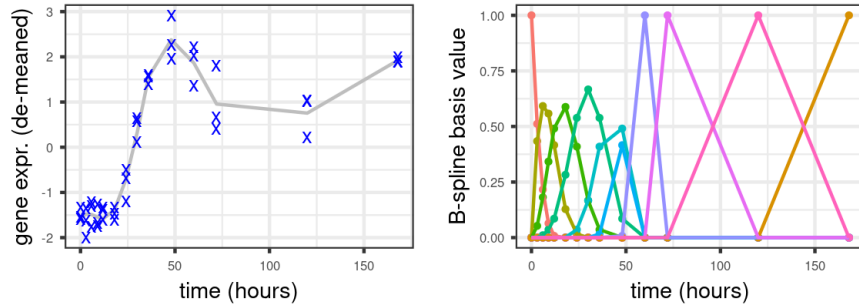


Figure 14: (Left) An example gene and its expression measured at 14 unique time points with three biological replicates at each time point. (Right) The cubic B-spline basis with 7 degrees of freedom, along with three indicator functions for the last three time points, $T = 72, 120, 168$.

The B-spline basis. Notice from Figure 14, which shows an example time-course for a single gene, that the time points are unevenly spaced, with more frequent observations at the beginning. Following Luan and Li [2003] we use cubic B-splines to smooth the time course expression data. Specifically, we model the first 11 time points using cubic B-splines with 7 degrees of freedom. For the last three time

points, $T = 72, 120, 168$ hours, we use indicator functions. That is, if \tilde{A} is the design matrix where each column is a B-spline basis vector evaluated at the M measurement times, we append to \tilde{A} three additional columns: in these columns, entries are 1 if $T = 72, 120$, or 168, respectively, and 0 otherwise. The resulting matrix is the full design matrix A . We use indicators for the last three time points for numerical stability; without the indicator columns, the matrix $\tilde{A}^T \tilde{A}$ is nearly singular because the later time points are more spread out. The left column of Figure 14 shows our basis functions.

The generative model. Eq. 21 gives the per-component conditional likelihood. We use a normal prior for the shifts b_n , a multivariate normal prior for the coefficients μ_k , and a gamma prior for the inverse variance τ_k . The prior on the mixture weights π are constructed using the stick-breaking construction in the main-text, and the cluster assignments z_n are drawn from a multinomial with weights π , as usual.

The variational approximation. The variational approximation, factorizes as

$$\mathcal{Q}(\zeta|\eta) = \left(\prod_{k=1}^{K_{\max}-1} \mathcal{Q}(\nu_k|\eta) \right) \left(\prod_{k=1}^{K_{\max}} \mathcal{Q}(\beta_k|\eta) \right) \left(\prod_{n=1}^N \mathcal{Q}(z_n|\eta) \mathcal{Q}(b_n|z_n, \eta) \right).$$

Note that the variational distribution for b_n conditions on z . We set $\mathcal{Q}(b_n|z_n = k, \eta)$ to be Gaussian with variational parameters dependent on k . For simplicity in this application, we let $\mathcal{Q}(\beta_k|\eta) = \delta(\beta_k|\eta)$, where $\delta(\cdot|\eta)$ denotes a point mass at a parameterized location.

As discussed in Example 6, the optimal distribution $\mathcal{Q}(z_n|\eta)$ is multinomial whose parameters can be set in closed form as a function of the global variational parameters only. We allow the distribution of b_n to depend on z_{nk} so that the its optimal distribution can also be set in closed form as a function of global parameters.

The optimal distribution $q(b_n|z_{nk} = 1, \eta)$ is Gaussian,

$$q(b_n|z_{nk} = 1, \eta) = \mathcal{N}(b_n|\hat{\mu}_{b_{nk}}, \hat{\sigma}_{b_{nk}}^2).$$

To define the optimal parameters $\hat{\mu}_{b_{nk}}, \hat{\sigma}_{b_{nk}}^2$, let

$$\begin{aligned} \rho_{nk}^{(1)} &= \mathbb{E}_{\mathcal{Q}(\beta_k|\eta)} \left[\sum_{m=1}^M \tau_k(x_{nm} - A_m \mu_k) \right] + \tau_0 \mu_0 \\ \rho_{nk}^{(2)} &= M \mathbb{E}_{\mathcal{Q}(\beta_k|\eta)} [\tau_k] + \tau_0, \end{aligned}$$

where μ_0 and τ_0 are the prior mean and information on b_n , respectively.

The optimal parameters for the Gaussian distribution on b_n are given by

$$\begin{aligned} \hat{\mu}_{b_{nk}} &= \rho_{nk}^{(1)} / \rho_{nk}^{(2)} \\ \hat{\sigma}_{b_{nk}}^2 &= 1 / \rho_{nk}^{(2)}. \end{aligned}$$

Figure 15 shows the inferred smoothers $A \mathbb{E}_{\mathcal{Q}} [\mu_k]$ for selected clusters.

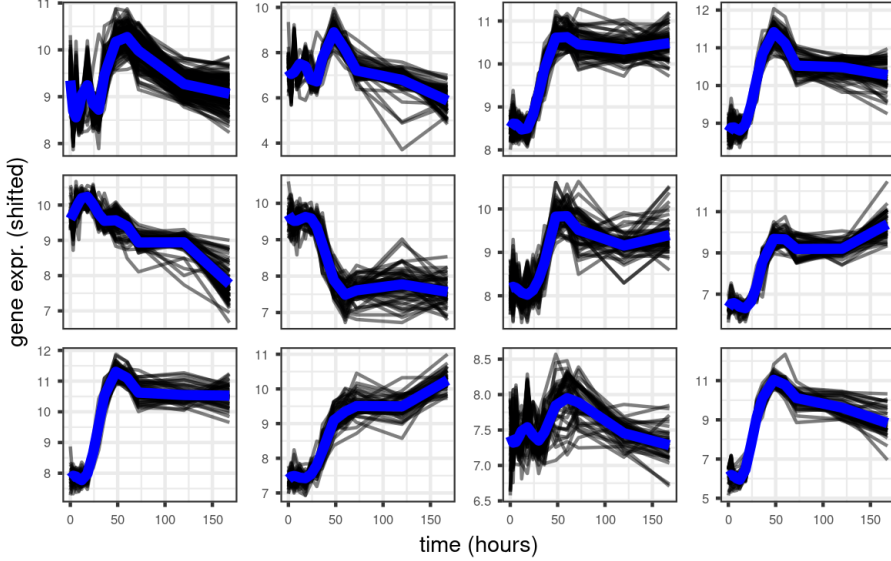


Figure 15: Inferred clusters in the mice gene expression dataset. Shown are the twelve most occupied clusters. In blue, the inferred cluster centroid. In grey, gene expressions averaged over replicates and shifted by their inferred intercepts.

E.4 fastSTRUCTURE

The generative process was described in the main text (Section 7.3). We detail here the variational approximation. Like in all our examples, the variational distribution is mean-field:

$$\mathcal{Q}(\zeta|\eta) = \left(\prod_{n=1}^N \prod_{k=1}^{K_{\max}-1} \mathcal{Q}(\nu_{nk}|\eta) \right) \left(\prod_{k=1}^{K_{\max}} \prod_{l=1}^L \mathcal{Q}(\beta_{kl}|\eta) \right) \left(\prod_{n=1}^N \prod_{l=1}^L \prod_{i=1}^2 \mathcal{Q}(z_{nli}|\eta) \right).$$

We let all distributions be conditionally conjugate except for the sticks, which are logit-normal. Each membership indicator z_{nli} is categorical, and the allele frequencies β_{kl} are Dirichlet distributed.

In this model, we still call (β, ν) the global latent variables, even though they scale with the number of individuals N ; they do not, however, scale with both the number of individuals and the number of loci like z does. Thus, we call z the local latent variables. The local variational parameters η_z can be set optimally in an analogous way as Example 6, except with the indices nk replaced with $nlik$.

The posterior quantities of interest in this application are the admixtures π_n . Figure 16 plots the inferred admixtures $\mathbb{E}_{\mathcal{Q}(\pi_n|\hat{\eta})} [\pi_n]$ for all individuals n .

In the approximate posterior with $\alpha_0 = 3$, there appear to be three dominant latent populations, which we arbitrarily label as populations 1, 2, and 3 (Figure 16).

The inferred admixture proportions generally correspond with geographic regions: Mbololo individuals are primarily population 1; Ngangao individuals are primarily population 2; and Chawia individuals are a mixture of populations 1, 2, and 3.

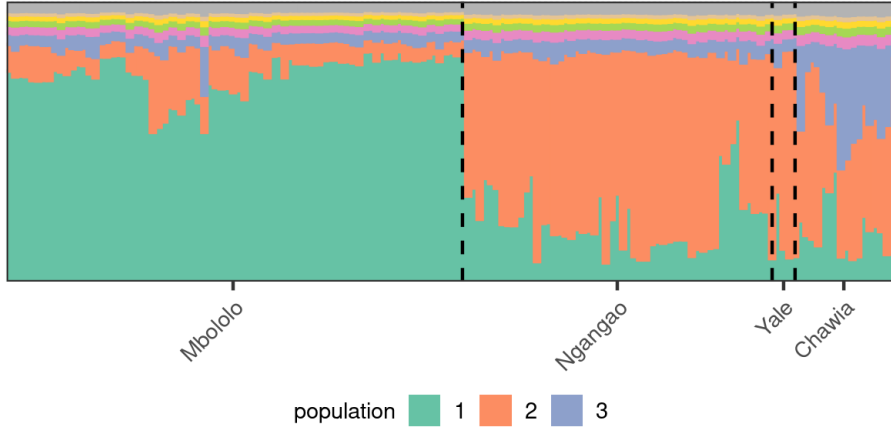


Figure 16: The inferred individual admixtures at $\alpha_0 = 3$. Each vertical strip is an individual and each color a latent population. Lengths of colored segments represent the inferred admixture proportions. Individuals are ordered by the geographic region from which they were sampled (Mbololo, Ngangao, Yale, and Chawia). In the text, we refer to the green, orange, and purple latent populations as population 1, 2, and 3, respectively.

F fastSTRUCTURE Supplemental Results

F.1 The expected number of populations

One posterior quantity of interest is the expected number of in-sample populations. Define

$$g_{\text{cl}, \tau}(\eta) = \mathbb{E}_{\mathcal{Q}(z|\eta)} \left[\sum_{k=1}^{K_{\max}} \mathbb{I} \left(\left(\sum_{n=1}^N \sum_{l=1}^L \sum_{i=1}^2 z_{nlki} \right) > \tau \right) \right],$$

which is the expected number of populations in the data set that contains at least τ loci. We allow the option of setting $\tau > 0$ in order to count only the populations that comprise a non-negligible fraction of the data set.

The expected number of latent populations is sensitive to α (Figure 17). Without any thresholding ($\tau = 0$), the expected number of populations quickly increases as α increases; in fact, it nearly saturates at $K_{\max} = 20$ when $\alpha = 7$. This sensitivity is due to the fact that the non-thresholded quantity is highly dependent on the behavior of small, nearly unoccupied populations; even though the probability

of a single locus belonging to these rare populations is small, the probability that *none* of the $N \times L \times 2$ observed genotypes belong to these rare populations is non-negligible.

This motivates the use of thresholding in reporting the number of populations. We consider two thresholds, $\tau = 20$ and $\tau = 40$, corresponding to approximately 2% and 4% of the total number of loci in the data set, respectively. The thresholded estimates for the number of populations is still moderately sensitive to the value of α . When refitting the variational approximation at $\alpha = 0.5, 1, \dots, 7$, the thresholded quantities vary between two and four latent populations.

The linearized variational parameters $\hat{\eta}_\gamma^{\text{lin}}(t)$ imperfectly captures the results observed by refitting. The linearized parameters and the refitted parameters almost perfectly agree on values of $g_{\text{cl},\tau}$ with $\tau = 0$. However, when $\tau = 20$, the linearized parameters underestimated the true sensitivity of $g_{\text{cl},\tau}$ found by refitting. In particular, the linearized parameters failed to produce the reduction to two latent populations at $\alpha = 0.5$ observed in the refits.

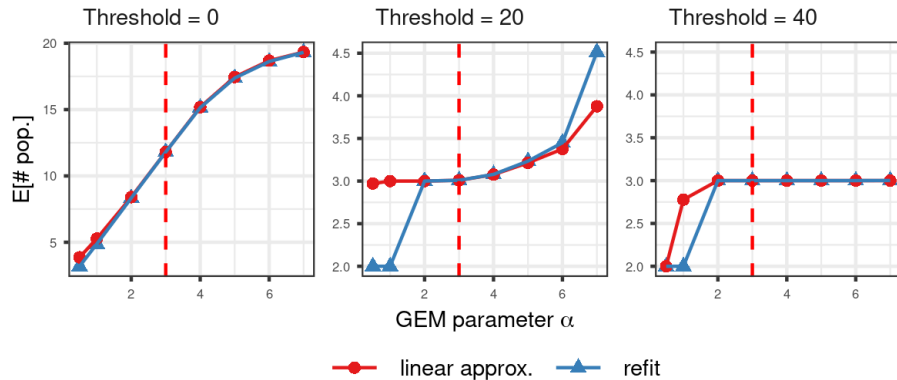


Figure 17: The expected number of (thresholded) populations in the thrush data as α varies. We computed the linear approximation at $\alpha_0 = 3$, and we compare the results under the linearly approximated variational parameters with the results observed after refitting. Thresholds at $\tau = 20$ and $\tau = 40$ corresponding to approximately 2% and 4% of the total number of loci in the data set, respectively.

We provide some more intuition concerning the thresholded estimate for the number of populations. The posterior quantity $g_{\text{cl},\tau}$ is closely related to the expected number of loci belonging to each population, defined as

$$g_{\text{loci}}(\eta; k) = \mathbb{E}_{\mathcal{Q}(z|\eta)} \left[\sum_{n=1}^N \sum_{l=1}^L \sum_{i=1}^2 z_{nlk} \right].$$

Figure 18 plots g_{loci} for the first six populations as α varies. The expected number of loci at the initial fit, $g_{\text{loci}}(\hat{\eta}(\alpha_0); k)$, is at least 100 for populations

$k = 1, 2$, and 3 and less than 15 for the remaining populations. A sample of assignments $z \sim \mathcal{Q}(z|\hat{\eta}(\alpha_0))$ will almost always have at least τ loci allocated to populations $1, 2$, and 3 , while the allocations to each remaining population will almost always be below τ , for either $\tau = 20$ or $\tau = 40$. Thus, at $\alpha = \alpha_0$ there then are clearly 3 populations by our definition of $g_{\text{cl},\tau}$, for either τ .

At $\alpha = 7$, the expected number of loci belonging to population 4 increases to approximately 20 , and a new population emerges above the threshold at $\tau = 20$. Both the linearized and the refitted variational parameters agree on this shift in allocation to population 4 . On the other hand, under the refitted variational parameters at $\alpha = 0.5$, the expected number of loci belonging to population 3 decreases to seven, below the threshold $\tau = 20$. Thus, the expected number of latent populations with allocations above the threshold $\tau = 20$ decreases to two. The linearized parameters under-estimated this decrease in allocation to population 3 , and therefore continued to estimate three latent populations even at $\alpha = 0.5$.

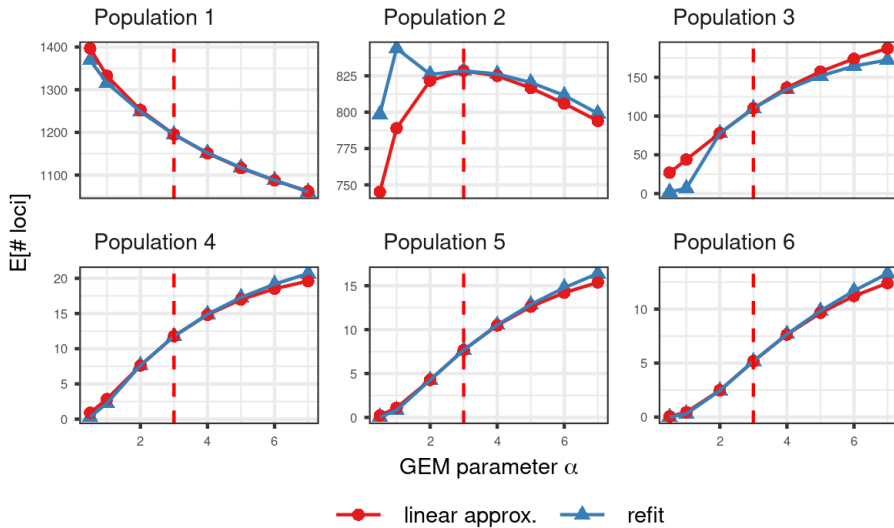


Figure 18: The expected number of loci per population as α varies.

F.2 Limitations of local sensitivity

Recall from Section 7.3 and Figure 10 that the linear approximation failed to capture the change in the admixture proportion of an individual, $n = 25$ after a worst-case functional perturbation.

Figure 19 examines individual $n = 25$ more closely. The bottom row plots this individual's admixture proportions as t varies from 0 to 1 in the perturbed prior $\mathcal{P}(\nu|t) = \mathcal{P}_0(\nu_k) \exp(t\phi_{\text{wc}}(\nu_k))$. The linearized parameters poorly captured

the change in admixture proportions observed after refitting, particularly for populations 1 and 2, for values of t close to 1. Even though we retain non-linearities in the mapping from variational parameters to the posterior statistic, for this perturbation, the mapping from prior parameter t to the relevant variational parameters is highly non-linear. This latter mapping is what we linearize and what causes our approximation to fail in this case. Specifically, the variational location parameter on the first stick-breaking proportion is concave as a function of t – the location parameter increases for small t , then decreases as $t \rightarrow 1$. However, $\hat{\eta}^{\text{lin}}(t)$ linearizes the relationship between the location parameter and t . Therefore, the corresponding admixture mixture proportion of population 1 is over-estimated under the linearized variational parameters. Furthermore, because our linearized variational parameters over-estimated the length of the first stick, and the second admixture proportion is a product of the remaining stick times the second stick-breaking proportion, the linearized variational parameters then under-estimates the admixture proportion of population 2.

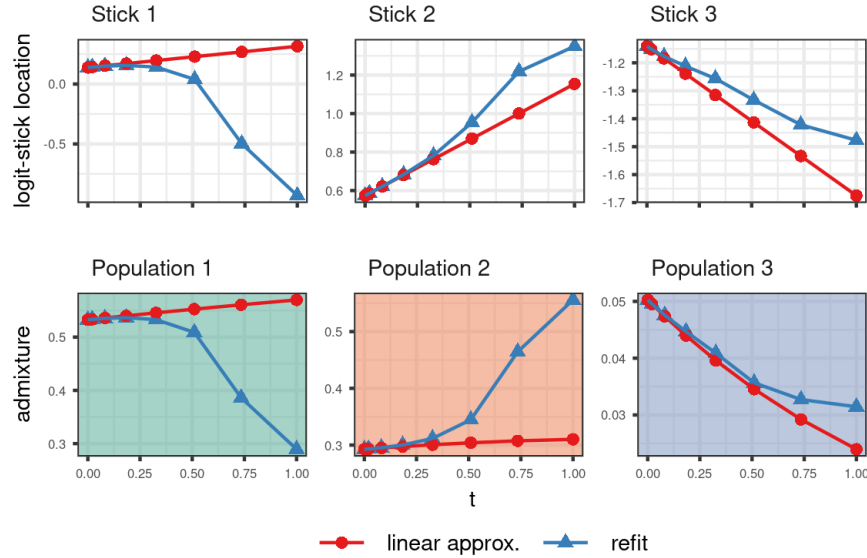


Figure 19: An individual ($n = 26$) for which the linearly approximated variational parameters poorly captured the change in admixture observed after refitting as $t \rightarrow 1$. (Top row) the change in location parameter of the normally distributed logit-sticks, for the first three sticks. The response here is a variational parameter, so the approximation (red) is necessarily linear with respect to t . (Bottom row) the change in the inferred admixtures for populations 1, 2, and 3.

Figure 20 shows a similar situation for individual $n = 74$. The linearized variational parameters grossly over-estimated the length of the first stick, resulting in the later admixture proportions being under-estimated. The third admixture proportion was particularly poorly approximated under the linearized variational parameters. Given the recursive nature of the relationship between admixtures and stick-breaking proportions, errors at early sticks affect later admixture proportions. Fully linearizing the mapping $t \mapsto g(\hat{\eta}(t))$ to form the approximation $g^{\text{lin}}(t)$ avoids this problem. In this example, $g^{\text{lin}}(t)$ outperforms $g(\hat{\eta}^{\text{lin}}(t))$, with g being the admixture proportion of population 3. In our experience, computing $g(\hat{\eta}^{\text{lin}}(t))$, and thus retaining non-linearities in the mapping from $\eta \mapsto g(\eta)$, is usually beneficial to the quality of the approximation. It is likely that $g(\hat{\eta}^{\text{lin}}(t))$ outperforms $g^{\text{lin}}(t)$ for most posterior quantities, though as we see in Figure 20, this is not guaranteed to always be true.

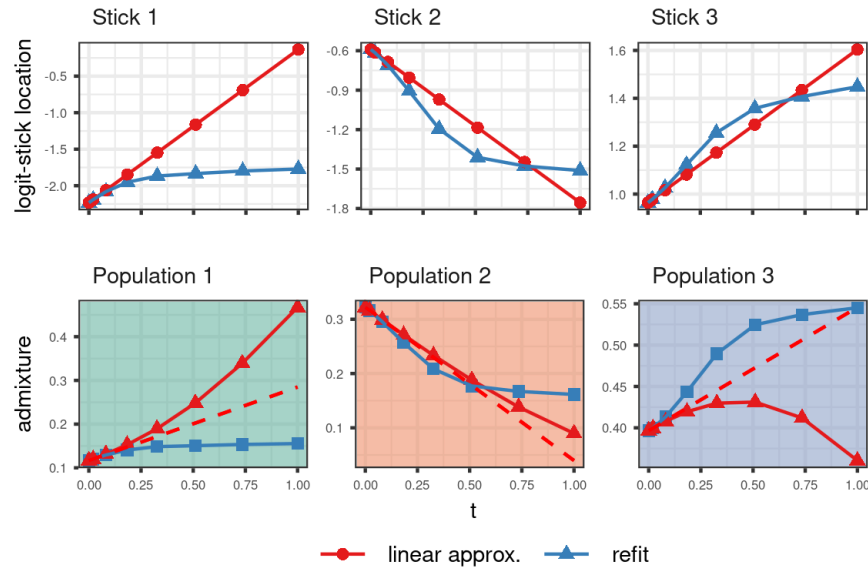


Figure 20: An example where linearizing the posterior quantity itself outperforms linearizing the variational parameters only. Shown are logit-stick location parameters (top row) and inferred admixtures (bottom row) for individual $n = 74$ and populations $k = 1, 2$ and 3 . Dashed red is the approximation $g^{\text{lin}}(t)$ formed by linearizing the inferred admixture $\mathbb{E}_Q[\pi_{nk}]$ with respect to prior parameter t . On the admixture proportion of population 3, $g^{\text{lin}}(t)$ outperforms $g(\hat{\eta}^{\text{lin}}(t))$ (solid red).